ADVANCING GLOBAL COMMUNICATIONS

TIA TELECOMMUNICATIONS SYSTEMS BULLETIN

Wireless Communications Systems Performance in Noise and Interference Limited Situations

Part 2: Propagation and Noise

TSB-88.2-E

January 2016

TELECOMMUNICATIONS INDUSTRY ASSOCIATION

tiaonline.org

NOTICE

TIA Engineering Standards and Publications are designed to serve the public interest through eliminating misunderstandings between manufacturers and purchasers, facilitating interchangeability and improvement of products, and assisting the purchaser in selecting and obtaining with minimum delay the proper product for their particular need. The existence of such Standards and Publications shall not in any respect preclude any member or non-member of TIA from manufacturing or selling products not conforming to such Standards and Publications. Neither shall the existence of such Standards and Publications preclude their voluntary use by Non-TIA members, either domestically or internationally.

Standards and Publications are adopted by TIA in accordance with the American National Standards Institute (ANSI) patent policy. By such action, TIA does not assume any liability to any patent owner, nor does it assume any obligation whatever to parties adopting the Standard or Publication.

This Standard does not purport to address all safety problems associated with its use or all applicable regulatory requirements. It is the responsibility of the user of this Standard to establish appropriate safety and health practices and to determine the applicability of regulatory limitations before its use.

Any use of trademarks in this document are for information purposes and do not constitute an endorsement by TIA or this committee of the products or services of the company.

(From Project No. TIA-PN-88.2-E, formulated under the cognizance of the TIA TR-8 Mobile and Personal Private Radio Standards, TR-8.18 Subcommittee on Wireless Systems Compatibility-Interference and Coverage).

Published by
©TELECOMMUNICATIONS INDUSTRY ASSOCIATION
Technology & Standards Department
1320 N. Courthouse Road, Suite 200
Arlington, VA 22201 U.S.A.

**PRICE: Please refer to current Catalog of
TIA TELECOMMUNICATIONS INDUSTRY ASSOCIATION STANDARDS
AND ENGINEERING PUBLICATIONS
or call IHS, USA and Canada
(1-877-413-5187) International (303-397-2896)
or search online at http://www.tiaonline.org/standards/catalog/**

NOTICE OF DISCLAIMER AND LIMITATION OF LIABILITY

The document to which this Notice is affixed (the "Document") has been prepared by one or more Engineering Committees or Formulating Groups of the Telecommunications Industry Association ("TIA"). TIA is not the author of the Document contents, but publishes and claims copyright to the Document pursuant to licenses and permission granted by the authors of the contents.

TIA Engineering Committees and Formulating Groups are expected to conduct their affairs in accordance with the TIA Procedures for American National Standards and TIA Engineering Committee Operating Procedures, the current and predecessor versions of which are available at http://www.tiaonline.org/standards/ec-procedures)/TIA's function is to administer the process, but not the content, of document preparation in accordance with the Manual and, when appropriate, the policies and procedures of the American National Standards Institute ("ANSI"). TIA does not evaluate, test, verify or investigate the information, accuracy, soundness, or credibility of the contents of the Document. In publishing the Document, TIA disclaims any undertaking to perform any duty owed to or for anyone.

If the Document is identified or marked as a project number (PN) document, or as a standards proposal (SP) document, persons or parties reading or in any way interested in the Document are cautioned that: (a) the Document is a proposal; (b) there is no assurance that the Document will be approved by any Committee of TIA or any other body in its present or any other form; (c) the Document may be amended, modified or changed in the standards development or any editing process.

The use or practice of contents of this Document may involve the use of intellectual property rights ("IPR"), including pending or issued patents, or copyrights, owned by one or more parties. TIA makes no search or investigation for IPR. When IPR consisting of patents and published pending patent applications are claimed and called to TIA's attention, a statement from the holder thereof is requested, all in accordance with the Manual. TIA takes no position with reference to, and disclaims any obligation to investigate or inquire into, the scope or validity of any claims of IPR. TIA will neither be a party to discussions of any licensing terms or conditions, which are instead left to the parties involved, nor will TIA opine or judge whether proposed licensing terms or conditions are reasonable or non-discriminatory. TIA does not warrant or represent that procedures or practices suggested or provided in the Manual have been complied with as respects the Document or its contents.

If the Document contains one or more Normative References to a document published by another organization ("other SSO") engaged in the formulation, development or publication of standards (whether designated as a standard, specification, recommendation or otherwise), whether such reference consists of mandatory, alternate or optional elements (as defined in the TIA Procedures for American National Standards) then (i) TIA disclaims any duty or obligation to search or investigate the records of any other SSO for IPR or letters of assurance relating to any such Normative Reference; (ii) TIA's policy of encouragement of voluntary disclosure (see TIA Procedures for American National Standards Annex C.1.2.3) of Essential Patent(s) and published pending patent applications shall apply; and (iii) Information as to claims of IPR in the records or publications of the other SSO shall not constitute identification to TIA of a claim of Essential Patent(s) or published pending patent applications.

TIA does not enforce or monitor compliance with the contents of the Document. TIA does not certify, inspect, test or otherwise investigate products, designs or services or any claims of compliance with the contents of the Document.

ALL WARRANTIES, EXPRESS OR IMPLIED, ARE DISCLAIMED, INCLUDING WITHOUT LIMITATION, ANY AND ALL WARRANTIES CONCERNING THE ACCURACY OF THE CONTENTS, ITS FITNESS OR APPROPRIATENESS FOR A PARTICULAR PURPOSE OR USE, ITS MERCHANTABILITY AND ITS NONINFRINGEMENT OF ANY THIRD PARTY'S INTELLECTUAL PROPERTY RIGHTS. TIA EXPRESSLY DISCLAIMS ANY AND ALL RESPONSIBILITIES FOR THE ACCURACY OF THE CONTENTS AND MAKES NO REPRESENTATIONS OR WARRANTIES REGARDING THE CONTENT'S COMPLIANCE WITH ANY APPLICABLE STATUTE, RULE OR REGULATION, OR THE SAFETY OR HEALTH EFFECTS OF THE CONTENTS OR ANY PRODUCT OR SERVICE REFERRED TO IN THE DOCUMENT OR PRODUCED OR RENDERED TO COMPLY WITH THE CONTENTS.

TIA SHALL NOT BE LIABLE FOR ANY AND ALL DAMAGES, DIRECT OR INDIRECT, ARISING FROM OR RELATING TO ANY USE OF THE CONTENTS CONTAINED HEREIN, INCLUDING WITHOUT LIMITATION ANY AND ALL INDIRECT, SPECIAL, INCIDENTAL OR CONSEQUENTIAL DAMAGES (INCLUDING DAMAGES FOR LOSS OF BUSINESS, LOSS OF PROFITS, LITIGATION, OR THE LIKE), WHETHER BASED UPON BREACH OF CONTRACT, BREACH OF WARRANTY, TORT (INCLUDING NEGLIGENCE), PRODUCT LIABILITY OR OTHERWISE, EVEN IF ADVISED OF THE POSSIBILITY OF SUCH DAMAGES. THE FOREGOING NEGATION OF DAMAGES IS A FUNDAMENTAL ELEMENT OF THE USE OF THE CONTENTS HEREOF, AND THESE CONTENTS WOULD NOT BE PUBLISHED BY TIA WITHOUT SUCH LIMITATIONS.

TABLE OF CONTENTS

FOREWORD xiii
INTRODUCTION xv
1. SCOPE 1
1.1 The TSB-88 Series 1
1.2 TSB-88.2-E 3
2. REFERENCES 4
3. DEFINITIONS AND ABBREVIATIONS 5
3.1 Definitions 5
3.2 Abbreviations 11
4. TEST METHODS 14
5. NOISE 15
5.1 Environmental RF Noise 15
5.2 Environmental RF Noise Data 15
5.2.1 Measurements Referenced to Land Cover Categories 15
5.2.2 Historical RF Noise Data 20
5.3 RF Noise Measurement Methodology 21
5.3.1 Receiver Selection 21
5.3.2 Antenna Selection 21
5.3.3 RF Noise Measurement in a Mobile Environment 22
5.3.4 Fixed RF Noise Measurement 26
5.3.5 Site Isolation 26
5.4 Symbolic RF Noise Modeling and Simulation Methodology 27
5.4.1 Receiver/Multicoupler Interference 27
5.4.2 Intermodulation 28
5.4.3 The Symbolic Method 31
5.4.4 Multicoupler Parametric Values 35
5.4.5 Non-Coherent Power Addition Discussion 36
5.4.6 Determining Unknown Power from Sum Plus One Known Value 38
5.5 Noise-Adjusted Faded Performance Threshold 39
6. ELECTROMAGNETIC WAVE PROPAGATION PREDICTIONS 41
6.1 Sub-Gigahertz Prediction Models Compared 41
6.1.1 Bullington [Bullington 47, 57, 77] 41
6.1.2 FCC (R-6406 & R-6602) [Carey 64] [Damelin 66] 41
6.1.3 Longley-Rice [Longley 68] [Hufford 79, 82, 85] 42
6.1.4 Okumura [Okumura 68] 43
6.1.5 TIREM [Frazier 83] 46
6.1.6 ITU-R (Rec P.452, 1238, 1411, 1546, & 1812) 46
6.1.7 Allsebrook & Parsons [Allsebrook 77] 48

6.1.8 Dadson,Durkin,Edwards (including JRC) [Edwards 69], [Dadson 75, 79], [Durkin 77] ... 48
6.1.9 CRC [Palmer 78, 79], [Whitteker 85a, 85b] ... 49
6.1.10 Blomquist & Laddell [Blomquist 74] ... 49
6.1.11 Egli [Egli 57] ... 49
6.1.12 3GPP Path Loss Models ... 49
6.1.13 3GPP Path Loss Models for Device-to-Device Applications ... 50
6.1.14 Air-to-Ground Path Loss Models ... 50
6.2 Comparison of Shadow Loss Calculation Algorithms ... 50
6.2.1 Bullington Shadow Loss Model ... 51
6.2.2 Delta-Bullington Shadow Loss Model ... 52
6.2.3 Epstein-Peterson Shadow Loss Model ... 53
6.2.4 EBU Shadow Loss Model ... 53
6.2.5 Deygout Shadow Loss Model ... 53
6.2.6 Edwards-Durkin Shadow Loss Model ... 54
6.2.7 López Shadow Loss Model [López 84] ... 55
6.2.8 Other Shadow Loss Models ... 55
6.2.9 Shadow Loss Modeling with the 3GPP Path Loss Models ... 55
6.2.10 Shadow Loss Modeling with the 3GPP Path Loss Models for Device-to-Device Applications ... 56
6.3 Comparisons of Small-Scale Prediction Methods ... 56
6.3.1 Probability distributions commonly used to characterize signal variations 56
6.3.2 Channel modeling ... 57
6.3.3 Delay Profiles & Delay Spread ... 57
6.4 Adjustments to R-6602 calculations ... 59
6.4.1 Terrain Roughness ... 59
6.4.2 Short Paths ... 60
6.4.3 Low HAATs ... 61
6.4.4 High HAATs ... 61
6.4.5 Number of Radials ... 62
6.4.6 Database Resolution ... 62
6.4.7 Contour Representation ... 63
6.5 Contour Calculations ... 63
6.5.1 Background ... 63
6.5.2 Basis ... 63
6.5.3 Frequency Assignment Criteria ... 63
6.6 HAAT Calculation ... 66
6.6.1 Terrain Database ... 67
6.6.2 HAAT DEFINITION ... 68
6.7 Terrain Elevation Dataset ... 68
6.7.1 Establishing Terrain Elevation Points Along a Profile Using the Terrain Dataset ... 70
6.8 Local Clutter Loss Attenuation Standard Values ... 71
6.8.1 Classification Values ... 71
6.8.2 NLCD Re-sampling ... 75
6.8.3 Clutter Loss Measurement in a Mobile Environment ... 76

6.9 Propagation Modeling and Simulation Benchmarks 78
6.10 Recommendations Concerning Tiled vs. Radial Metaphors 79
6.10.1 Radial Method 79
6.10.2 Stepped Radial Method 79
6.10.3 Grid Mapped from Radial Data Method 79
6.10.4 Tiled Method 80
6.10.5 Discussion of Methods 80
6.10.6 Summary and Recommendations 81
6.11 Reliability Prediction 82
6.12 Interference Calculations 83
6.12.1 Equivalent Interferer Method 84
6.12.2 Monte Carlo Simulation Method 87
6.12.3 Alternative Methods 88
6.13 Building Losses 89

7. SITE DIVERSITY 92

7.1 Aperture Gain 92
7.2 Fading Gain 93
7.3 Fading Gain Conclusions 96
7.4 Antenna Configurations 96
7.5 Horizontal Separation 97
7.5.1. Tall Towers 98
7.5.2. Shorter Towers on High HAAT Sites 98
7.5.3. Building Tops 98
7.5.4. Low HAAT Sites 98
7.6 Radius of Local Scatterers 99
7.7 Combiner Types 99
7.7.1 Selective Combiner 99
7.7.2 Equal Gain Combiner 99
7.7.3 Maximal-ratio Combiner 100
7.8 Theoretical Gain 100
7.8.1 Measured Comparisons 101
7.8.2 Rayleigh vs. Rician fading distributions 104
7.9 System imbalances effect on Gain 105
7.10 Macro-Diversity (Voting) 106
7.11 Summary 106

BIBLIOGRAPHY 107

TABLE OF FIGURES

Figure 1 - Amplifier Intermodulation Performance Specifications 30
Figure 2 - Noise Figure Calculation 31
Figure 3 - Symbolic Method 32
Figure 4 - Multicoupler IMR Performance Example 34
Figure 5 - Receiver Multicoupler 36
Figure 6 - Adding Non-Coherent Powers 37
Figure 7 - Determine Unknown Power from Sum and One Value 38
Figure 8 – Bullington Construction 52
Figure 9 – Epstein – Peterson Construction 53
Figure 10 – Deygout Construction 54
Figure 11 – Edwards – Durkin Construction 54
Figure 12 – López Construction 55
Figure 13 Typical Delay Profile 57
Figure 14 -Terrain Roughness Correction 59
Figure 15 -Definition of Terrain Roughness 60
Figure 16 - Probability of Interference vs. Mean C/I 66
Figure 17 - Radial Crossings in a 2-Site System 81
Figure 18 - Tile Reliability, No Uncertainty Margin 83
Figure 19 - Generalized Medium Building Penetration Loss 91
Figure 20 - Standard Deviation, Generalized Medium Buildings 91
Figure 21 Model of Cross-correlation Factors 93
Figure 22 Cross-correlation Example 94
Figure 23 Estimated Diversity Gain 95
Figure 24 Fading Gain Example 96
Figure 25 Cross-correlation vs. Arrival Angle 97
Figure 26 Theoretical Diversity Gain for Maximal-ratio combining, ... 101
Figure 27 Full Rayleigh Fading 102
Figure 28 Rayleigh Faded, Medium Cross-correlation 103
Figure 29 Rician Fading 104
Figure 30 Rayleigh vs. Rician Fading 105

TABLE OF TABLES

Table 1- Noise Considerations ... 15
Table 2- Recommended Environmental Noise Values (dB) LULC Categories at 162 MHz ... 16
Table 3 - Recommended Environmental Noise Values (dB) NLCD-92 Categories at 162 MHz ... 17
Table 4 - Recommended Environmental Noise Values (dB) NLCD-01/06 Categories at 162 MHz ... 18
Table 5 - Comparison of Land Cover Classifications ... 19
Table 6 - Adding Non-Coherent Powers ... 37
Table 7 - Determine Unknown Power from Sum and One Value ... 39
Table 8 - Characteristics of the Okumura "Family" of Algorithms ... 45
Table 9 - ITU-R Propagation Algorithms ... 47
Table 10 - Summary of Air Ground Models ... 50
Table 11 - Recommended Field Strength in dB/µV for 10,000 feet HAAT ... 62
Table 12 – Recommended Modified PSA Co-channel Values ... 64
Table 13 - Interaction Between Shared and PSA Users ... 64
Table 14 - Probability of Interference ... 65
Table 15 - Re-Classification of USGS NLCD-01, NLCD-06, and NLCD-11 Classes ... 72
Table 16 - Re-Classification of USGS National Land Cover Dataset (NLCD92) Codes ... 73
Table 17 - Reclassification of General Ground Cover Categories ... 74
Table 18 - Local Clutter Attenuation in dB as a Function of Frequency and Land Use Classification ... 75
Table 19 - NLCD Re-sampling Weights ... 76
Table 20 - Tile Reliability Margins ... 82

DOCUMENT REVISION HISTORY

Version	Date	Description
TSB-88 Issue O	January 1998	Original Release
TSB-88 Issue O-1	December 1998	Added Annex F
TSB-88 Issue A	June 1999	Added Information and moved many tables from Annexes into the main body.
TSB-88 Issue A-1	January 2002	Added Annexes G & H and Corrigenda
TSB-88 Issue B	September 2004	Consolidated Annexes F, G & H into document. Updated the ACCPR modulations and methodology, ACCPR tables moved to Annex A. Modified building loss section. Added new terrain data base information and new NLCD information. Numerous editing changes and examples added. A CD with spreadsheets for each modulation is now included in a new Annex F.
TSB-88.2 Issue C	April 2009	Split TSB-88 into three documents. Replaced the VHF/low UHF propagation model Added NLCD-01 and removed LULC for clutter loss Added NLCD-01 and removed LULC for noise Added material on Land Clutter loss and noise measurement Added discussion of space diversity Updated clutter losses for Agricultural land cover categories Added material on the use of directional antennas
TSB-88.2 Issue D	June 2012	Replaced the recommended propagation prediction model with a general discussion of models applicable to land mobile radio in the VHF and low UHF ranges. Updated the discussions of the land cover and elevation datasets.
TSB-88.2 Issue E		Revised Foreword, Introduction, and Scope Added new shadow loss method Added discussion of building loss with Low-E glass Added references to new NLCD-11 Inserted new §6.3 on short range statistics and re-numbered old §6.3 and succeeding clauses. Revised §§6.9, 6.11 and 6.12 (new numbering) for compatibility with broadband. Inserted new §§6.1.12,13,14 on 3GPP path loss methods and 6.2.8,9 on 3GPP shadow loss modeling.

FOREWORD
(This foreword is not part of this bulletin.)

Working Group WG-8.18.2 prepared this document. Subcommittee TR-8.18 of TIA Engineering Committee TR-8 approved this document.

Changes in technology, narrowbanding some existing frequency bands have recently occurred. In addition, increased reporting of interference continues. These events support keeping this document current and that it provide the methodology of modeling the various interference mechanisms to support frequency coordinators in determining the best assignments to be made for the available pool of frequencies and mixtures of technology.

This document, Wireless Communications Systems --- Performance in Noise- and Interference- Limited Situations --- Part 2: Propagation & Noise, includes a Bibliography, but no Annexes nor other supplementary material.

This is Part 2, Revision E of this Bulletin and it supersedes TSB-88.2-D. Other parts of this Bulletin cover the following areas:

- Part 1: Performance Modeling
- Part 2: Propagation Modeling, including Noise
- Part 3: Performance Verification
- Part 4: Broadband Performance Modeling[2]
- Part 5: Broadband Performance Validation[2]

Patent Identification

The reader's attention is called to the possibility that using this document may necessitate the use of one or more inventions covered by patent rights. By publication of this document no position is taken with respect to the validity of those claims or any patent rights in connection therewith. The patent holders so far identified have, we believe, filed statements of willingness to grant licenses under those rights on reasonable and nondiscriminatory terms and conditions to applicants desiring to obtain such licenses.

The following patent holders and patents have been identified in accordance with the TIA intellectual property rights policy:

– None identified

TIA is not be responsible for identifying patents for which licenses might be referenced by this document or for conducting inquiries into the legal validity or scope of those patents that are brought to its attention.

INTRODUCTION

The TSB-88 series of documents is intended to address the following issues:

- Addressing migration and spectrum management issues involved in the transition either to narrowband/bandwidth efficient digital and analog technologies or to broadband technologies. Provide information on new and emerging Land Mobile bands;

- Assessing and quantifying the interference impact between narrowband technologies and broadband technologies;

- Address the methodology of minimizing system interference between current or proposed Noise Limited Systems in spectral and spatial proximity to current or proposed Interference Limited Systems;

- Assessing and quantifying the impact of new narrowband/bandwidth efficient digital and analog technologies on existing analog and digital technologies; Address the methodology to minimize intersystem interference between systems at national boundaries;

- Accommodating the design and frequency coordination of bandwidth-efficient narrowband technologies likely to be deployed as a result of the Federal Communications Commission “Spectrum Refarming” efforts; and

- Accommodating the design and frequency coordination of broadband technologies to be deployed in support of FirstNet’s nationwide interoperable broadband public safety network;

The TSB-88 series of documents was prepared partially in response to specific requests from three particular user organizations: the Association of Public Safety Communications Officials, International (APCO), the Land Mobile Communications Council (LMCC) and the National Coordination Committee (NCC). In 2003, the National Public Safety Telecommunications Council (NPSTC) assumed the reponsibilites of NCC[1]

This document TSB-88.2-E is intended to address propagation and noise issues within the context described above.

[1]NPSTC's Broadband Requirements Report "Defining Public Safety Grade Systems and Facilities" describes best practices for coverage modeling based on recommendations from TSB-88 [NPSTC 14].

[BLANK PAGE]

Wireless Communications Systems – Performance in Noise and Interference-Limited Situations – Part 2: Propagation and Noise

1. SCOPE

1.1 The TSB-88 Series

The TSB-88 series of bulletins gives guidance on the following areas:

- Establishment of standardized methodology for modeling and simulating either narrowband/bandwidth efficient technologies or broadband technologies;
- Establishment of a standardized methodology for empirically confirming the performance of either narrowband/bandwidth efficient systems or broadband systems;
- Aggregating the modeling, simulation and empirical performance verification reports into a unified "Spectrum Management Tool Kit" which can be employed by frequency coordinators, systems engineers, software developers, and system operators;
- Recommended databases that are available for improved results from modeling and simulation; and
- Providing current information for new and emerging bands.

The purpose of these documents is to define and advance a scientifically sound standardized methodology for addressing technology compatibility. This document provides a formal structure and quantitative technical parameters from which automated design and spectrum management tools can be developed based on proposed configurations that can temporarily exist during a migration process or for longer term solutions for systems that have different technologies.

As wireless communications systems evolve, the complexity in determining compatibility between different types of modulation, different operational geographic areas, and application usage increases.

Spectrum managers, system designers and system maintainers have a common interest in utilizing the most accurate and repeatable modeling and simulation capabilities to determine likely wireless communication system performance. A standardized approach and methodology is needed for the modeling and simulation of wireless communications system performance, considering both analog and digital practices in all frequency bands of interest.

In addition, subsequent to wireless communications system implementation, validity or acceptance testing is often an issue subject to much debate and uncertainty. Long after a system is in place and optimized, future interference dispute resolution demands application of a unified quantitative methodology for assessing system performance and interference.

These documents also provide a standardized definition and methodology to a process for determining when various wireless communications configurations are compatible. The document contains performance recommendations for public safety and non-public safety type systems that are recommended for use in the modeling and simulation of these systems. These documents also satisfy the desire for a standardized empirical measurement methodology that is useful for routine proof-of-performance and acceptance testing and in dispute resolution of interference cases.

To provide this utility necessitates that specific manufacturers define various performance criteria for the different modulations and their specific implementations. Furthermore, sufficient reference information is provided so that software applications can be developed and employed to determine if the desired system performance can be realized.

Wireless system performance can be modeled and simulated with the effects of single or multiple potential distortion sources taken into account. These sources include:

- Performance parameters
- Co-channel users
- Off-channel users
- Internal noise sources
- External noise sources
- Equipment non-linearity
- Transmission path geometry
- Delay spread and differential signal phase
- Over the air and network protocols
- Performance verification methods

Predictions of system performance can then be based on the desired RF carrier versus the combined effects of single or multiple performance degrading sources. Performance is then based on a faded environment to more accurately simulate actual usage and considers both signal magnitude and phase attributes.

It is anticipated that this series of documents will serve as the standard reference for developers and suppliers of land mobile communications system design, modeling, simulation and spectrum management software and automated tools.

1.2 TSB-88.2-E

This document, Part 2 of TSB-88, addresses propagation and noise issues within the context described in §1.1, above.

2. REFERENCES

This Telecommunications System Bulletin contains informative information. There may be references to other TIA standards which contain normative elements. These references are primarily to indicate the methods of measurement contained in those documents. At the time of publication, the edition indicated was valid. All standards are subject to revision, and parties to agreements based on this document are encouraged to investigate the possibility of applying the most recent edition of the standard indicated in Section 3. ANSI and TIA maintain registers of currently valid national standards published by them.

3. DEFINITIONS AND ABBREVIATIONS

There is a comprehensive Glossary of Terms, Acronyms, and Abbreviations listed in Annex-A of TIA TSB-102. In spite of its size, numerous unforeseen terms still might have to be defined for the compatibility aspects. Additional TIA references will also be included as applicable. Items being specifically defined for the purpose of this document are indicated as (New). All others will be referenced to their source as follows:

ANSI/IEEE 100-2000 Standard Dictionary	[IEEE]
Recommendation ITU-R P.1407-4	[ITU3]
TIA-845-B	[845]
TSB-88.1-D	[88.1]
TSB-88.3-D	[88.3]
TSB-88.4[2]	[88.4]

The preceding documents are referenced in this bulletin. At the time of publication, the editions indicated were valid. All such documents are subject to revision, and parties to agreements based on this document are encouraged to investigate the possibility of applying the most recent editions of the standards indicated below:

3.1 Definitions

For the purposes of this document, the following definitions apply:

ACCPR Adjacent Channel Coupled Power Ratio: The ratio of the average power of a transmitter under prescribed conditions and moduation to the energy coupled into a victim receiver. The selectivity of the victims receiver, the offset frequency and the Spectral Power Density of the interfering carrier interact to calculate this parameter. ACCPR = 1/ACCP

ACP Adjacent Channel Power: The energy from an adjacent channel transmitter that is intercepted by prescribed bandwith, relative to the power of the emitter. Regulatory rules determine the measurement bandwidth and offset for the adjacent channel. ACP = 1/ ACPR

Adjacent Channel: The RF channel assigned adjacent to the licensed channel. The difference in frequency is determined by the channel bandwidth.

[2] Editor's Note: *The above document is a work in progress and should not be referenced unless and until it is approved and published. Until such time as this Editor's Note is removed, the inclusion of the above document is for informational purposes only.*

Aperture Gain: Diversity Gain (*q.v.*) resulting solely from effects similar to the addition of phased antenna elements resulting in co-phased signal power adding, and ignoring any effects due to de-correlation of signals at the respective antennas.

"Area" Propagation Model: A model that predicts power levels based upon averaged characteristics of the general area, rather than upon the characteristics of individual path profiles. *Cf:* Point-to-point Model.

Beyond Necessary Band Emissions (BNBE): All unwanted emissions outside the necessary bandwidth. This differs from OOBE (*q.v.*) in that it includes spurious emissions.

Boltzmann's Constant (k): A value 1.3805x 10^{-23} J/K (Joules per Kelvin). Room temperature, T, is typically taken as 290 K.

Broadside: An arrangement of antennas or antenna elements whereby the radiation or reception location is perpendicular to the plane of the elements. *Cf:* End-fire.

Co-Channel: Another licensee, potential interferer, on the same center frequency.

Confidence Interval: A statistical term where a confidence level is stated for the probability of the true value of something being within a given range which is the interval.

Confidence Level: also called Confidence Coefficient or Degree of Confidence, the probability that the true value lies within the Confidence Interval.

Correlation: The strength of the relationship between two random variables, represented by a single number called the *correlation coefficient*.

Cross-correlation: The correlation between two different random variables, as opposed to the correlation between a variable and itself offset by a given time interval, which is called the *autocorrelation*.

Channel Performance Criterion [CPC]: The CPC is the specified design performance level in a faded channel.

Delivered Audio Quality (DAQ): The acronym for Delivered Audio Quality, a reference similar to Circuit Merit with additional definitions for digitized voice and a static SINAD equivalent intelligibility when subjected to multipath fading.

Delay Spread [ITU3]: The power-weighted standard deviation of the excess delays, given by the first moment of the impulse response.

Dipole: A half wave dipole is the standard reference for fixed station antennas. The gain is relative to a half wave dipole and is expressed in dBd.

Directional Height Above Average Terrain (DHAAT): The Height Above Average Terrain within a defined angular boundary. Used for determining co-channel site separations by the FCC

Diversity Gain: The total effective gain relative to a non diversity system for the same level of performance due to all diversity-related effects.

Diversity Reception: The technique of receiving systems incorporating multiple antennas or sites to improve signal capture.

End-fire: An arrangement of antennas or antenna elements whereby the radiation or reception location is in-line with the elements. *Cf:* Broadside.

Equivalent Noise Bandwidth (ENBW): The frequency span of an ideal filter whose area equals the area under the actual power transfer function curve and whose gain equals the peak gain of the actual power transfer function. In many cases, this value can be close to the 3-dB bandwidth. However, there exist situations where the use of the 3-dB bandwidth can lead to erroneous results.

Estuarine: Pertaining to a water passage where the tide meets a river current. *Cf:* Palustrine.

Faded Reference Sensitivity [102.CAAA]: The faded reference sensitivity is the level of receiver input signal at a specified frequency with specified modulation which, when applied through a faded channel simulator, results in the standard BER at the receiver detector.

Fading Gain: The portion of the Diversity Gain (*q.v.*) related to fading reduction due to the capture of uncorrelated copies of the same signal.

Fading Penalty: The difference in C/N between a static signal level and a fading signal level needed for the same level of performance

Height Above Average Terrain (HAAT): The height of the radiating antenna center above the average terrain that is determined by averaging equally spaced data points along radials from the site or the tile equivalents. Average only that portion of the radial between 3 and 16 km inclusive.

Inferred Noise Floor: The noise floor of a receiver calculated when the Reference Sensitivity is reduced by the static C_s/N necessary for the Reference Sensitivity. This is equivalent to kTB + Noise Figure of the receiver.

Isotropic: An isotropic radiator is an idealized model where its energy is uniformly distributed over a sphere. Microwave point-to-point antennas are normally referenced to dBi.

Macro Diversity: Commonly used as "voting", where sites separated by large distances are compared and the best is "voted" to be the one selected for further use by the system. *Cf:* Micro Diversity

Measurement Error: The variability of measurements due to the measuring equipment's accuracy and stability.

Micro-diversity: Diversity reception accomplished through the placement of antennas on a single site, with diversity processing typically taking place pre-detection. *Cf:* Macro Diversity

National Elevation Dataset (NED): An elevation dataset with 30-meter horizontal resolution. It is available from the USGS. For more information see http://nationalmap.gov/elevation.html .

Noise Limited: The case where the CPC is dominated by the Noise component of C/(I+N).

Palustrine: Pertaining to inland wetlands lacking flowing water and containing ocean-derived salts in low concentrations. *Cf:* Estuarine.

Point-to-Point Model: A model that uses path profile data to predict path loss between points. Cf: "Area" propagation model.

Power Loss Exponent: The exponent of range (or distance from a signal source) that calculates the decrease in received signal power as a function of distance from a signal source, e.g. the received signal power is proportional to transmitted signal power time r^{-n} where r is the range and n is the power loss exponent.

Propagation Loss: The path loss between transmit and receive antennas. The loss is in dB and does not include the gain or pattern of the antennas.

Protected Service Area (PSA): That portion of a licensee's service area or zone that is to be afforded protection to a given reliability level from co-channel and off-channel interference and is based on predetermined service contours.

Radius of Local Scatterers: A term used to describe the distance between the mobile and its most significant scatterers. Its value in m can be estimated by dividing the rms delay spread in ns by 3.33564 ns/m.

Reference Sensitivity [102.CAAA]: An arbitrary signal strength value used in receiver C/N calculations. A given value Reference Sensitivity doesn't specifically relate to a defined audio quality or other measurement value. If its corresponding value of C_s/N is known, an inferred noise floor can be determined.

Rician Fading: Formally, signal fading that follows a Nakagami-Rice distribution [Rice 59] [Rice 67]. As used herein, the Rician distribution that includes a substantial fixed vector in addition to the Rayleigh-distributed (scattered) vector typical of line-of-sight paths.

Service Area: A specific user's geographic bounded area of concern. Usually a political boundary such as a city limit, county line or similar definition for the users business. Can be defined relative to site coordinates or an irregular polygon where points are defined by latitude and longitude.

Signal to Interference plus Noise Ratio (SINR): This term is the same as $C_f/(I+N)$, except the latter term makes it explicit that the carrier is faded.

SINAD: SINAD is a test bench measurement used to compare analog receiver performance specifications, normally at very low signal power levels, e.g., 12 dB SINAD for reference sensitivity. It is defined as:

$$SINAD(dB) = 20\log_{10}[\frac{Signal + Noise + Distortion}{Noise + Distortion}]$$

where: Signal = Wanted audio frequency signal voltage due to standard test modulation. Noise = Noise voltage with standard test modulation. Distortion = Distortion voltage with standard test modulation.

Simulcast: In a land mobile radio system, a technique in which identical baseband information is transmitted from multiple sites operating on the same assigned frequency. Quasi-synchronous transmission.

Site Isolation: The antenna port to antenna port loss in dB for receivers close to a given site. It includes the propagation loss as well as the losses due to the specific antenna gains and patterns involved.

Spectral Power Density (SPD) [IEEE]: The power density per unit bandwidth.

Standard Deviate Unit (SDU): Also "Standard Normal Deviate." That upper limit of a truncated normal (Gaussian) curve with zero mean and infinite lower limit which produces a given area under the curve (e.g., Z = +1.645 for Area =0.95).

Surplus Gain: The sum of all gains and losses from the input of the first amplified stage until the input to the base receiver.

Tile Reliability: The tile reliability is the probability that the received local median signal strength predicted at any location with a given tile equals or exceeds the desired CPC margin. See [88.1] §5.3.4.

Tile Reliability Margin: The tile reliability margin, in dB, is the difference between the predicted value of $C_f/(I+N)$ and the desired value of $C_f/(I+N)$ for the CPC. See [88.1] §5.3.3.

Uncertainty Margin: An additional margin necessary due to measurement error.

Voting: The process of comparing received signals and selecting the instantaneous best value and incorporating it into the system. [See also macro diversity.]

3.2 Abbreviations

ACP	Adjacent Channel Power
ACPR	Adjacent Channel Power Ratio
ACR	Adjacent Channel Rejection
ACRR	Adjacent Channel Rejection Ratio
ANSI	American National Standards Institute
APCO	Association of Public Safety Communications Officials International, Inc.
BAPC	Bounded Area Percent Coverage
BDA	Bi-Directional Amplifier
BNBE	Beyond Necessary Band Emissions.
C4FM	4-ary FM QPSK-C; Compatible Four-Level Frequency Modulation
CCIR	International Radio Consultative Committee (Now ITU-R)
$C_f/(I+N)$	Faded Carrier to Interference plus Noise ratio
C_f/N	Faded Carrier to Noise ratio
C/I	Carrier to Interference signal ratio
CPC	Channel Performance Criterion
CQPSK	AM QPSK-C; Compatible Quadrature Phase Shift Keying
C_s/N	Static Carrier to Noise ratio
CSPM	Communications System Performance Model
CTG	Composite Theme Grids
DAQ	Delivered Audio Quality
dBd	Decibels relative to a half wave dipole
dBqw	Decibels relative to a quarter wave antenna
dBi	Decibels relative to an isotropic radiator
dBm	Power in decibels referenced to 1 milliWatt
dBμ	Decibels referenced to 1 microvolt per meter (1 μV/m)
dBS	SINAD value expressed in decibels
DEM	Digital Elevation Model
DHAAT	Directional Height Above Average Terrain
DIMRS	Digital Integrated Mobile Radio Service
DLCD	Digital Land Coverage Dataset

DMA	Defense Mapping Agency (former name of NGIA, National Geospatial Intelligence Agency)
E_b / N_0	Energy per bit divided by the noise power in one Hertz bandwidth
EMG	Effective Multicoupler Gain
ENBW	Equivalent Noise Bandwidth
erf	Error Function
erfc	Complementary Error Function *(erfc x = 1 - erf x)*
ERP_d	Effective Radiated Power, relative to a $\lambda/2$ dipole
F4FM	Filtered 4-ary FM, not compatible with C4FM
FPT	Faded Performance Threshold
HAAT	Height above Average Terrain
HAGL	Height above Ground Level
IMBE	Improved Multi-Band Excitation
ITU-R	International Telecommunication Union Radiocommunication Sector
LM	Linear Modulation
LOS	Line of Sight
LULC	Land Usage/Land Cover
MOS	Mean Opinion Score
N/A	Not Applicable
NED	National Elevation Dataset
NF	Noise Factor
NF_{db}	Noise Figure
NGDC	National Geophysical Data Center
NLCD	National Land Cover Dataset
NLOS	Non-Line-of-Sight
OOBE	Out-of-Band Emissions
PEC	Perfect Electrical Conductor
PSA	Protected Service Area
QPSK	Quadrature Phase-Shift Keying
QPSK-c	Quadrature Phase-Shift Keying - Compatible
RF	Radio Frequency
RSSI	Receiver Signal Strength Indication
SINAD	Signal plus Noise plus Distortion -to-Noise plus Distortion Ratio

SINR	Signal to Interference plus Noise Ratio (cf.: $C_f/(I+N)$)
SPD	Spectral Power Density
TBD	To Be Determined
TIREM	Terrain-Integrated Rough Earth Model
UHF	Ultra-High Frequency
USGS	United States Department of the Interior Geological Survey
UTM	Universal Transverse Mercator
VHF	Very High Frequency
Z	Standard Deviate Unit

4. TEST METHODS

A recommended test method is defined in the following subsection:

- §5.3 RF Noise Measurement Methodology

5. Noise

5.1 Environmental RF Noise

To determine effective receiver sensitivity, it is essential that the level of environmental noise be known. Note that it is seldom necessary to measure environmental noise in a mobile environment at frequencies higher than 400 MHz because it is rare for the total environmental noise to exceed *kTB*. A major exception to the foregoing statement is for frequencies near 866-869 MHz in which the mobile can experience noise generated by CMRS and A-band Carrier cell sites and when near the CMRS cell sites within the 851-861 MHz portion of the band that utilize frequencies interleaved with other licensees. Table 1 summarizes this recommendation.

Table 1- Noise Considerations

Frequency Range	Environment	Action
All	Fixed (site)	Consider Noise
< 400 MHz	Mobile	Consider Noise
between 866-869 MHz	Mobile	Consider Noise
≥ 400 MHz, but not near CMRS or A block Cellular sites	Mobile	Noise rarely an issue

5.2 Environmental RF Noise Data

5.2.1 Measurements Referenced to Land Cover Categories

Measurements [Rubinstein 98] have been made which correlate RF environmental noise levels with USGS Land Use Land Clutter (LULC) [Anderson 76] categories at 162 MHz . These measurements ought to be useful in system design over the entire VHF land mobile band (138 - 174 MHz). Of the 37 LULC categories, Table 2 contains data for 14 categories.

Further analysis has correlated a subset of the aforementioned data to NLCD-92 [Vogelman 01] categories, again in the 138-174 MHz band. Those results are shown in Table 3. Further analysis has correlated a different subset of the aforementioned data to the NLCD-01 [USGS 07] categories in the 138-174 MHz band (Table 4). Note that the NLCD-06 [USGS 11] and NLCD-11 [Homer 15] data use the NLCD-01 categories. Because of the different categorization schemes, where the newer schemes sometimes overlapped older ones and sometimes contained portions of more than one older one, the number of categories of the newer schemes that could be correlated to the data based on the LULC categories was smaller than the original number of LULC categories.

Table 2- Recommended Environmental Noise Values (dB) LULC Categories at 162 MHz

LULC Category	Major Metro			Medium Metro			Rural		
	dB_{kTB}	Rel	dBm_{1kHz}	dB_{kTB}	Rel	dBm_{1kHz}	dB_{kTB}	Rel	dBm_{1kHz}
11	15.6	36.3	-128.4	12.6	18.2	-131.4	12.1	16.2	-131.9
12	15.8	38.0	-128.2	12.8	19.1	-131.2			
13	16.1	40.7	-127.9						
14	14.6	28.8	-129.4						
16	15.3	33.9	-128.7						
17	16.4	43.7	-127.6				13.0	20.0	-131.0
21	13.6	22.9	-130.4				12.1	16.2	-131.9
22	13.1	20.4	-130.9						
23	13.6	22.9	-130.4						
24							12.7	18.6	-131.3
32	16.9	49.0	-127.1						
41							11.7	14.8	-132.3
43				12.3	17.0	-131.7	11.6	14.5	-132.4
76	16.8	47.9	-127.2						

dB_{kTB} ≡ decibels relative to kTB

Rel ≡ the ratio of the noise power to kTB. Multiply this value by 290 to calculate noise temperature.

dBm_{1kHz} ≡ dBm for a bandwidth of 1 kHz. To calculate the noise power in dBm for a particular bandwidth, add $10 \times \log_{10}(ENBW_{kHz})$ to the Table value

If the proposed system is not covered by (i.e., it is not at VHF high band or its category/development level combination is not in the table), use the information in §5.2.2 to calculate the environmental noise level. However, caution is recommended in applying §5.2.2, because the results indicate that noise levels have been increasing over the years since the Spaulding & Disney measurements were made.

Table 3 - Recommended Environmental Noise Values (dB) NLCD-92 Categories at 162 MHz

NLCD-92 Category)	Major Metro			Medium Metro		
	dB_{kTB}	Rel	dBm_{1kHz}	dB_{kTB}	Rel	dBm_{1kHz}
21	17.7	58.9	-128.3	12.7	18.6	-131.3
22	17.6	57.5	-128.4	12.6	18.2	-131.4
23	16.0	39.8	-128.0	12.6	18.2	-131.4
31	16.6	45.7	-127.4			-
41				12.7	18.6	-131.3
42	17.6	57.5	-128.4	12.8	19.1	-131.2
43	17.6	57.5	-128.4	12.8	19.1	-131.2
51	17.7	58.9	-128.3			
71	17.1	51.3	-128.9			
82	12.7	18.6	-131.3			
85	15.0	31.6	-129.0			

dB_{kTB} ≡ decibels relative to kTB

Rel ≡ The ratio of the noise power to kTB. Multiply this value by 290 to calculate noise temperature.

dBm_{1kHz} ≡ dBm for a bandwidth of 1 kHz. To calculate the noise power in dBm for a particular bandwidth, add $10 \times \log_{10}(ENBW_{kHz})$ to the Table value.

If the proposed system is not covered by Table 3 (i.e., it is not at VHF high band or its category/development level combination is not in the table), use the information in §5.2.2 to calculate the environmental noise level. However, caution is recommended in applying §5.2.2, because the results indicate that noise levels have been increasing over the years since the Spaulding & Disney measurements were made.

Table 4 - Recommended Environmental Noise Values (dB) NLCD-01/06 Categories at 162 MHz

NLCD-01/06/11 Category (Table 15	Major Metro			Medium Metro			Rural		
	dB_{kTB}	Rel	dBm_{1kHz}	dB_{kTb}	Rel	dBm_{1kHz}	dB_{kTb}	Rel	dBm_{1kHz}
22	15.6	36.3	-128.4	12.6	18.2	-131.4	12.1	16.2	-131.9
23	16.1	40.7	-127.9	12.8	19.1	-131.2			
41							11.7	14.8	-132.3
43				12.3	17.0	-131.7	11.6	14.5	-132.4
52	16.9	49.0	-127.1						
81	13.6	22.9	-130.4				12.1	16.2	-131.9
82	13.1	20.4	-130.9						

dB_{kTB} ≡ decibels relative to kTB

Rel ≡ the ratio of the noise power to kTB. Multiply this value by 290 to calculate noise temperature.

dBm_{1kHz} ≡ dBm for a bandwidth of 1 kHz. To calculate the noise power in dBm for a particular bandwidth, add $10 \times \log_{10}(ENBW_{kHz})$ to the Table value

If the proposed system is not covered by Table 4 (i.e. it is not at VHF high band or its category/development level combination is not in the table), use the information in §5.2.2 to calculate the environmental noise level. However, caution is recommended in applying §5.2.2, because the results indicate that noise levels have been increasing over the years since the Spaulding & Disney measurements were made.

Table 5 - Comparison of Land Cover Classifications

Scheme Data Year	Land Use Land Cover (LULC) 1972 - 1983	National Land Cover Dataset (NLCD) 1992	National Land Cover Dataset (NLCD) 2001/2006/2011
Class			
11	Residential	Open Water	Open Water
12	Commercial & Services	Perennial Ice / Snow	Perennial Ice / Snow
13	Industrial		
14	Transport, Comm, Utilities		
15	Industrial & Comm'l Complexes		
16	Mixed Urban or Built-up		
17	Other Urban or Built-up		
21	Cropland & Pasture	Low Intensity Residential	Developed, Open Space
22	Orchards, Groves, Vinyards	High Intensity Residential	Developed, Low Intensity
23	Confined Feeding Operations	Commercial / Industrial / Transport	Developed, Medium Intensity
24	Other Agricultural Land		Developed, High Intensity
31	Herbaceous Rangeland	Bare Rock/Sand/Clay	Barren Land
32	Shrub & Brush Rangeland	Quarries/Strip Mines/Gravel Pits	Unconsolidated Shore
33	Mixed Rangeland	Transitional	
41	Deciduous Forest	Deciduous Forest	Deciduous Forest
42	Evergreen Forest	Evergreen Forest	Evergreen Forest
43	Mixed Forest	Mixed Forest	Mixed Forest
51	Streams & Canals	Shrubland	Dwarf Scrub
52	Lakes		Shrub / Scrub
53	Reservoirs		
54	Bays & Estuaries		
61	Forested Wetland	Orchards/Vineyards/Other	
62	Nonforested Wetland		
71	Dry Salt Flats	Grasslands/Herbaceous	Grasslands/Herbaceous
72	Beaches		Sedge/Herbaceous
73	Sandy Areas except Beaches		Lichens
74	Bare Exposed Rock		Moss
75	Strip Mines/Quarries/Gravel Pits		
76	Transitional Areas		
77	Mixed Barren Land		

Table 5 (concluded)

Scheme Data Year	Land Use Land Cover (LULC) 1972 - 1983	National Land Cover Dataset (NLCD) 1992	National Land Cover Dataset (NLCD) 2001/2006/2011
81	Shrub & Brush Tundra	Pasture/Hay	Pasture/Hay
82	Herbaceous Tundra	Row Crops	Cultivated Crops
83	Bare Ground Tundra	Small Grains	
84	Wet Tundra	Fallow	
85	Mixed Tundra	Urban/Recreation Grasses	
90			Woody Wetlands
91	Perennial Snowfields	Woody Wetlands	Palustrine Forested Wetland
92	Glaciers	Emergent Herbaceous Wetlands	Palustrine Shrub/Scrub Wetland
93			Estuarine Forested Wetland
94			Estuarine Scrub/Shrub Wetland
95			Emergent Herbaceous Wetland
96			Palustrine Emergent Wetland
97			Estuarine Emergent Wetland
98			Palustrine Aquatic Bed
99			Estuarine Aquatic Bed

5.2.2 Historical RF Noise Data

Many investigators have conducted noise measurements. One representative noise survey was that of Spaulding and Disney [Spaulding 74]. Their work resulted in the following RF noise equation:

$$N_r = 52 - 29.5 \log_{10} f_{MHz} \quad \text{dB} \qquad (\text{Relative to } kTB) \qquad (1)$$

Where: N_r is the “quiet rural” noise level relative to kTB.

They also arrived at the following corrections for environments other than “quiet rural” to be added to N_r:

Rural: 15 dB Residential: 18 dB Business: 25 dB

The total cannot be less than 0 dB (relative to *kTB*).

Environmental noise is highly variable even within the same environment and the only certain means of determining the level of environmental noise (and thus the effective sensitivity) is to conduct a noise measurement program.

5.3 RF Noise Measurement Methodology

5.3.1 Receiver Selection

The preferred tool for making a noise measurement is a receiver designed specifically for that purpose.

A communications receiver can also be used for making noise measurements. Although they do not have the many features provided by a measuring receiver, they are adequate for the job when properly applied and do have a small number of advantages over measuring receivers, including low cost and having the exact bandwidth that is needed for the given application.

If a communications receiver is to be used, consider adding a low noise preamplifier to increase the measurable range in the low signal power region. Without the addition of the low noise preamplifier, noise that is below the communication receiver’s internal noise level might not be measurable and yet this noise level might degrade the performance of the target system. Care is recommended when adding the low noise preamplifier since the additional gain can produce elevated intermodulation products that could, distort the measurements.

5.3.2 Antenna Selection

Since noise originates from all directions, an argument can be made for measuring noise by using an antenna that is sensitive in all directions; i.e., one with an isotropic pattern. In practice, specific types of antennas are used in land mobile communications and they typically have a great deal of vertical directivity and can also have horizontal directivity. To match the results to the hardware that a user might be deploying, it is recommended that the measurements be taken with the type of antenna that is used by the typical user.

Radio frequency noise is frequently expressed in terms of dB above the noise floor (*kTB*) or in terms of spectral power density (in units such as dBm/kHz). Using such terms rather than the received signal level has the advantage of making the measurement “portable” to receivers with any noise bandwidth. To do so, of course, it is necessary to know the following in addition to the received signal level: (a) the gain or loss of the antenna system (including cable and connector losses), and (b) the measuring receiver’s ENBW.

5.3.3 RF Noise Measurement in a Mobile Environment

Noise floor measurements are useful in determining a necessary baseline design signal strength while considering that the noise is not necessarily coming from the clutter objects themselves but from man-made sources within the suburban, urban and industrial areas.

5.3.3.1 Methodology

A typical receiver's sensitivity can be stated in terms of a carrier-to-noise value; e.g., a particular receiver might need a 7 dB C_s/N to produce the static reference sensitivity. Knowing the noise power at the frequency of interest at a given location and the values from Table A-1 in TSB-88.1 [TIA 12] allows the user to calculate the necessary signal level for the desired CPC in that environment.

A standard communications receiver can be used for the noise measurement. If the receiver's Received Signal Strength Indicator (RSSI) bus is considerably more sensitive than the sensitivity corresponding to the desired CPC, a preamplifier might not be necessary to extend the measurable range; otherwise, a low noise preamplifier can be connected between the antenna and the receiver. The receiver can now be calibrated. Connect a signal generator to the input of the preamplifier (or the receiver if no preamplifier is used). In the low signal range, use 1-decibel intervals. For each calibration point repeat measurement many ($\geq$ 30) times to ensure a valid reading. All of this could be automated by a data acquisition device/system. It is recommended that calibration be done in accordance with TSB-176 [TIA 09].

The actual readings are taken by driving around the evaluation area using a test setup to take readings in an automated fashion[3]. A typical test setup would consist of the antenna and receiver, a notebook computer, and an analog-to-digital (A/D) converter on a PCMCIA card. A more fully automated system could include Global Positioning System (GPS) or Differential Global Positioning System (DGPS) data to eliminate user interface for location information.

A computer program can be written to take the necessary readings subtract the effects of the antenna system, compare the results to the calibration curve, and note the results corresponding to a given location. This gives a noise power value, typically in dBm. To arrive at the noise level relative to *kTB*, one needs to know the Equivalent noise bandwidth. Knowing that, one merely subtracts *kTB* from the (already determined) noise power.[4] It is preferable to try to calculate the external noise when it is greater than or equal to the internal thermal noise. Since the thermal noise varies with time, values of external noise that are less than the thermal noise become more difficult to measure with reasonable

[3] TIA 845, *Radiowave Propagation – Path loss – Measurement, Validation and Presentation* [TIA 10] is recommended for data recording formats and processes.
[4] For use when bandwidth is expressed in kHz, the value of kT_0 is -144 dBm.

accuracy as the thermal noise contribution is dominant and varying. This is why a preamplifier configuration might be necessary so that the internal thermal noise is reduced.

After taking the data, the user can then establish noise contours for the area and frequency band of interest. With this information and the receiver's C_s/N performance for a given CPC, it is possible to establish the receiver's effective sensitivity on a geographic basis.

5.3.3.2 Associating Local Noise Measurements with Land Cover categories

The noise measurements that Table 2, Table 3, and Table 4 are based upon were taken in specific areas. While many of the values are based upon measurements [Rubinstein 98] that were taken in three different types of terrain (urban and suburban with sparse trees, suburban with dense trees, and forested rural), locally taken measurements are best for predicting those values over a wider, but still local, set of terrain. Where practical, it is recommended that noise measurements be taken over a local sample area. The values in Table 2, Table 3, and Table 4 provide a good estimate where such measurements are not practical.

To implement a local land cover survey, consider the following material:

a. Choose a Land Cover dataset to use in categorizing the data. If available in the area of interest, use NLCD-11 as it is the most up-to-date.

b. Based upon the Land Cover category data create a route that covers as many tiles containing each Land Cover Category of interest as possible. It is recommended that at least 30 tiles for each category be covered and that the test sample area be selected, insofar as is practical, such that each category is found in more than one portion of the sample area; i.e. not a single grouping. Note also that, because the shadow loss affecting measurements can vary greatly over small distances and is difficult to predict, measurements ought to be made only along unshadowed paths.

c. Make a noise power survey according to the principles described in §5.3.3.1 above and in TIA-845 [TIA 10].

d. Gather the data on a Category-by-Category basis. Plot the data for each category using box-and-whisker plots[5] [Hoaglin 83]. See sidebar box.

[5] While other methods of considering spread, skewness, and outliers of a dataset exist, the box-and-whisker plot is recommended because of its simplicity and intuitiveness.

Visually inspect the plots to determine whether the data is reliable[6]. If it is, use the median value in preference to the more general values in Table 2, Table 3, and Table 4.

[6] Indications of possible data unreliability include the following: (i) widely-spread inter-quartile range, (ii) greatly unbalanced 2nd vs. 3rd quartiles, (iii) large number of outliers.

Box-and-Whisker Plots

A box-and-whisker plot ("boxplot") is constructed as follows:

- A rectangle of random width is constructed, with the height scaled so that the top corresponds to the boundary between the third and fourth quartiles and the bottom corresponds to the boundary between the first and second quartiles.
- A line is drawn through the box, scaled to correspond to the median value.
- A line is extended upward from the center of the top of the rectangle, scaled so that it reaches the last "non-outlier" value. The last "non-outlier" point is the largest actual data point that is ≤ a value that is within 1.5 × the inter-quartile range added to the value of the boundary between the third and fourth quartiles.
- A line is extended downward from the center of the bottom of the rectangle, scaled so that it reaches the last "non-outlier" value. The last "non-outlier" point is the smallest actual data point that is ≥ a value that is within 1.5 × the inter-quartile range subtracted from the value of the boundary between the first and second quartiles.
- Outliers (those values not represented by either the box or either of the whiskers) are plotted individually with symbols.
- If multiple boxplots are plotted on the same page (useful for comparison), it is advisable that all use the same vertical scale (in dB units).

NOTE: The term "inter-quartile range" refers to the scaled distance between the top and the bottom of the rectangle.

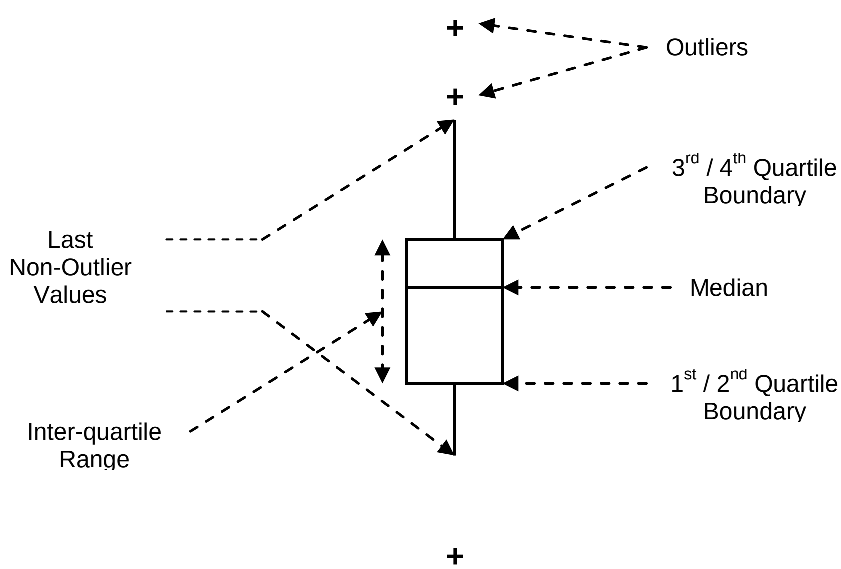

5.3.4 Fixed RF Noise Measurement

An entirely different approach is taken to doing site noise measurements. Connect a coaxial switch so that one pole is connected to a simulation of the proposed antenna system, and the other pole is connected to a matched coaxial load. The moving contact is connected via an isolated RF coupler (such as a directional coupler) to a receiver similar to the one that is to be used in the proposed system. Switch the coaxial switch so that the load is connected in. Connect a (1 kHz 60% system deviation) modulated RF signal generator to the isolated port of the coupler. Increase the RF level of the RF signal generator until the SINAD and/or BER produced by the receiver approaches the value that corresponds to the desired CPC. Note the RF level. Next, switch the coaxial switch to the antenna system. Increase the RF level until the SINAD reading again reaches the desired level. Note the RF level. The difference in levels is the amount by which the specified sensitivity has to be increased to reestablish the effective sensitivity. It is recommended to make this measurement at several times throughout the workday to account for variations in the use of the RF sources on the site.

The noise power can be ascertained from this measurement by knowing the C_s/N needed for the target CPC. (See §5.5.2 and Table A-1 of Annex-A of TSB-88.1-D) Using the (previously calculated) effective sensitivity and subtracting out the C_s/N needed, yields the received noise power. Knowing the receiver's ENBW, it is a simple matter to calculate the noise relative to *kTB* merely by subtracting *kTB* (in dB units) from the received noise power (in dB units).

5.3.5 Site Isolation

Site Isolation is used to evaluate the effects of strong field strengths in close proximity to those sites. Site isolation includes the propagation losses due to distance as well as the gains and losses due to antenna patterns. The site isolation is defined as the total loss, in dB, between the input port of the transmit antenna and the output port of the receive antenna.

The importance is that strong interfering signals can cause receiver intermodulation or contain strong BNBE that falls directly on the victim receiver's frequency.

Generally site isolation has been estimated to be around 70 dB at 800 MHz and decreased by 5 dB to 450 MHz and an additional 5 dB to VHF high band. This was based on typical private user sites deployed on relatively tall towers and using omnidirectional antennas. More recent deployments have seen reduced tower heights and an increased utilization of directional antennas often employing down-tilted antenna patterns. As a result, the previously estimated values have been steadily decreasing and cannot be assumed to be the older values. Cases of site isolation of less than 55 dB have been measured. Where practical, it is advisable to measure actual site isolation.

If 20 Watts (+43 dBm) is input into the transmit antenna and the site isolation is 55 dB, the resultant interfering power level would be -12 dBm. This strong and interfering level can produce intermodulation when multiple signals are present that is essentially impossible to overcome in a noise-limited system. The BNBE power that is specified at some value (e.g. -70 dBc) could produce a -82 dBm interfering power level on the victim's desired frequency.

The propagation loss in close proximity to an interfering site can be modeled as free space loss. This does not consider local obstructions that increase the loss nor ground reflections that can decrease the loss. In most cases where this type of interference is prevalent, there is a line of sight path between the antennas and the free space loss assumption is justified. Include actual antenna patterns.

Section 5.4.2 "Intermodulation" of this document and §5.11 "Identifying Interference" of TSB-88.3-C provide additional examples.

5.4 Symbolic RF Noise Modeling and Simulation Methodology

5.4.1 Receiver/Multicoupler Interference

Receiver intermodulation effects are rarely considered in system interference. When a tower-mounted amplifier or tower-mounted amplifier and amplified receiver multicoupler are used they can dramatically increase the link margins, but introduce intermodulation that is detrimental.

The amount of gain provided has a direct impact on the overall noise figure of the cascaded combination of elements and on the intermodulation performance. As linear systems come into existence an increased awareness of the tradeoffs is necessary to more accurately calculate the effect. Adding gain without determining its overall effect on system performance and interference potential is not a recommended practice.

Some base stations specify the performance sensitivity at the input to the receiver multicoupler. Most base stations receiver noise figures fall between 9 and 12 dB, with a typical design noise figure of 10 dB. The overall receiver multicoupler scheme has a composite noise figure of between 5 and 7 dB, with 6 dB being a typical design value. With a true noise figure of 4 dB, 25 dB of gain, followed by 16 dB of splitting loss and one dB of cable loss, the resulting noise figure of the cascaded chain can be calculated using equation (2):

$$NFc = NF_1 + [NF_2 \ -1]/G_1 \ + \ [NF_3 - 1]/[G_1 \bullet G_2] \qquad (2)$$

Where:

NF is the Noise Factor (*numeric*)

G is the Gain of an Amplifier (*numeric*)

NF_1 = 4.0 dB = ***2.5***. G_1 = 25 dB = ***316***

NF_2 = 17 dB = ***50*** G_2 = -17 dB = ***0.02***

NF_3 = 10 dB = ***10***

NF_C = 2.5 + [50 -1]/316 + [10 – 1]/[316 x 0.02] = 4.08 = 6.1 dB

The generalized form of Equation (2) is:

$$NF_C = NF_1 + \sum_{i=2}^{n} \frac{NF_{i-1}}{\prod_{j=1}^{i-1} G_j} \tag{3}$$

From this example, the overall noise figure of the combination is improved over the base station receiver by itself but degraded from the noise figure of the multicoupler amplifier. By increasing the gain of the amplifier, and reducing the loss in the splitter, the cascaded noise figure trends toward the noise figure of the multicoupler. However, all the excess gain tends to increase the level of intermodulation products for components downstream. With linear systems, a specification that limits the amount of "excess gain" that can be introduced prior to the base receiver could be necessary to keep the entire system operating within a linear region.

To determine the absolute power level of the intermodulation products use the the Third Order Intercept point (IP^3). Considerable confusion exists around the IP^3 due to manufacturers' specmanship. Most manufacturers use the Output Third Order Intercept Point (OIP^3) as it produces a higher number. Reducing the manufacturers OIP^3 by the gain of the amplifier calculates the Input Third Order Intercept Point (IIP^3). This is more useful as one can now determine the intermodulation products with respect to the desired carrier and design noise threshold, adjusting absolute levels by selecting gain and loss elements.

5.4.2 Intermodulation

A receiver with an 80 dB Intermodulation Rejection (IMR) has an IIP^3 in the 0 to +5 dBm range[7]. To measure the IMR[8], start with the static sensitivity criterion, such as 12 dB SINAD, C_s/N = 5 dB for an analog FM radio with ±4 kHz deviation. The desired signal is increased by 3 dB and two interfering signals are injected. One is the adjacent channel and the other is the alternate channel. In this case, 2 times the adjacent channel, minus the alternate channel creates a product that falls back on the same frequency as the desired. The two signals are increased at the same level until the 12 dB SINAD performance specification is again reached. The difference between the equal levels of the intermodulation signals and the original reference is the IMR of the receiver.

---

[7] The value depends upon the reference sensitivity and Cs/N at reference sensitivity.
[8] [603], §2.1.9.

In Figure 1, if the IMR specification is 80 dB, and the 12 dB SINAD is -119 dBm, (0.25 µV); the following test would be conducted. Inject -119 dBm and measure 12 dB SINAD.

The inferred design noise threshold would be -124 dBm. Increase the desired signal level to -116 dBm, a 3 dB boost. Inject the adjacent and alternate channels; increasing them until 12 dB SINAD is once again obtained. With a receiver of 80 dB IMR, the adjacent and alternate channels would be 80 dB above the 12 dBS, -39 dBm. This once again produces a C_s/N of 5 dB, 12 dBS, comprised of the -124 dBm design thermal noise and another -124 dBm noise equivalent from the interference from the IMR. The combined noise sources equal -121 dBm versus the desired signal at -116 dBm. Figure 1 illustrates a graphical solution for the IIP^3 of +3.5 dBm. Two slopes are constructed, a 1:1 relationship from the design noise threshold and a 3:1 slope for the third order products offset by (80 + 5) 85 dB at the design noise threshold. The equation for this relationship is:

$$IMR = 2/3\ (IIP^3 - Sens) - 1/3\ (C_s/N\ @\ \text{Sens}) \qquad (4)$$

In this example, sensitivity for 12 dB SINAD was -119 dBm with a C_s/N of 5 dB. If the *IMR* is 80 dB, the IIP^3 is = +3.5 dBm. Equation (4) can be re-arranged to solve for IIP^3, as shown in equation (4a):

$$IIP^3 = Sens + 1/2(C_s / \text{N}) + 3/2(\text{IMR}) \qquad (4a)$$

The preceding calculation was for a single receiver. The process becomes more complex when a receiver multicoupler is cascaded with the receiver. The IIP^3 of the receiver has to be known to determine the interaction with the parameters of the receiver multicoupler chain.

See also [88.3] §5.8.4.

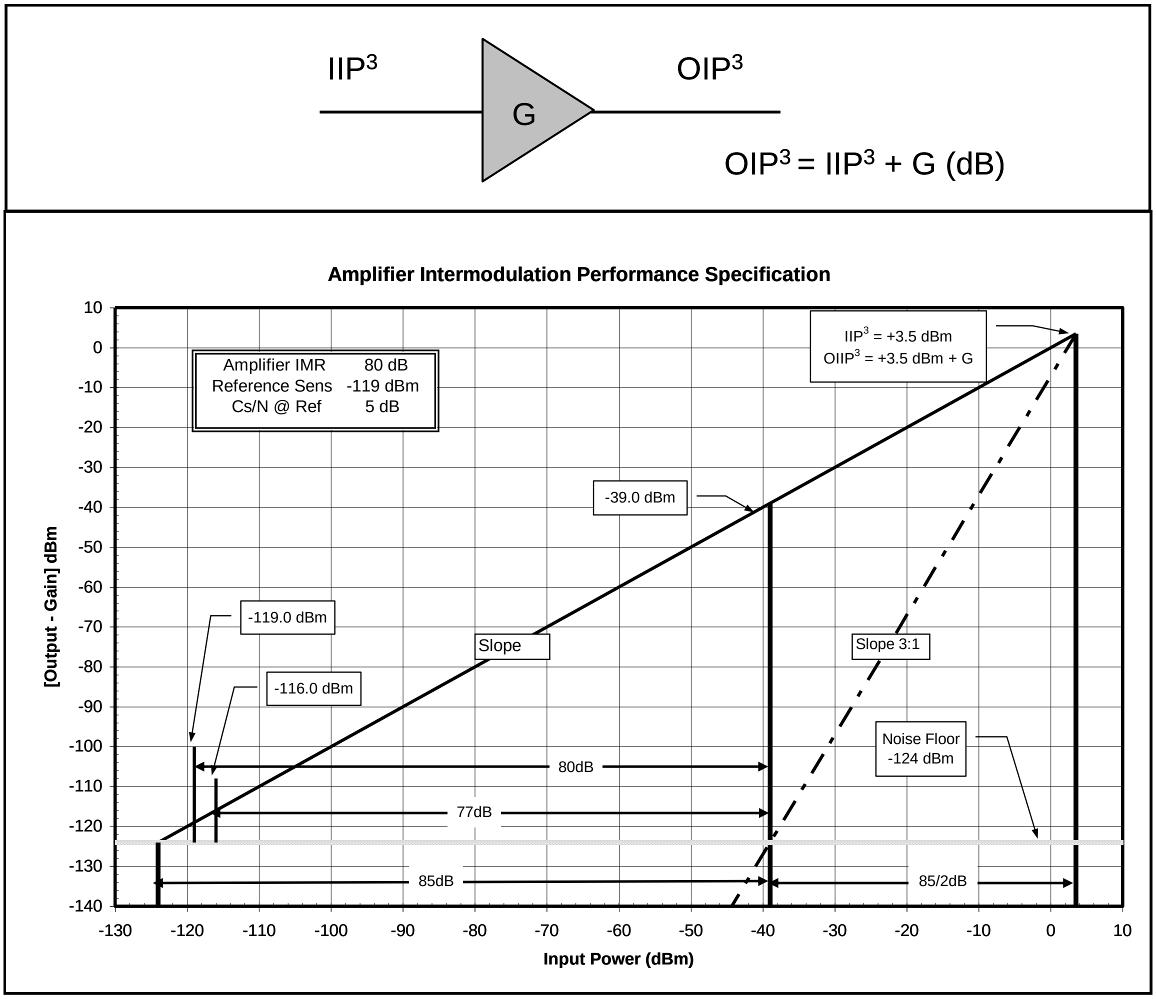

Figure 1 - Amplifier Intermodulation Performance Specifications

Receiver multicoupler manufacturers typically use the OIP^3 for their specification. Knowing the gain of the amplifier and the splitting losses one can calculate the impact on the desired and undesired portions. This also highlights the case of when there are two amplifiers in the multicoupler chain and the gain inserted to lower the cascaded effective noise figure reduces IMR performance too much. Tower top amplifiers normally involve three amplifiers, the tower top amp, a distribution amplifier and the actual receiver.

An example can illustrate the issues. Consider the previously described base station configuration with a receiver multicoupler. The parameters and lineup are shown in Figure 2. The noise figure is calculated to be 9.2 dB, based on 12 *dBS* = -119 dBm, C_s/N = 5 dB and the *ENBW* = 12 kHz.

The receiver multicoupler has 25 dB of gain and 17 dB of losses prior to the receiver's antenna port. The OIP^3 is given as +34 dBm. By subtracting the gain we calculate an IIP^3 of +9 dBm.

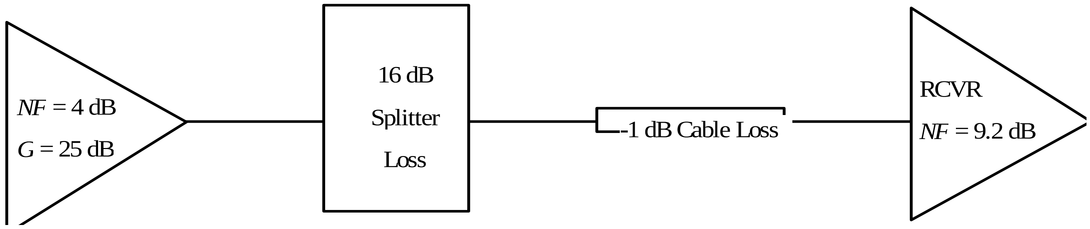

NF_1 = 4 dB = 2.51 $G1$ = 25 dB = 316

NF_2 = 17 dB = 50 $G2$ = -17 dB = 0.02

NF_3 = 9.2 dB = 8.32

$$NFc = 2.51 + \frac{(50-1)}{316} + \frac{(8.32-1)}{(316)(0.02)}$$

$$NFc = 2.51 + 0.16 + 1.16 = 3.83 = 5.83\,\text{dB}$$

NF_{imp} = 9.2 - 5.83 = <u>3.37 dB</u>

Figure 2 - Noise Figure Calculation

The traditional cascaded noise figure approach calculates an effective noise figure at the input of the multicoupler of 5.83 dB, indicating a 3.37 dB improvement in the noise figure for the combination.

5.4.3 The Symbolic Method

Symbolically all active devices are shown, in Figure 3, as a single amplifier with some known amount of gain. Inputs to the amplifier include another amplifier which has the gain of the device's noise figure which is fed from a noise source equal to the *kTB* value of the actual receiver. Following the flow from the first amplifier, the noise source is amplified and attenuated until it arrives at the input of the final receiver. In this case the accumulated noise power is -121.2 dBm. The receiver has its own noise source which is -124.0 dBm. The sum of these two noise sources is -119.37 dBm. To achieve a C_s/N of 5 dB the C needs to be -114.37 dBm. Considering the gain and losses, the signal at the input to the first amplifier needs to be -122.37 dBm. The receiver's sensitivity by itself for a C_s/N of 5 dB is -119 dBm so the improvement of the combination is -119 - (-122.37) = 3.37 dB, the same as calculated by the cascaded noise figure equation(2).

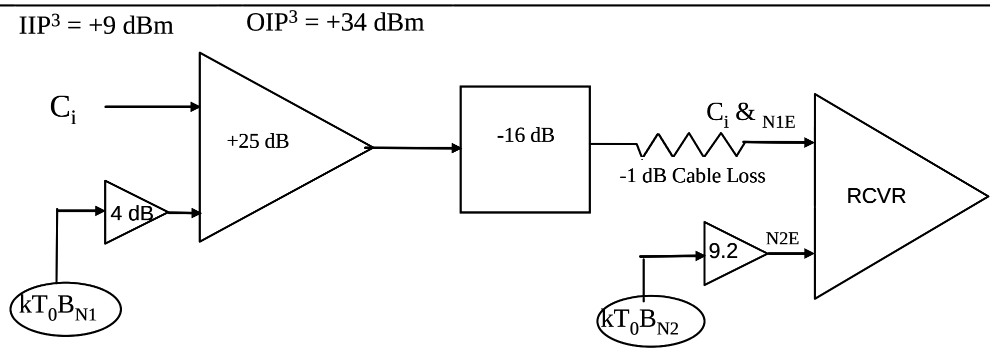

N1E = -133.2	N2E = -133.2	IIP^3 = +3.5 dBm
+4.0	+9.2	12 dBS = -119 dBm
+25.0	**-124.0 dBm**	ENBW = 12 kHz
-17.0		Cs/N @ 12 dBS = 5 dB
-121.2 dBm		NF_{dB} = 9.2 dB
		***kT0B* = -133.2 dBm**

Σ(*N1E* + *N2E*) = -119.37 dBm

Ci= [-119.37 + 5] -25 +16 +1 = -122.37 dBm

Performance Improvement = -119.0 - (-122.37) = **3.37 dB**

Figure 3 - Symbolic Method

This approach allows evaluating the effect of system IMR noise power. Equations (7) and (8) can be used to calculate either a relative or absolute power level for the third order product. First a calculated equivalent signal power level is necessary to use in this evaluation. For the classic IMR case as measured by the TIA method, the equivalent signal power C_i[9], is:

$$C_i = \frac{2(\text{Adjacent Channel Power}) + \text{Alternate Channel Power}}{3} \tag{5}$$

For the TIA test method, both the adjacent and alternate channels are held at the same power level. However in the field, users frequently have to deal with IMR where the frequency relationships aren't that close and are unequal in power. In these cases the equivalent power to use for C_i would be to consider only the specific case which would be where the two signals have different average powers and the effect of the actual mixing process where one frequency is

[9] All powers are in the same units of dB with an absolute reference, typically dBm.

doubled and the other not, so the resultant power falls into the victim's bandwidth. The example is for third order intermodulation. It is also assumed that the mixer remains constant and that no additional selectivity is available. In this case:

$$\mathrm{Ci} = \frac{2(P_a) + P_b}{3} \tag{6}$$

Where P_a is the power in absolute dB of the signal whose frequency is doubled and P_b is the power in absolute dB of the signal whose frequency is not doubled.

An application with specific frequencies, calculates the interfering carrier levels and the intermodulation power that results for a specific design or problem evaluation. At the input of an amplifier:

$$\textit{Relative IM} = 2\,(IIP^3 - C_i) \tag{7}$$

Where C_i = Equivalent interferer.

$$\textit{Absolute IM Level} = C_i - \textit{Relative IM} \tag{8}$$

Combining Equations (8) and (7) plus accounting for the Gains and Losses the result is:

$$\text{Absolute IM Level}_{\text{dBm}} = Ci - 2(IIP^3 - Ci) + (G - L) \tag{9}$$

Where Ci and IIP^3 are in dBm and Gains (G) and Losses (L) are in dB.

In most cases system designers are interested in the level of the IM and can then follow it through the chain of amplifiers and loss elements until it arrives at the input of the last amplifier stage. At the final stage, the individual carriers also will be present and can once again produce IM. The total noise would then be the sum of the individual noise sources and the individual IM products, $C/(\Sigma N + \Sigma IM)$. Continuing with the example, consider the following case.

The Adjacent channel power, C_{a1}, at the input to our multicoupler amplifier is -30 dBm, and the Alternate channel, C_{a2}, is -42 dBm. This is the classic 2A-B IM case. From equation(6):

$$C_i = [2(-30) + (-42)] / 3 = -34 \text{ dBm} \tag{10}$$

The IIP^3 of the first amplifier is +9 dBm. From equation (9), the absolute IM level at the input of the receiver is calculated to be -34 dBm -2(9-(-34)) + 25 -17 = -112 dBm. The individual C_{a1} and C_{a2} would be amplified (25 -17) = 8 dB to -22 dBm and -34 dBm respectively. From equation (6), their C_i is now -26 dBm.

Using the same 80 dB IMR receiver with an IIP^3 = +3.5 dBm that was previous described, below equation (4), the absolute IM level, using equation (9) calculate that the IM noise introduced by the receiver itself is -85 dBm.

In Figure 4, there are now five different inputs to the final receiver that impact its performance; the desired C, and the four noise sources, $N_1 + N_2 + IMR_1 + IMR_2$. In this example, the IMR due to the high adjacent and alternate channels are controlling. In a 25 kHz analog FM system, to achieve a CPC with a DAQ = 3, [88.1] Table A-1, a $C_f/(I+N)$ = 17 dB is needed, therefore the necessary desired signal level at the input of the receiver is -68 dBm or greater. As shown from this example, additional amplifiers in the "gain chain" can amplify high interfering signals to such a high level that IMR in unavoidable. The proper addition of attenuation (pad) is necessary to optimize the sensitivity versus IMR performance.

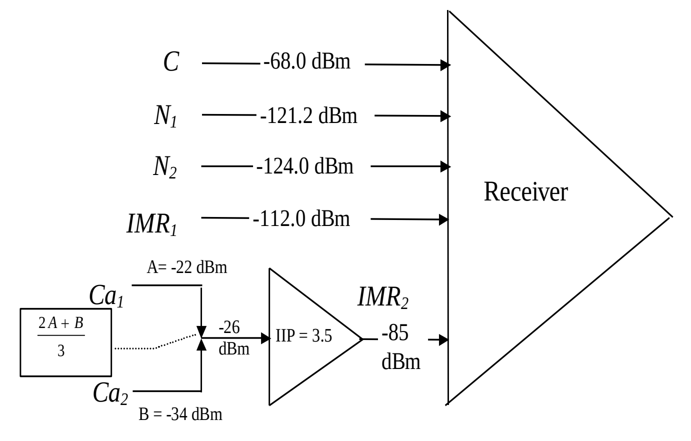

$$\Sigma Ns = N_1 + N_2 + IMR_1 + IMR_2 = -85dBm$$

$$\frac{C}{\Sigma(N + IMR)} \equiv 17dB, \therefore C = -68dBm$$

Figure 4 - Multicoupler IMR Performance Example

It is important to remember that there is a probability consideration that needs to be included, and that the type of interference also needs to be considered. For example, if the interfering adjacent channel had the same CTCSS code, a receiver would open whenever the interference was present and no desired carrier was present. This would dramatically impact the users perception of the amount of interference.

5.4.4 Multicoupler Parametric Values

Using the listed parameters, the improvement of the receiver reference sensitivity used in the Noise Figure examples, Figure 2 and Figure 3 are: 2.6 dB using a tower top amplifier; -0.24 dB for a multicoupler only.

Therefore, a simple method for frequency coordination would be to assume the values indicated are typical and that a base sensitivity improvement of +3 dB can be assumed for a tower top amplifier with all transmission line losses eliminated. This is equivalent to having the receiver input at the input to the tower top amplifier and adding 3 dB of increased sensitivity. If the receiver sensitivity improves beyond -119 dBm (0.25 μV), use the value of -119 dBm.

For the receiver multicoupler configuration, the assumption is that the receiver reference sensitivity can be referenced to the input of the receiver multicoupler. This is equivalent to eliminating the receiver line losses between the multicoupler and the receiver being evaluated.

More detailed evaluations might be undertaken if specific values of the parameters are made available by the applicant, or victim, when a proposed coordination is being challenged.

The values in Figure 5 represent common receiver multicoupler deployments to use if specific information is unavailable or the recommendation that the receiver reference sensitivity can be referenced to the input of the receiver multicoupler is unacceptable in a challenge.

Filter	Bandwidth	Band of Interest			
	Insertion Loss	1.0 *dB*			
Amp_1	Noise Figure	3.0 *dB*			
	IIP^3	+10 *dBm*			
	1-*dB* Compression	-2 *dBm*			
	Gain	20.0 *dB*			
Line / Pad	Loss (*dB*)	Based on antenna HAGL			
Attenuator	Loss (*dB*)	Assume surplus gain limited to < 9			
Filter / Power Inj	Insertion Loss (*dB*)	0 *dB*, special case usage			
Amp_2	Noise Figure	4.5 *dB*			
	IIP^3	+15 *dBm*			
	1-*dB* Compression	-3 *dBm*			
	Gain	+20 *dB*			
Splitter (Bold is typical value)	N Ways	8	16	32	64
	Loss	10 *dB*	13 *dB*	**16 *dB***	19 *dB*
Line	Loss	1 dB typical for local distribution			

Figure 5 - Receiver Multicoupler

5.4.5 Non-Coherent Power Addition Discussion

When adding powers, the values need to be in some form of Watts before they are added. In microwave systems the picowatt is commonly used. To add the powers, it is not necessary to convert them to a specific watt level, milliwatt, microwatt, or picowatt. As long as they all are at the same pseudowatt level they can be added and converted back and forth to the nonlinear form of decibels.

The following simple method can be used to combine powers in the decibel form. Take the dB difference of two powers and look up in Table 6 or Figure 6 for a value to add to the higher power. For example, if a -113 dBm and -108 dBm are to be combined, the difference is 5 dB which from Figure 6 add +1.2 dB to the -108 dBm for a composite -106.8. For cases with more than two power levels, the process can be repeated multiple times. $P1$ and $P2$ can be combined to Pc which can then be combined with P3 for the average power of all three.

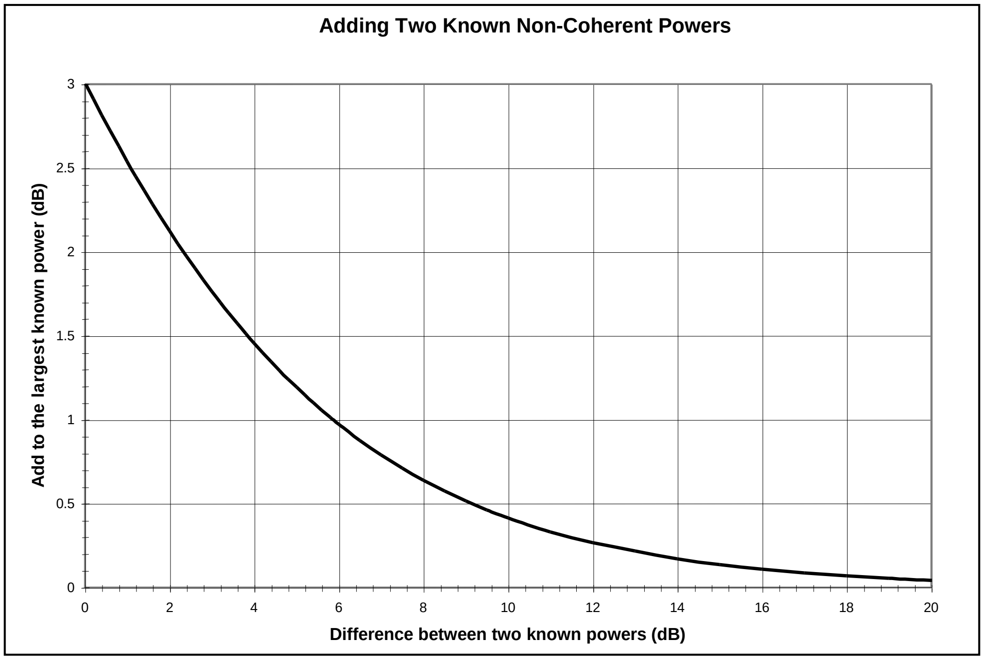

Figure 6 - Adding Non-Coherent Powers

Table 6 - Adding Non-Coherent Powers

dB Difference	Add To Largest	dB Difference	Add To Largest	dB Difference	Add To Largest	dB Difference	Add To Largest
0.0	3.01	2.6	1.902	5.2	1.146	11	0.331
0.2	2.911	2.8	1.832	5.4	1.1	12	0.266
0.4	2.815	3.0	1.764	5.6	1.056	13	0.216
0.6	2.721	3.2	1.698	5.8	1.014	14	0.17
0.8	2.629	3.4	1.635	6.0	0.973	15	0.135
1.0	2.539	3.6	1.573	6.5	0.877	16	0.108
1.2	2.451	3.8	1.513	7.0	0.79	17	0.086
1.4	2.366	4.0	1.455	7.5	0.71	18	0.068
1.6	2.284	4.2	1.399	8.0	0.639	19	0.054
1.8	2.203	4.4	1.345	8.5	0.574	20	0.043
2.0	2.124	4.6	1.293	9.0	0.515	25	0.016
2.2	2.048	4.8	1.242	9.5	0.461	30	0.004
2.4	1.974	5.0	1.193	10.0	0.414		

5.4.6 Determining Unknown Power from Sum Plus One Known Value

Figure 7 or Table 7 can be used to identify the magnitude of an unknown when the total power (sum) and one specific value is known. For example, if the total power is measured to be -100 dBm and one contributor is known to be -106 dBm then the other contributors can be found to be -101.25 dBm, 1.25 dB below the total power. See §5.8.1 [88.3] for using this method to identify interference sources.

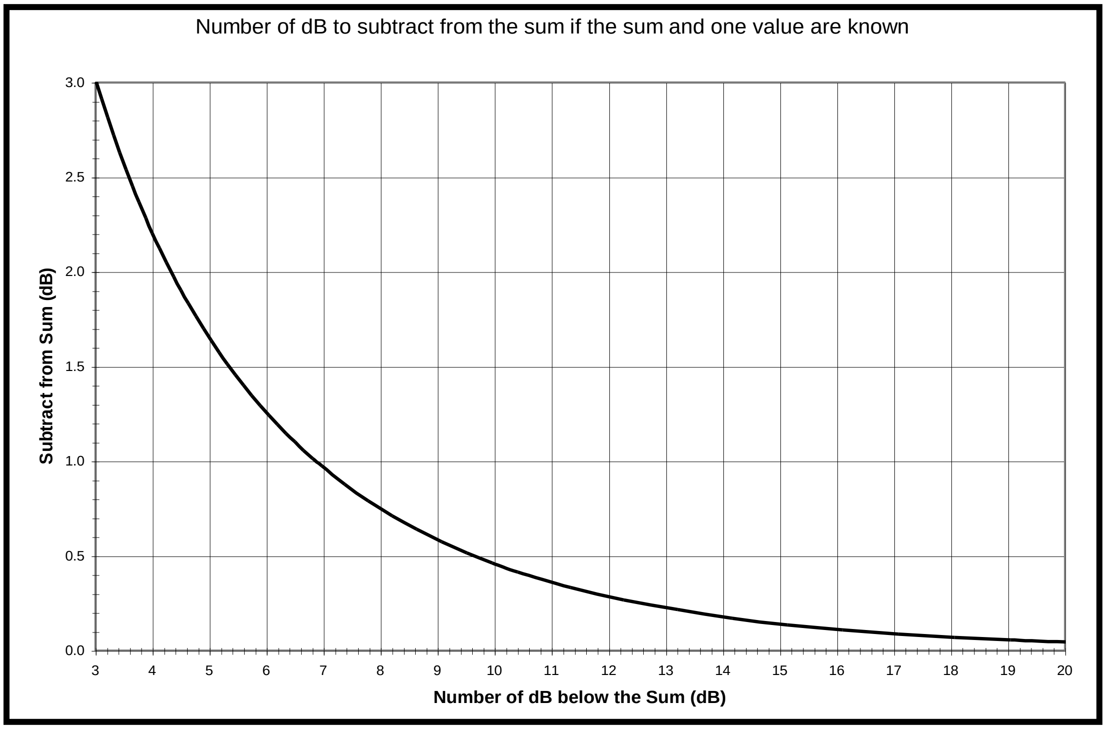

Figure 7 - Determine Unknown Power from Sum and One Value

Table 7 - Determine Unknown Power from Sum and One Value

dB Difference	Subtract From Sum	dB Difference	Subtract From Sum	dB Difference	Subtract From Sum
3	3.01	7	0.97	14	0.17
3.25	2.78	7.5	0.85	14.5	0.15
3.5	2.57	8	0.75	15	0.14
3.75	2.38	8.5	0.67	15.5	0.12
4	2.21	9	0.59	16	0.11
4.25	2.05	9.5	0.52	16.5	0.10
4.5	1.90	10	0.46	17	0.09
4.75	1.77	10.5	0.41	17.5	0.08
5	1.65	11	0.36	18	0.07
5.25	1.54	11.5	0.32	18.5	0.06
5.5	1.43	12	0.28	19	0.05
5.75	1.34	12.5	0.25	19.5	0.04
6	1.25	13	0.22	20	0.03
6.5	1.10	13.5	0.19		

5.5 Noise-Adjusted Faded Performance Threshold

Environmental noise causes a receiver's apparent Faded Performance Threshold to algebraically increase. This "Noise-Adjusted Faded Performance Threshold", FPT_{Adj}, is calculated as follows:

$$\text{Adjustment} = 10 \log10(1 + \text{Nr/NF}) \qquad (11)$$

$$\text{FPTAdj} = \text{FPT} + \text{Adjustment} \qquad (12)$$

Where,

$N_r \equiv$ The environmental noise (relative to kTB), expressed in linear (not dB) units. See §5.2.

$NF \equiv$ The receiver's Noise Factor, expressed in linear (not dB) units.

FPT $\equiv$ The receiver's Faded Performance Threshold, expressed in dB units.

An example of this adjustment is contained in Annex C of TSB-88.1-D, §C.2.4.

[BLANK PAGE]

6. Electromagnetic Wave Propagation Predictions

Two general types of propagation models exist: the “path-general” type and the “path-specific” type. A “path-general” type of model categorizes each path based on a small number of characteristics (for example, path roughness and base height above average terrain), and applies general rules based on those characteristics. A “path-specific” model may include the former considerations into account, but its defining characteristic is that it takes the path’s actual geometry into account. For studies involving spectrum management, and particularly for frequency coordination of systems requiring a “Protected Service Area” (PSA), or other conditions where a detailed assessment of interference is desired, a path specific model is necessary.

Studies (see, for example, [Daly 10]) have shown that, in interference-limited situations such as frequency coordination, the calculated signal-to-interference ratio is not strongly dependent upon the selection of the specific propagation model so long as the same propagation model is applied consistently throughout. For that reason, this document does not recommend a specific propagation prediction model. Instead, a comparison of the major characteristics of some well-known models is presented.

6.1 Sub-Gigahertz Prediction Models Compared

6.1.1 Bullington [Bullington 47, 57, 77]

The Bullington method is a path-specific model that gives the user a choice of two algorithms, depending upon path characteristics: the plane Earth method and the three-loss method. Both are semi-empirical methods; i.e., Bullington made an attempt to fit theory to measurements. Bullington’s Plane Earth method is suitable in cases with low antenna heights, whereas his Three-Loss method is more suitable with high antenna height. Neither method is suitable in areas where the antenna height is high but the path is shorter than the line-of-sight. The Bullington method has been tested over the frequency range 54-216 MHz, so it should not be used at frequencies far outside that range. Bullington included a shadow loss routine as part of his algorithm. For a description, see §6.2.1.

6.1.2 FCC (R-6406 & R-6602) [Carey 64] [Damelin 66]

FCC OCE Report R-6406 (popularly known as the “Carey curves”) is a generalized model that was prepared to assist in the assignment of frequencies in the old mobile telephone service (Domestic Public Land Mobile Radio Service). The curves were prepared for the 35-, 152-, and 450-MHz bands. The curves were derived from the 1963 version of CCIR (now known as ITU-R) Recommendation 370. In deriving the curves, the FCC assumed a terrain roughness factor (Δh) of 50 meters. The FCC adjusted the curves by 9 dB to account for the difference between the CCIR’s 10 meter (TV) and the FCC’s 2 meter (mobile) receiving antenna heights.

OCE Report R-6602, also a generalized model, is sometimes mistakenly called the “Carey curves”. The purpose of R-6602 was to provide guidance for FM and TV broadcasting. Land Mobile was not envisioned as a possible use when the report was written. Measurements taken were centered around three frequencies: 75, 195, and 650 MHz. They were intended to be applied over the ranges 54-108, 174-216, and 470-890 MHz, respectively.

The method of R6602 is analogous to that of the Area Method of Longley-Rice. No parameters other than HAAT and h are used in the method. The portion that uses Δh is considered to be a correction to the basic curves and is NOT used by the FCC for licensing. In applying R6602 to Land Mobile situations, it is important to take a 10 dB correction factor to account for the fact that the curves were developed for a home TV antenna height of 30 feet and the typical mobile antenna is at 5 feet.

6.1.3 Longley-Rice [Longley 68] [Hufford 79, 82, 85]

The Longley-Rice algorithm is, like Bullington, a path-specific semi-empirical model. It is, however, much more detailed than the Bullington model and requires many more input values. In particular, it requires the ground constants (the surface dielectric constant) and (the ground conductivity) and the surface refractivity, N_0. The algorithm classifies propagation into the following four categories with increasing distance from the transmitter:

- Free Space
- Line-of-sight
- Diffraction
- Scatter

Except for interference calculations from extremely distant stations, the scatter category is typically not reached. Longley-Rice works in two possible “modes”: area mode and point-to-point mode. To a land mobile engineer, this may be confusing terminology. The point-to-point mode is not for use with point-to-point radio links; it is, rather, the mode that takes into account all profile data when doing point-to-area predictions. The area mode does point-to-area predictions based upon average values, rather than actual profiles. Thus, it does not calculate shadow loss at all.

Longley-Rice’s calculation of shadow loss is a modification to Epstein-Peterson as described in §6.2.2. The modification is that only the largest obstacle as seen from each site is considered. All intervening obstacles between the two considered are ignored. This method *is*, however, more accurate than Bullington’s shadow loss algorithm.

The Longley-Rice model is also sensitive to the locations of horizon-defining obstacles. An error flag is returned to indicate that internal parameters are out of range, yet the program still returns the median transmission loss. It is highly advisable to check the value of the error flag"

In sum, Longley-Rice is more complicated than any of the algorithms mentioned thus far, but does not provide substantially better results.

6.1.4 Okumura [Okumura 68]

Original Model

The Okumura algorithm is based solely upon measurements with no attempt to reconcile it with theory; i.e. it is purely empirical. When the full model is used, the Okumura model is path-specific. However, it has also been used as a generalized model by excluding all calculations except for the Basic Median Attenuation and the antenna factors. Okumura's method consists of adding a "Basic Median Attenuation" (A_{mu}) to the free space loss (Friis formula):

$$LFS = 32.3 + 20 \log_{10} d + 20 \log_{10} f, \qquad (13)$$

where antennas are dipoles, d is in miles, and f is in MHz.

The A_{mu} prediction curves are based upon the following assumed conditions:

- Urban environment
- Quasi-smooth
- Base antenna height = 200 m
- Mobile antenna height = 3 m

The A_{mu} value extracted from the curve is based upon the frequency and distance.

Various correction factors are applied to bring the loss to that associated with the actual (as opposed to assumed) conditions. Additional correction factors are available for the following:

- Isolated ridges
- Sloped paths
- Mixed land-sea paths
- Path orientation with respect to street direction

Okumura's Isolated Ridge factor is intended for use with a very specific type of obstacle. It is advisable to substitute a more general diffraction model, such as one of those discussed in §6.2. However, adjustments should be made to account for the fact that the aforementioned diffraction models are intended to be added to free space.

Most technical papers indicate that land-sea effects diminish with frequency, so Okumura's Land-Sea correction should be applied with caution.

In an automated program, it is extremely difficult to account for street orientation, so that factor has been eliminated in many implementations of Okumura's model. Okumura's A_{mu} curve applies to mean street orientation.

The Okumura/Hata/Davidson Method

Previous versions of TSB-88 and 88.2 recommended the Okumura model. Since Okumura's method is completely graphical, the method needed to be computerized. Starting from Hata's equations [Hata 80] which are based on Okumura's work but limited to short range and medium antenna heights, Allen Davidson extended Hata's (and, indeed, Okumura's) limits. Table 8 summarizes the characteristics of the Okumura, Hata, ITU Hata, and the Okumura/Hata/Davidson (OHD) method.

Table 8 - Characteristics of the Okumura "Family" of Algorithms

Characteristic	Okumura	Hata	ITU Hata	OHD	COST-231 Hata
Freq Range (MHz)	150 - 2000	150 - 1500	150-1500	30 - 1500	1500-2000
Base Height Range (m)	20-1000	30-200	30-200	20 - 2500	30-200
Rolling Terrain Factor?	Y	N	N	N	N
Shadow Loss	Isolated Ridge	None	None	Epstein-Peterson	None
Slope Factor?	Y	N	N	N	N
Land/Sea Factor?	Y	N	N	N	N
Clutter Factor	Okumura	Okumura	Okumura	Land Cover-based Okumura	3 dB for Dense Urban
Max Distance (km)	100	20	100	300	20

6.1.5 TIREM [Frazier 83]

The TIREM method was developed from TN-101 [Rice 67] which is also the starting point of Longley-Rice, so there is an obvious family resemblance. TIREM increases the number of line-of-sight modes to three (L-R has 2) and the number of beyond line-of-sight modes to six (L-R has 2). This does not necessarily make it a better method than Longley-Rice. For example, its multiple obstruction method is just straight Bullington shadow. TIREM has some very enthusiastic proponents, particularly in the U.S. military.

6.1.6 ITU-R (Rec P.452, 1238, 1411, 1546, & 1812)

ITU Recommendations are very important in some parts of the world. ITU-R produces different Recommendations for different situations. According to ITU-R Recommendation P.1144-5 [ITU 09a], they are applied as shown in Table 9.

Table 9 - ITU-R Propagation Algorithms

Service	Rec. P.452	Rec. P.1238	Rec. P.1411	Rec. P.1546	Rec. P.1812	Rec. P.2001
[Ref]	[ITU 15a]	[ITU 15b]	[ITU 15c]	[ITU 13e]	[ITU 15d]	[ITU 15e]
Base to Fixed	1-3 GHz	No	No	0.03-1 GHz	No	No
Base to Base	1-3 GHz	No	No	0.03-1 GHz	No	.03-50 GHz
Base to Mobile	No	0.9-100 GHz	0.3–100 GHz	0.03-1 GHz	0.03–3 GHz	No
Base to Brdcst	No	No	No	0.03-1 GHz	No	No
Short Path	No	No	0.3-100 GHz	No	No	No
In-Building	No	0.9–100 GHz	No	No	No	No
Mobile to Fixed	1-3 GHz	No	No	0.03-1 GHz	No	No
Mobile to Base	1-3 GHz	0.9-100 GHz	0.3-100 GHz	0.03-1 GHz	0.03–3 GHz	No
Mobile to Mobile	No	No	No	0.03-1 GHz	No	No
Mobile to Brdcst	No	1-3 GHz	No	No	No	No

Note 1: In all but the “Planning” services, the recommendations are for interference scenarios.

6.1.7 Allsebrook & Parsons [Allsebrook 77]

In their paper, Allsebrook and Parsons attempted a number of things. They published an extension of Okumura, bringing its frequency range down to 75 MHz. Their principal contributions were to the prediction of urban propagation models. Starting with the Blomquist and Laddell model, they came up with improved methods for both flat and hilly cities.

6.1.8 Dadson,Durkin,Edwards (including JRC) [Edwards 69], [Dadson 75, 79], [Durkin 77]

The Joint Research Committee (JRC) of the Nationalized Power Industries (UK) among other U.K. agencies has participated in creating a rather complete coverage algorithm. The algorithm takes into account the following factors:

- line-of-sight loss
- diffraction loss due to obstacles
- loss due to inadequate Fresnel-zone clearance
- earth curvature refraction

For the “line-of sight loss”, the program chooses between Plane Earth and Free Space loss. For obstacle loss, the program uses a unique hybrid between Epstein-Peterson and Bullington. For a discussion of this method see §6.2.6. Earth curvature is taken into account by the alteration of K when calculating the profile.

6.1.9 CRC [Palmer 78, 79], [Whitteker 85a, 85b]

The Communications Research Centre of Canada's Department of Commerce has developed a program which gives the selection of four algorithms: (a) a smooth earth model, (b) an urban area model, (c) an irregular terrain model, and (d) a detailed model. The smooth-earth is similar in characteristics to the Bullington 3-loss model. The urban area model is essentially an Egli model. The irregular terrain model is the same as Longley-Rice model in "Area" mode. The only truly original model is the detailed model. This model takes the method of Soares de Assis [Soares 71] for multiple rounded obstacles and adds a reflection component to it. Scatter loss is also calculated and is substituted for the diffraction loss if it is less than the diffraction loss. The program then adds some unique clutter loss corrections. With an adequate database, the CRC detailed method is a good one. A likely drawback is that it is likely to take excessive calculation time because of the detailed diffraction calculation.

6.1.10 Blomquist & Laddell [Blomquist 74]

Blomquist and Laddell advocate a method which uses two calculations: an earth curvature diffraction calculation and an Epstein-Peterson obstacle diffraction calculation. They then apply either of the following two rules to the calculations: (a) take the lesser loss of the two calculations, or (b) take the root sum square of the two calculations. They don't recommend which to use nor do they provide any theoretical foundation for their method. Their results, however, seem to be reasonably good.

6.1.11 Egli [Egli 57]

Egli's method is essentially a modification of Plane Earth which incorporates a 20 log (f_{MHz}/40) correction. He also includes a statistical irregular-terrain correction factor. He also discusses antenna height gains. His method is very simple and not very accurate.

6.1.12 3GPP Path Loss Models

In Annex B, Section B.1.2.1 of [3GPP 10], various path loss models are defined for use in modeling of Evolved Universal Terrestrial Radio Access (E-UTRA) systems (i.e. LTE), and can also be used for other broadband technologies. Models are defined for Urban Micro (UMi), Urban Macro (UMa), Suburban Macro (SMa), and Rural Macro (RMa) scenarios, with Line-of-Sight (LOS) and Non-Line-of-Sight (NLOS) versions for each scenario. They are presented in Table B.1.2.1-1. Like the models presented above, these models are slope and intercept based, where the slope is related to the propagation assumption (LOS or NLOS) and the intercept is based on factors such as carrier frequency and heights of the base station and device, and they also include shadowing standard deviation terms based on the scenario. However, these models have two key differences compared to the models presented above. First, they are applicable for the frequency range of 2-6 GHz, with the RMa model applicable from 450 MHz to 6 GHz. Also, these models are valid for distances as small as 10m, with

UMi, UMa, and SMa extending to 5km and RMa to 10km. Thus, these models may be considered for use with smaller cell size broadband data systems deployed at higher frequencies.

6.1.13 3GPP Path Loss Models for Device-to-Device Applications

Appendix A.2.1.2 of [3GPP 14b] defines path loss and channel models for use in LTE device-to-device applications. These models can be used for other broadband systems, with Outdoor to Outdoor, Outdoor to Indoor, and Indoor to Indoor scenarios addressed. Like the models above, these too are slope and intercept based. They are defined for 2GHz carrier frequency, but can be used at 700MHz or other bands below 2GHz by applying a “20log(fc)” correction term to adjust the intercept point. The models are based on free space path loss, but include adjustments for NLOS as well as penetration loss for the Outdoor to Indoor case. For the Indoor to Indoor scenario, this reference leverages path loss modeling techniques originally proposed in [3GPP 10] for E-UTRA small cells.

6.1.14 Air-to-Ground Path Loss Models

The antenna heights and coverage ranges found in air-to-ground scenarios will typically fall outside of the tuning ranges of the path loss models presented to this point and hence require different path loss modeling techniques. Air-to-ground path loss models will typically assume free-space propagation while also capturing effects due to the curvature of the earth and diffraction from terrain. These effects are a function of distance and HAAT of the base station and device. Examples of path loss models that are appropriate for air-to-ground scenarios are EPM73 [Lustgarten 77] and ITU-R P.528-3 [ITU12]. The characteristics of these models are summarized in the table below. Note that these examples do not require additional margin for shadowing as both models are based on an assumption of line-of-sight propagation with parameters to consider terrain as needed.

Table 10 - Summary of Air Ground Models

Characteristic	EPM73	ITU-R Rec. P.528-3
Frequency Range (MHz)	1 - 10000	125 - 15500
Antenna Ht Range (m)	< 3000	1.5 - 20000
Max Distance (km)	400	1800

6.2 Comparison of Shadow Loss Calculation Algorithms

Some of the prediction algorithms described above include shadow loss calculation algorithms as an inherent part of the algorithm. Others do not. Still others (e.g., Okumura) use a shadow loss algorithm that is very restricted in its application. We therefore present a discussion of various shadow loss algorithms to give the user an idea of their characteristics.

When a receiver is situated so that it does not have radio line-of-sight to its associated transmitter it is said to be "shadowed". The amount of shadow loss present along a given path depends upon a number of characteristics of that path, but primarily upon the path's geometry. Paths can be shadowed by single or multiple obstacles and each obstacle can be modeled as having any of a number of profiles, including knife-edge, wedge, and cylinder. Although typically not done, a case can be made for modeling the path geometry on a three-dimensional basis, taking into account the horizontal profile as well as the (more usual) vertical profile.

For two-dimensional paths, two general "families" of solutions exist. The "exact" methods and the "simplified" methods. The "exact" methods include such techniques as Ray Tracing employing, for example, Uniform (Geometrical) Theory of Diffraction and Geometric Optics, or the Method of Moments. They require a very detailed knowledge of the terrain elevation and ground cover (i.e. very detailed databases). The simplified methods still require a great deal of detail, but not to the level required for the exact methods. In addition, the calculations required for the exact methods are much more complicated, requiring much more computer time than that required for the simplified methods.

For simplicity and speed of computation, most workers in the field have proposed modeling obstacles as knife edges. This has the danger of being overly liberal (insufficient shadow loss) because it does not take into account the actual profile of the obstacle. In practice, however, methods which take into account the obstacle profile have been found to be overly conservative more often than those that do not have been found to be liberal. The calculation of knife-edge loss is straightforward. See Parsons [Parsons 92] pp 40-45 for a detailed explanation. Modeling of multi-obstacle paths has proven to be more difficult.

6.2.1 Bullington Shadow Loss Model

The earliest simplification proposed to model multiple knife-edges was that of Bullington [Bullington 47]. Bullington proposed that a triangle be constructed such that its legs are formed by starting at the ends of the path and proceeding along the path with each leg tangent to the obstacle that appears largest (i.e. has the most positive elevation angle) from the end from which it was drawn. The legs are extended until they cross. See [Bullington 47]. The position and height of the crossing are used to establish the parameters of a single "effective knife-edge" which is used to calculate the effective shadow loss. The Bullington method usually underestimates the shadow loss.

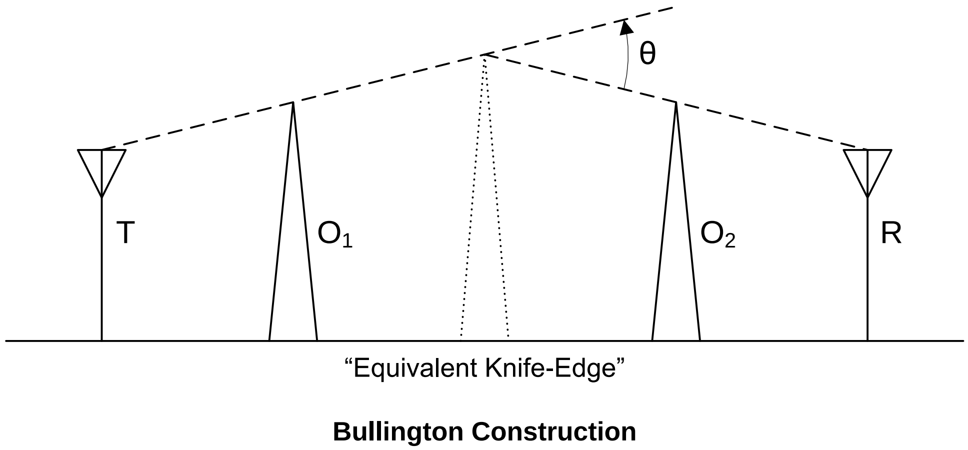

Figure 8 – Bullington Construction

6.2.2 Delta-Bullington Shadow Loss Model

As a result of 2 papers presented at the 2008 ISART conference [DeMinco 08] [Craig 08], ITU-R Study Group 3 undertook to create an improved diffraction calculation model for use in Recommendations P.452 [ITU 15a], P.526 [ITU 13b], P.1812 [ITU 15d], and P.2001 [ITU 15e]. The ISART studies had shown the existing ITU-R model to be sufficiently accurate in rolling terrain but inaccurate in rugged terrain. A new model, which maintains accuracy in both rolling and rugged terrain is called the "delta Bullington" model.

The method, described in §4.5.2 of [ITU 13b] involves first performing a traditional Bullington calculation on the actual path then constructing a smooth surface based on the path geometry. Both the Bullington loss and the true spherical diffraction for the newly-constructed surface are then calculated. If the spherical diffraction for the smooth surface exceeds the Bullington loss for the same surface, then the Bullington loss for the actual path is corrected by the difference between spherical diffraction for the smooth surface and the Bullington loss for the same surface. Otherwise, the Bullington loss for the actual path geometry stands.

$$L = L_{ba} + \max\{L_{sph} - L_{bs}, 0\} \tag{13}$$

Where

L is the total diffraction loss

L_{ba} is the Bullington loss calculated for the actual path geometry

L_{sph} is the spherical diffraction around the smooth surface

L_{bs} is the Bullington loss around the same smooth surface

6.2.3 Epstein-Peterson Shadow Loss Model

Epstein and Peterson [Epstein 53] were next to propose a multiple obstacle model. Their model consisted of calculating each individual shadow loss as though it was the only obstacle in the path, then adding the calculated losses. See [Epstein 53]. This method tends to be conservative, especially for paths with many obstacles. For paths with more than three obstacles, it should not be used.

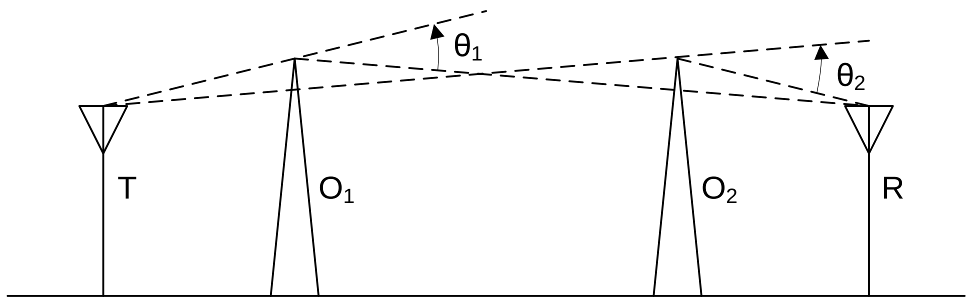

Epstein-Peterson Construction

Figure 9 – Epstein – Peterson Construction

6.2.4 EBU Shadow Loss Model

The European Broadcasting Union (EBU) proposed and the International Telecommunications Union (ITU) adopted a method called the “clearance angle” method [ITU-13e, p.44]. In this method (which is even simpler than Bullington’s), the user calculates the “clearance angle”, which is the angle that a line to the horizon from the receiver site (only) makes with horizontal. A correction in dB is calculated based on that angle and the frequency range. This is the very simplest and least accurate method.

6.2.5 Deygout Shadow Loss Model

Deygout [Deygout 66, 91] followed with a method where he selected the “main obstacle” (the one with the greatest negative Fresnel clearance). He calculated for that obstacle as though it was the only obstacle, then broke the path into two subpaths, with the main obstacle as one end of each of the two subpaths. He performed the same process on either or both subpaths depending on whether they were obstructed. Each obstructed subpath had its own main obstacle. He continued in this manner, constructing sub-subpaths until there were no more obstructed sub-subpaths. See Figure 10. He then added up all of the losses. Deygout’s method is somewhat conservative, although not nearly so much as the Epstein-Peterson method.

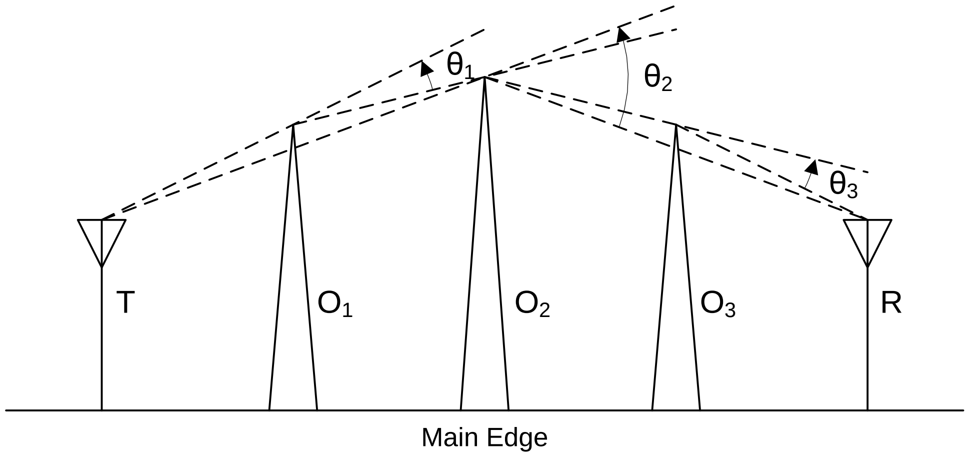

Deygout Construction

Figure 10 – Deygout Construction

6.2.6 Edwards-Durkin Shadow Loss Model

The JRC (Edwards & Durkin) Method [Edwards 69 §3.2] is a compromise in level of detail and calculation between the very simple methods (such as Bullington) and the more complicated (but not exact) methods (such as Deygout). This model finds the obstacles with the largest positive elevation angles from each of the 2 sites (as done by Longley & Rice). Unlike Longley & Rice, however, it doesn't ignore anything between the two obstacles. It acts as if there is a new path between those obstacles and constructs a Bullington-like triangle between them. It then calculates and adds the three attenuations from the three resulting diffraction angles. This method is more accurate than Bullington or Epstein-Peterson, but less computer intensive than the Deygout-like methods.

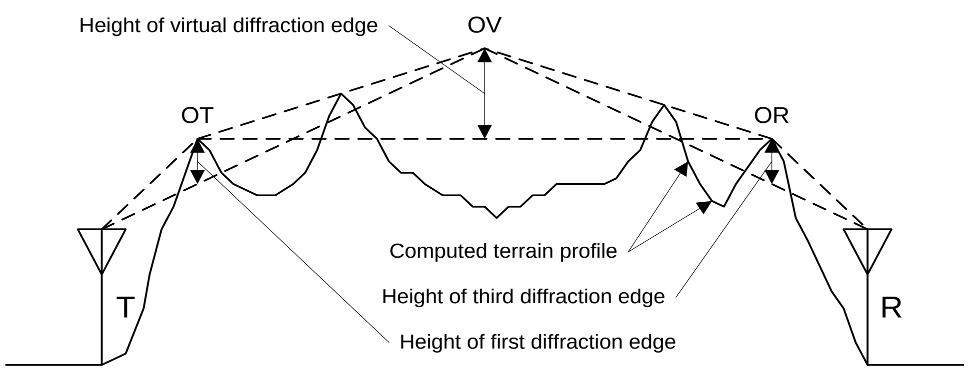

Edwards-Durkin Method

Figure 11 – Edwards – Durkin Construction

6.2.7 López Shadow Loss Model [López 84]

López came up with a slight modification to Deygout's method. He observed that the signal diffracted by the main obstacle originates at the transmitter and ends at the receiver only if those subpaths are unobstructed. If either subpath is obstructed, the signal originates at the largest obstacle for that subpath; i.e. the main obstacle for that subpath. See [López 84]. Applying this observation, he reduced the diffraction angle, thus reducing conservatism. López' method is the most accurate of the known "simplified" methods.

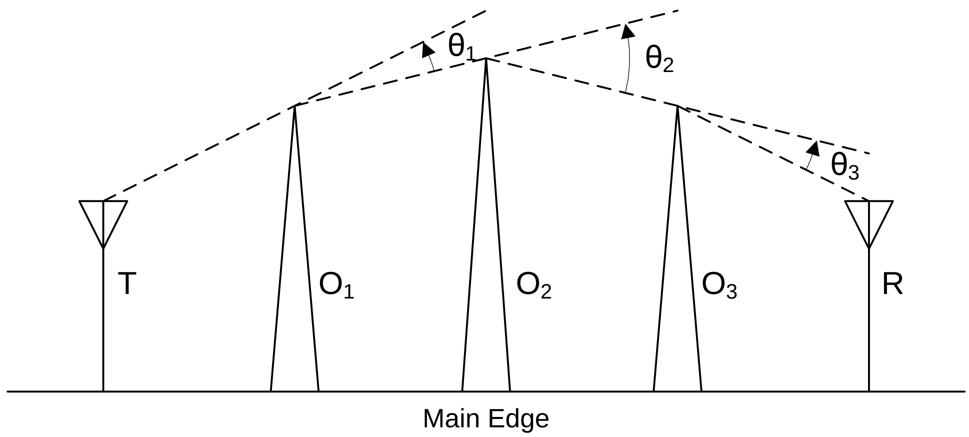

López Construction

Figure 12 – López Construction

6.2.8 Other Shadow Loss Models

Other simplified methods include those due to Picquenard [Picquenard 74] and Shibuya [Shibuya 87] and are similar in concept, complexity, and accuracy to Deygout.

6.2.9 Shadow Loss Modeling with the 3GPP Path Loss Models

The 3GPP UMi, UMa, SMa, and RMa path loss models that were introduced in Section 6.1.12 assume that the distribution of the shadow fading is log-normal and provide a shadow fading standard deviation term for each channel scenario. This term is found in Table B.1.2.1-1 of [3GPP 10] and can be used to calculate the additional margin needed on top of the path loss to account for shadow loss. In addition, Section B.1.2.1.1, "Autocorrelation of shadow fading", presents a technique for modeling the spatial correlation between fading values, with the correlation dependent on the environment. Table B.1.2.2.1-4 presents correlation parameters for shadowing and other large scale parameters for use with this technique.

6.2.10 Shadow Loss Modeling with the 3GPP Path Loss Models for Device-to-Device Applications

The 3GPP path loss models for device-to-device applications that were introduced in Section 6.1.13 assume that the distribution of the shadow fading is log-normal and provide a shadow fading standard deviation term for each channel scenario. Shadowing correlation for these scenarios is assumed to be independent and identically distributed (i.i.d.).

6.3 Comparisons of Small-Scale Prediction Methods

Radiowave propagation can be characterized as being composed of three components; namely, large-scale, medium scale, and small scale. Large-scale signal variations result from signal spreading (i.e. free space loss) and terrain variations. Terrain variations are accounted for using prediction methods based on the path profile. Medium- and small-scale variations are typically accounted for statistically. Medium-scale variations, where the signal varies over several wavelengths, are typically caused by signal shadowing due to local obstructions, such as trees, billboards, bridges, and buildings. Such variations are typically lognormal in nature. Small-scale variations, where the period of the variation is on the order of a wavelength, are typically caused by reflections off of objects, such as buildings, bridges, freeway cuts, etc. They are most frequently modeled by the use of the Nakagami-Rice ("Rician") [Nakagami 40] [Rice 48] distribution. The Rayleigh distribution [Strutt 80], a special case of the Rician where the direct signal is zero, can be used in non-line-of-sight (NLoS) situations.

6.3.1 Probability distributions commonly used to characterize signal variations

As discussed earlier, the medium term variations are commonly characterized as being lognormal, whereas the short term variations are commonly characterized as being Rician, with the Rayleigh distribution just being a special case of the Rician distribution. Clearly, predictions could be made more easily on the micro scale if a distribution combining the above two were available. Suzuki observed this [Suzuki 77] and created such a distribution. However, the distribution is a combined lognormal/Rayleigh so it is not applicable to situations where the direct component is significant (i.e. line-of sight situations). Many years later, Prasad developed a true lognormal/Rician distribution [Prasad 96].

Other distributions, such as the Nakagami-m (not to be confused with the Nakagami-Rice), and Wiebull have been proposed to characterize short term fading. Indeed, a combined lognormal/Wiebull distribution has been developed [Karadimas 09].

It should be borne in mind, however, that for coverage prediction the short-term fading is generally accounted for in the faded sensitivity of the receiver and, therefore, the only statistical consideration for such predictions is the medium term fading.

6.3.2 Channel modeling

A "channel model" is a portrayal of the time-varying characteristics of a radio channel. Channel models can include information regarding the channel's delay characteristics, its statistical characteristics, and its directional characteristics. In most applications, the directional characteristics are not of interest. Channel models are used in simulators to test equipment performance in a simulated real-world environment. These simulations can produce performance curves for such characteristics as throughput vs. signal strength.

6.3.3 Delay Profiles & Delay Spread

The performance of a broadband radio system depends upon a number of factors; notably, signal strength and the delay characteristics. The delay profile (also known as a Channel Impulse Response) is a description of the radio path's environment from a time vs. power perspective. Figure 13 is an example of a delay profile.

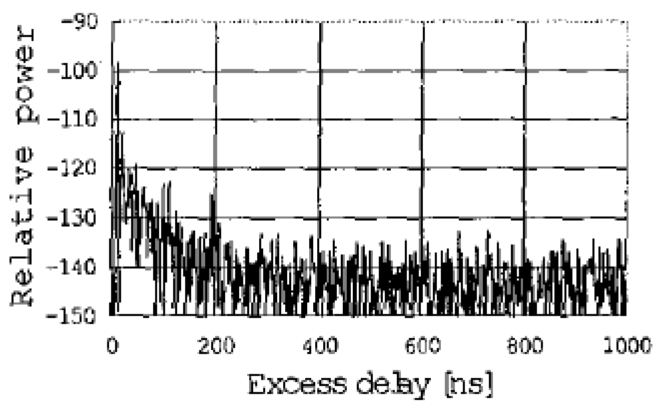

Figure 13 Typical Delay Profile

The choice of a particular delay profile for a given application depends largely on the frequency of interest and the intended environment. Because of radio propagation characteristics, it is obvious that the delay profile for a given environment will vary with frequency. Fortunately, these variations are not so large as to require more than one measurement for a given frequency band. However, caution is urged when trying to apply results over, say, a 2:1 frequency range. The environment over which a delay profile is applied should match the environment over which the measurements were made. General environment characterizations such as "Urban", "Suburban", and "Rural" appear to be adequate for predictions.

However, other factors can greatly affect the delay profile. One particularly strong factor is whether the path is line-of-sight (LoS). LoS paths tend to have the strongest signals very dominant and at the least delay. With non-line-of sight (NLoS) paths, the strongest signal is less dominant and may or may not have the least delay. Antenna height and directivity also affect the delay profile. For example, an implementation with an antenna placed above rooftop level will have an entirely different delay profile than will one in the same environment with its antenna placed below rooftop level. Similarly, an implementation using an omni-directional antenna will see an entirely different delay profile than will one with a unidirectional antenna because some reflections originating from “behind” the unidirectional antenna will be attenuated by that antenna’s directivity. Vertical directivity also has an effect, but in practical situations it usually turns out to be less pronounced. Numerous measurement campaigns have been run with channel sounders to determine the delay profiles for various combinations of environment versus. It should be noted, though, that any individual measurement of a delay profile is just a “snapshot” of a particular set of conditions. Given the amount of topological variability within any given set of conditions, it is not necessarily suitable as a model for that same set of conditions.

Some standardization bodies have affirmed particular delay profiles as part of their standard channel models[10]. For example, 3GPP has standardized LTE channel models [ETSI 14a] [ETSI 14b].

Another measure of delay characteristics is the so-called delay spread. The rms delay spread is defined as the square root of the second central moment of the impulse response. It is given in continuous form in Equation (14) and in discrete form in Equation (15). The multipath delay spread (Tm), used for simulcast predictions at traditional Land Mobile frequencies, is twice the value of the rms delay spread.

$$T_{rms} = \sqrt{\frac{1}{P_m}\int_{t_0}^{t_3} t^2 P(t)dt - \left[\frac{1}{P_m}\int_{t_0}^{t_3} tP(t)dt\right]^2} \tag{14}$$

$$T_{rms} = \sqrt{\frac{\sum_{i=1}^{N} P_i t_i^2}{\sum_{i=1}^{N} P_i} - \frac{\left(\sum_{i=1}^{N} P_i t_i\right)^2}{\left(\sum_{i=1}^{N} P_i\right)^2}} \tag{15}$$

[10] Non-LTE examples include the following: [3GPP 06], [3GPP 14a], [3GPP2 03], [Correia 99], [Correia 01], [Erceg 03], [ETSI 98], [IEEE 04], [ITU 97]

6.4 Adjustments to R-6602 calculations

6.4.1 Terrain Roughness

The FCC Rules and Regulations requirement in §73.313(i) and (j) and §73.684(k) and (l) is to implement the R-6602 terrain roughness correction. However, the rule sections stating this FCC requirement have been stayed indefinitely. In Part 90, this FCC requirement is neither stated nor discarded, so the FCC requirement for its use in Part 90 services is unclear.

Informal studies have shown that this adjustment can produce contour dimensions that are far too short when applied in mountainous terrain. Therefore, the methodology of this document specifically recommends that the R-6602 terrain roughness correction be implemented for land mobile interference contour predictions only to the extent that it increases the dimensions of the contour. Adjustments that decrease the dimensions of the contour are not recommended. In practical terms, this generally implies that it is unnecessary to calculate the terrain roughness correction when the terrain roughness is greater than or equal to 50 meters.

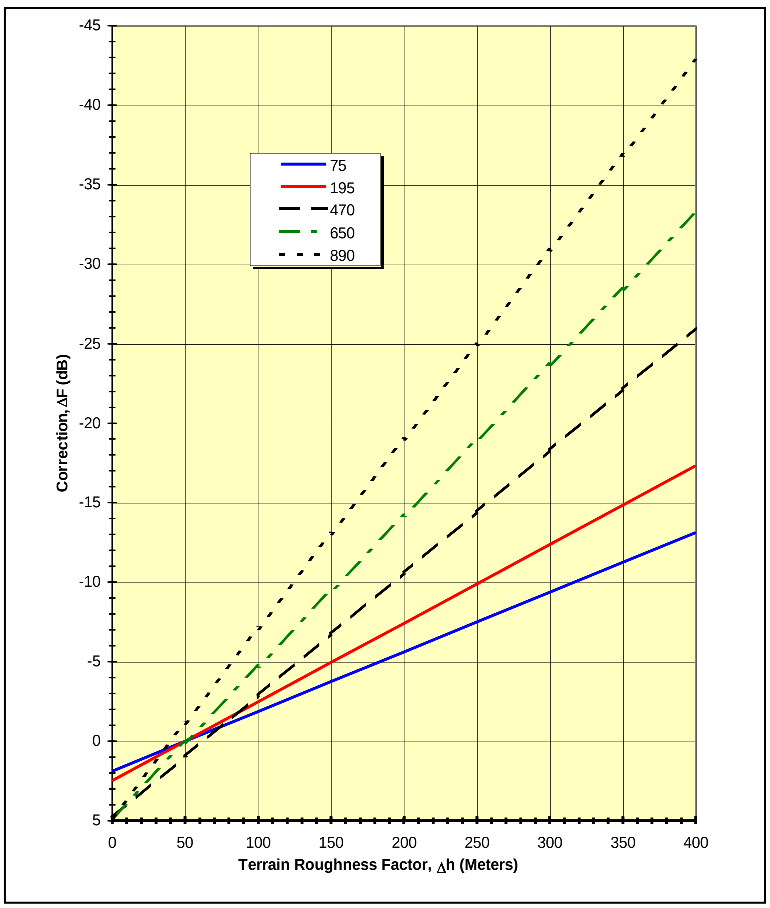

Figure 14 -Terrain Roughness Correction

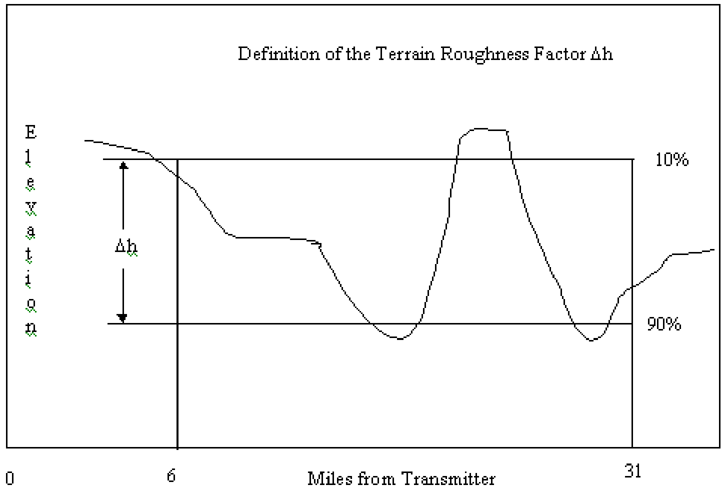

Figure 15 -Definition of Terrain Roughness

Note: 6 and 31 miles are approximately 10 and 50 km, respectively Aa

6.4.2 Short Paths

It is noted that the lowest distance R-6602 curve is for a distance of 1 mile (~1.6 km). That is, there is no curve corresponding to situations where the field strength exceeds that shown for 1 mile. For these situations, it is recommended that the calculation be made as though the R-6602 curves were extended at a 20 $\log_{10}$ d rate. See Equations (16) and (17).

$$F = F_1 - 20\ log_{10}\ d_{mi} \tag{16}$$

$$F = F_1 - 20\ log_{10}\ (d_{km}/1.6) \tag{17}$$

where,

F = Field strength in dB above 1 μV/m for 1 kW ERP at the distance of interest

F_1 = Field strength in dB above 1 μV/m for 1 kW ERP at 1 mile distance, per FCC Report R-6602 [Damelin 66]

d_{mi} = distance of interest in miles; $d_{mi} \leq 1.0$

d_{km} = distance of interest in kilometers; $d_{km} \leq 1.6$

Solving for d, we have equations (18) and (19).

$$d_{mi} = 10^{\frac{F_1 - F}{20}} \tag{18}$$

$$d_{km} = 1.6 \times 10^{\frac{F_1 - F}{20}} \tag{19}$$

Where the symbols are as indicated above.

6.4.3 Low HAATs

R-6602 does not address base antenna heights of less than 100 feet/30 meters. Since such cases do occur, the following method is recommended for HAATs between 30 and 100 feet. No method is recommended for HAATs of less than 30 feet, because antennas below roof level cannot be treated in this manner.

Adjust the calculated field strength downward relative to the 100 foot / 30 meter value by the appropriate formula for the units being used:

$$Adj = 20 \log10 (h_{ft}/100) \tag{20}$$

or

$$Adj = 20 \log10 (h_m/30) \tag{21}$$

Where,

Adj is the adjustment in decibels

h_{ft} is the antenna height in feet; $30 \le h_{ft} < 100$

h_m is the antenna height in meters; $10 \le h_m < 30$

This implies that the *target* field strength ought to be adjusted *upward* by the same amount.

In cases where the HAAT is calculated to have a value of less than 30 feet (10 meters), including negative values, the method of this subclause does not apply. In such cases, a detailed engineering study is recommended. See §§ 6.9 - 6.12.

6.4.4 High HAATs

R-6602 addresses HAATs only up to 5000 feet. However, numerous cases of land mobile base stations with HAATs in excess of 5000 feet exist in the United States. Therefore the following methodology is added for use along radials with HAATs exceeding 5000 feet, up to 10000 feet. Table 11 lists the (50, 50) values corresponding to 10000 feet. These form additional columns in the R6602-based interpolation tables found in [Kalagian 76]. If the FCC R-6602-based program [Kalagian 76] is being used, add program modifications to add to the appropriate DATA statements and to account for the larger matrix via allocation statements and loop index modifications.

Table 11 - Recommended Field Strength in dB/μV for 10,000 feet HAAT

	UHF	VHF HB	VHF LB
Distance Miles	Fig. 29 [Damelin 66] Fig. 5 [Kalagian 76]	Fig. 19 [Damelin 66] Fig. 3 [Kalagian 76]	Fig. 17 [Damelin 66] Fig. 1[Kalagian 76]
	Recommended Value @10,000 ft	Recommended Value @10,000 ft	Recommended Value @10,000 ft
1	102.8	102.8	102.8
2	96.8	96.8	96.8
3	93.0	93.0	93.0
4	90.8	90.8	90.8
5	88.8	88.8	88.8
10	82.4	82.8	82.8
20	76.7	76.5	77.2
30	67.0	69.9	70.8
40	59.8	63.4	64.1
50	54.0	57.1	57.4
60	49.1	51.1	51.0
70	44.6	45.7	45.2
80	40.2	40.7	40.0
90	35.9	36.3	35.5
100	31.4	32.3	31.5
110	26.9	28.8	28.1
120	22.5	25.6	25.1
130	18.2	22.7	22.4
140	14.3	19.9	19.9
150	10.8	17.3	17.4
160	7.9	14.8	14.9
170	5.6	12.4	12.4
180	3.7	10.1	9.9
190	2.1	7.9	7.6
200	0.5	5.9	5.7

6.4.5 Number of Radials

The maximum angular difference for calculating radials is 5 degrees. This creates a minimum number of radials of 72.

6.4.6 Database Resolution

Conform the database resolution to §6.6.1.1

6.4.7 Contour Representation

The contour is the locus of points of the individual radials.

6.5 Contour Calculations

6.5.1 Background

It has been observed that the interference contour calculation methodology in FCC Rules and Regulations Parts 73 and 90 has severe limitations. Part of the problem stems from the regulatory need to use closed contours, which is not realistic in actual deployments. Notwithstanding this limitation, it is possible to improve upon the FCC methodology. While still imperfect, the following methodology substantially improves upon that currently being used by the FCC

6.5.2 Basis

This method is based upon the FCC Report R-6602 [Damelin 66] methodology, with several modifications. In compliance with FCC regulations, the user first determines the maximum ERP by making reference to the HAAT or Station-to-Service Area HAAT (per §6.6) and to the appropriate FCC regulations. The user then uses this value, or a lesser value, if that is what is proposed, in determining the appropriate contours.

In addition to the R-6602 document, the FCC has published a computer program implementing an automated method [Kalagian 76] of interpolating the R-6602 curves. This method is recommended. If the FCC program is not used, remember that the values found in the R-6602 document are based upon an ERP of 1 kilowatt. Therefore, any “target” field strength value needs to be adjusted *upward* by the same amount that the actual ERP value is *below* 1 kilowatt.

Note that in FCC Rules and Regulations §90.689, the FCC uses a -9 dB adjustment to the R-6602 curves. This is to account for the difference in receiving antenna heights between broadcast receiving antennas, for which R-6602 was written, and land mobile receiving antennas. The current methodology preserves that -9 dB adjustment.

6.5.3 Frequency Assignment Criteria

It is good engineering practice that candidate frequency assignments be evaluated against both co-channel and adjacent channel incumbents. The current FCC method of requiring the (50,50)[11] contour of the desired to not be intersected by the interfering source’s (50,10) contour was originally based on broadcast stations. These criteria are based on measured data where receive antennas were above the local environmental clutter. As a result, the statistics

[11] The values represent (L%, T%) where L represents the locations probability and T represents the time probability.

included in the difference between the (50,10) data and the (50,50) data are not representative of the land mobile environment where receive antennas are immersed in the local clutter. To be applicable to land mobile applications, modify the (50,10) criteria to an adjusted (50,50) by adding the maximum difference between the (50,10) values and the (50,50) to the (50,50) values. These values were obtained from FCC Report R-6602 Figures 10 and 26 to be 11 dB for the VHF band and 14 dB for the UHF band.

Table 12 – Recommended Modified PSA Co-channel Values

Band (MHz)	Original Criteria	Modified Criteria	C/I provided
150	37(50,50)/19(50,10)	37(50,50)/8(50,50)	29 dB
220	38(50,50)/28(50,10)	38(50,50)/17(50,50)	21 dB
450	39(50,50)/21(50,10)	39(50,50)/7(50,50)	32 dB
700/800[12]	40(50,50)/22(50,10)	40(50,50)/8(50,50)	32 dB

Table 12 describes the recommended PSA co-channel levels. For shared channels these values are not applicable unless protecting a PSA. The primary direction of analysis is from applicant to incumbent. This allows an applicant to elect to receive additional interference as a condition of obtaining a license when the number of possibilities is small.

Table 13 - Interaction Between Shared and PSA Users

Incumbent	Applicant	Comment
Shared	Shared	Best Fit. Many subjective decisions involved
Shared	PSA	Applicant PSA has option to take greater Interference to obtain license
PSA	Shared	Shared needs to protect PSA
PSA	PSA	Applicant PSA has option to take greater Interference to obtain license

The probability of interference can be adjusted by varying the margin for interference and then evaluating the joint probability of achieving the *C/N* performance in the presence of *C/I*. The following formula, table, and graph can

[12] The Public Safety band, originally 821-824/866-869 MHz has been relocated to 806-809/851-854 MHz and has different requirements for different Regional Frequency Planning Committees. The 700 MHz Public Safety Band also has different criteria based on the degree of urbanization and Regional Frequency Planning Committees. In both cases, local requirements ought to be followed.

be used to estimate the interaction. Fortran programs[Kalagian 76] and [Wong 82] are available from the FCC to automate this process. The probability of interference is defined as the probability that the interference signal *(I)* is greater than the desired signal level *(C)* for a given mean *C/I* ratio. The mean *C/I* value does not include the necessary factor to achieve CPC for the modulation technique of the victim receiver. For example, if the mean *C/I* is 35 dB and the CPC of the victim is 15 dB, then the probability of interference would be calculated by reducing the mean *C/I* by the CPC margin, 35 dB - 15 dB = 20 dB. Then the probability of interference would be less than 4 % for a lognormal standard deviation of 8 dB and less than 0.6 % for a standard deviation of 5.6 dB.

For initial frequency coordination use the log normal standard deviation value of 8 dB.

$$\text{Probability of Interference}^{13} = \frac{1}{2}\left(erfc\left(\frac{C/I}{2\sigma} \right) \right) \qquad (22)$$

Table 14 - Probability of Interference

Probability of Interference σ = 8 dB	Mean *C/I* (dB) (Does not include necessary CPC margin)
0.5%	29.26
1.0%	26.36
2.0%	23.25
3.0%	21.28
4.0%	19.81
5.0%	18.61
6.0%	17.59
7.0%	16.69
8.0%	15.86
9.0%	15.16
10.0%	14.50

[13] In this situation, there are two variables, the desired and an interferer. Thus the denominator of the *erfc* function is root sum squared. This changes the equation from probability of achieving a margin for signal strength to the probability of achieving a margin over an interfering signal.

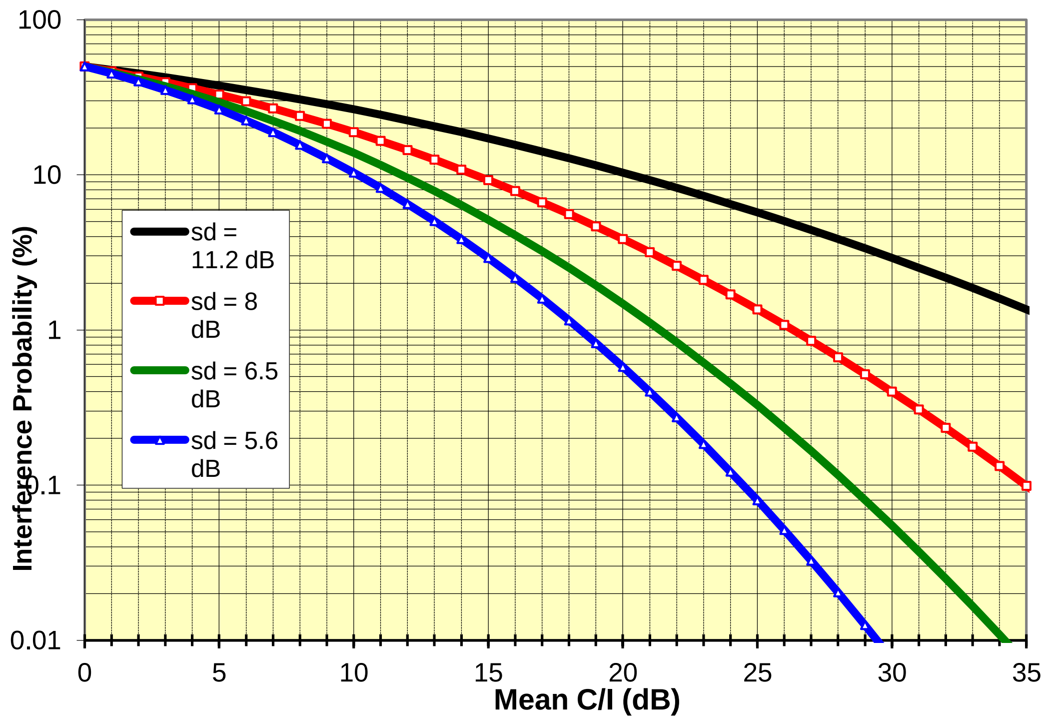

Figure 16 - Probability of Interference vs. Mean C/I[14]

6.5.4 Adjacent Channel Considerations

The adjacent channel contour can be determined by increasing the modified appropriate co-channel interference contour based on the source to victim ACPR, where the ACPR is adjusted for the frequency drift as defined in § 5.7.2.3 [88.1]. For easy reference, the stability values for use in the calculation are shown in Table 17 of [88.1].

6.6 HAAT Calculation

It has been observed that the methods contained in Federal Communications Commission Regulations Part 90 (§§ 90.309(a)(4), 90.621(b)(4)(i)) can give inconsistent results for the calculation of HAAT and DHAAT, respectively. This section is intended to be sufficiently specific that calculations made according to its principles always yield the identical results for identical situations.

---

[14] C/I does not include CPC requirement.

6.6.1 Terrain Database

6.6.1.1 Terrain Database resolution

The recommended resolution for the standard database at frequencies below 1 GHz is 3 arc seconds. Points are specified on the intersection of the 3-second grids. Thus the point at N. Latitude 30-0-3, W. Longitude 100-0-3 represent a tile whose corner coordinates are the following:

SE: 30-0-1.5, 100-0-1.5

NE: 30-0-4.5, 100-0-1.5

NW: 30-0-4.5, 100-0-4.5

SW: 30-0-1.5, 100-0-4.5

6.6.1.2 Basis and methodology for extracting values

Extract elevation values from the best available data having unrestricted distribution. In each case, where the source data is 3" or better, or, if registered to UTM (distance), 100 meters or smaller, use the nearest point from the source data to the desired output intersection point. In the case where the best available source data is coarser than 3” or 100 meters, use bilinear interpolation [Wong 82] of the data to derive output values.

6.6.1.3 Data extents

The published database includes all US States, Territories and Possessions, extended 320 km into any foreign land and ocean area around them.

6.6.1.4 Data format

The elevation values need to be in integral meters, and digitally published in 2 byte integer format above mean sea level in 1 x 1 degree blocks. Format can be compressed using any of the following “zip” formats: .Z, .ZIP or .GZ

6.6.1.5 Reissue

The standard database ought to be reissued with corrections and improvements (if any) every two years, with the status of updates indicated on the web site.

6.6.1.6 Availability

Terrain data re-sampled at 3 arc-second intervals from 30-meter data is available at the following URL: http://www.its.bldrdoc.gov/The US data is zipped. A FORTRAN routine to extract the data is available at the site. For Canada and Mexico data, a pointer is provided to the GLOBE database.

Higher resolution data should yield more accurate elevation estimates for the individual points along each path. However, depending on the situation, this may not yield an overall improvement in modeling accuracy.

6.6.2 HAAT DEFINITION

6.6.2.1 Station HAAT Definition

All terrain data intersection points within the database between 3 and 16 km are to be averaged to compute the average elevation. Points at distances of 3.0 km or greater and at 16.0 km or less are to be included in the average. Include points over water (lake or ocean) and points over foreign land. The HAAT is calculated by subtracting the average elevation from the elevation of the antenna.

This method, when compared with radial averages extracted at 5 degree increments or less, closely approximates but is not exactly equal to the average of the radial averages.

6.6.2.2 Radial HAAT Definition

At any single azimuth, points at 100-meter intervals are to be extracted from the terrain data, beginning at 3.0 km and ending at 16.0 km, and averaged (divide by 131).

6.6.2.3 Station-to-Service Area HAAT Definition

Find the range of azimuths from the station of interest that barely encompass the “victim” service area. HAAT is calculated as in §6.6.2.1, except that only points within the predetermined range of azimuths are included in the calculation.

Station-to-Service Area HAAT is intended to more accurately portray the same information that the Federal Communications Commission’s directional HAAT (DHAAT) portrays.

6.6.2.4 Radial Point extraction method

Calculate, using Great Circle methods, the latitude and longitude of each applicable point, and use the closest terrain data point (no interpolation).

6.7 Terrain Elevation Dataset

The propagation prediction model defined in this specification inherently depends on the terrain dataset to compute the effective base antenna height for use and for the geometry computations for the shadow loss equations. In the United States, there are currently seven terrain datasets that are commonly used:

1) The 30 arc second National Geophysical Data Center (NGDC) dataset

2) The 3 arc second (U.S. Geological Survey (USGS) or Defense Mapping Agency (DMA)[15]) dataset

[15] Former name of NGA (National Geospatial Intelligence Agency)

3) The 30 meter (USGS) National Elevation Dataset (NED). For more information see http://www.asprs.org/a/publications/pers/2002journal/january/highlight.html.

4) The updated, resampled 3 arc second data per §6.6.1.6

5) The 1 arc-second and 3 arc-second Shuttle Radar Topography Mission (SRTM) dataset. For more information see https://lta.cr.usgs.gov/SRTM

6) The 10-meter (USGS) National Elevation Dataset (NED). For more information see http://nationalmap.gov/elevation.html

7) The 3-meter (USGS) National Elevation Dataset (NED).

The 30 second dataset is primarily used by the FCC and those filing FCC applications to determine 2-10 miles (3-16 km) average terrain along radials emanating from a transmitter site for the purpose of determining the location of coverage of interference signal contours. Because of its wide point spacing (nearly 1 km), its use for more detailed propagation studies is not common.

The 3 arc second dataset is the one most commonly used for propagation studies in the conterminous United States. Its point spacing of about 90 meters north-south by an average of 70 meters east-west seems appropriate for many planning purposes, especially when wide-area systems with service radii of 50 km or more are being considered. Considering coverage and interference with a grid spacing of less than 100 meters is rarely necessary. The 3 arc second dataset is also a convenient size for use on personal computers since with reasonable compression techniques the entire dataset can fit and be used from an inexpensive CD-ROM drive.

The main drawback to the 3 arc second dataset is its vertical accuracy. For the most part it was derived from the 1:250,000 series of maps covering the US. Most of these maps have contour intervals of 200 feet. The result is that many ridges and hills with peak elevations that lie between 200 foot contour intervals are not properly represented. Even some peaks where USGS benchmarks are shown on the maps were not properly digitized. Occasionally, elevation errors occur, some as great as 200 meters.

The 1 arc second data contains elevation data points spaced at approximately 30 meter intervals rather than intervals based on latitude and longitude. Its development has been a on-going effort by the USGS over the last several years. It is fundamentally derived using contour and other information from the 7.5 minute quadrangle series maps which cover the US. Since the data source has a finer resolution than the data source for the 3 second dataset, the vertical accuracy achieved is significantly better.

The much-improved vertical accuracy of the 1 arc second data warrants consideration for a development effort of an up-to-date propagation model. “For the model defined here, the 3-arcsecond data re-sampled from 1 arc second data described in § 6.6.1.6 is the fundamental recommended dataset.

The ⅓ arc second NED data has identical vertical accuracy to the 1 arc second NED data, but has a horizontal resolution 3 times as fine, or about 10 meters. Because of the execution time and disc storage versus accuracy improvement tradeoff, it is not typically used for path studies at frequencies below ~1.5 GHz.

The $^1/_9$ arc second NED data has identical vertical accuracy to the 1 arc second NED data, but has a horizontal resolution 9 times as fine, or about 3 meters. However, it currently covers only a very small portion of the United States. At frequencies below ~1.5 GHz using the models described in this document, this improvement in spatial resolution will yield little or no improvement in prediction accuracy. Because of this and the execution time and disc storage issue, it is almost never used for path studies at frequencies below ~1.5 GHz.

6.7.1 Establishing Terrain Elevation Points Along a Profile Using the Terrain Dataset

In practice the model needs a terrain elevation profile to be defined between the transmitter and the receiver. This profile is fundamental to the path loss prediction techniques in §6.1. The elevation points on this profile are to be extracted from the terrain dataset by first determining the great circle path from the transmitter to the receiver. Spacing between adjacent data points ought not exceed 0.2 km or 0.2% of the path length, whichever is finer. Either method can be used regardless of the horizontal resolution of the dataset. Either of the following extraction techniques is acceptable.

6.7.1.1 Bilinear Interpolation

A profile elevation point spacing is selected. At a point some distance d from the transmitter along the great circle path where the profile elevation is to be found, the latitude-longitude or other coordinates of the point (the lookup point) are determined using double precision spherical trigonometry. These coordinates are then used to find the four surrounding elevation points; linear interpolation is used to establish the elevation at the lookup point. This process is used to find the elevation at each of the points along the profile from the transmitter to the receiver.

6.7.1.2 “Snap to Nearest Point” Method

The equation of the line segment between the transmitter and the receiver is established. Using conventional spherical trigonometry techniques, the distances from all points to the line are determined. The elevations of all points within 0.5 $\times$ (the horizontal resolution of the dataset) are used. Their corresponding horizontal positions along the profile are the crossing points of perpendiculars from the points to the line. This method produces profiles with unequal horizontal spacings, but the results produce equally valid results as those using the method described in §6.7.1.1.

6.8 Local Clutter Loss Attenuation Standard Values

The path loss predictions used in §6.1 can be improved by applying a local clutter loss factor. Apply an urban, suburban, or foliage loss correction that is determined by a land use or ground cover type associated with the user's receiver location. Four land cover datasets are currently available from the USGS: The Land Use / Land Cover (LULC) dataset [Anderson 76], the National Land Cover Dataset of 1992 (NLCD-92) [Vogelmann 01], the National Land Cover Dataset of 2001 (NLCD-01) [USGS 07], and the National Land Cover Dataset of 2006 (NLCD-06) [USGS 11] , and the National Land Cover Dataset of 2011 (NLCD-11) [Homer 15]. . However the LULC dataset is obsolete and will not be considered further in this document.

NLCD-92 is available as grid data in which one of 21 land cover types is assigned to each 30-meter square cell. The categorization scheme used for NLCD-92 is less than ideal for land mobile radio coverage analysis but is acceptable. The NLCD-01, NLCD-06, and NLCD-11 datasets have identical categorization schemes. These datasets are more recent but their categorization scheme is somewhat less useful than NLCD-92 for land mobile radio coverage analysis. On balance, however, NLCD-11 is the best choice given that recency of data is very important.

6.8.1 Classification Values

With the exception of categories 21-23 in NLCD-92 and 21-24 in NLCD-01, NLCD-06, and NLCD-11, the remaining land use classifications in the land cover datasets are much too fine-grained for radio propagation use. Table 15 shows a recommended way of reducing the 29 NLCD01/06/11 classifications to 10. Table 16 shows a recommended way of reducing the 21 NLCD92 classifications to 10. Table 18 shows the value of $A_{clutter}$ to be used for each of the reduced classifications as a function of frequency. If no land cover database is available for use, an alternative approach is to use local knowledge to classify the ground cover according to the general categories shown in Table 17, which also maps those categories to the classifications used in Table 18.

Table 15 - Re-Classification of USGS NLCD-01, NLCD-06, and NLCD-11 Classes

USGS Classification Number	USGS Classification Description	New Classification Number	New Classification Description
11	Open Water	4	Water
12	Perrenial Ice/Snow	10	Snow & Ice
21	Developed, Open Space	1	Open Land
22	Developed, Low Intensity	7	Residential
23	Developed, Medium Intensity	8	Mixed urban/buildings
24	Developed, High Intensity	9	Commercial/industrial
31	Barren Land (Rock/Sand/Clay)	1	Open Land
32	Unconsolidated Shore	1	Open Land
41	Deciduous forest	5	Forest land
42	Evergreen forest	5	Forest land
43	Mixed forest	5	Forest land
51	Dwarf Scrub	3	Rangeland
52	Shrub / Scrub	3	Rangeland
71	Grassland / Herbaceous	3	Rangeland
72	Sedge / Herbaceous	5	Rangeland
73	Lichens	1	Open land
74	Moss	1	Open land
81	Pasture / Hay	2	Agricultural
82	Cultivated Crops	2	Agricultural
90	Woody Wetlands	5	Forest land
91	Palustrine Forested Wetland	5	Forest land
92	Palustrine Scrub/Shrub Wetland	3	Rangeland
93	Estuarine Forested Wetland	5	Forest land
94	Estuarine Scrub/Shrub Wetland	3	Rangeland
95	Emergent Herbaceous Wetland	6	Wetland
96	Palustrine Emergent Wetland (Persistent)	6	Wetland
97	Estuarine Emergent Wetland	6	Wetland
98	Palustrine Acquatic Bed	6	Wetland
99	Estuarrine Acquatic Bed	6	Wetland

Table 16 - Re-Classification of USGS National Land Cover Dataset (NLCD92) Codes

USGS Classification Number	USGS Classification Description	New Classification Number	New Classification Description
11	Open Water	4	Water
12	Perennial Ice and Snow	10	Snow & Ice
21	Low-intensity Residential	7	Residential
22	High-intensity Residential	7	Residential
23	Commercial/Industrial/Transportation	9[1]	Commercial / Industrial
31	Bare Rock, Sand, Clay	1	Open Land
32	Quarries/Strip Mines/Gravel Pits	1	Open Land
33	Transitional	1	Open Land
41	Deciduous forest land	5	Forest land
42	Evergreen forest land	5	Forest land
43	Mixed forest land	5	Forest land
51	Shrub land	3	Rangeland
61	Orchards/Vineyards/Other	2	Agricultural
71	Grasslands/Herbaceous	3	Rangeland
81	Pasture/Hay	2	Agricultural
82	Row Crops	2	Agricultural
83	Small Grains	2	Agricultural
84	Fallow	2	Agricultural
85	Urban/Recreational Grasses	2	Agricultural
91	Woody Wetlands	5	Forest Land
92	Emergent Herbaceous Wetlands	6	Wetland

Table 17 - Reclassification of General Ground Cover Categories [For use when Land Cover Categories are not available]

Macroscopic Ground Cover Database Categories	Description	New Classification Number	New Classification Description
00	UNKNOWN	1	Open land
10	RURAL OPEN	[Further differentiation needed]	
11	Pastures, grassland	1	Open land
12	Low crop fields	2	Agricultural
13	High crop fields (vines, hops, ...)	3	Rangeland
19	Park land	3	Rangeland
20	TREE COVERED	5	Forest land
21	Irregularly spaced sparse trees	5	Forest land
22	Orchard (regularly spaced)	5	Forest land
23	Deciduous trees (irregularly spaced)	5	Forest land
24	Deciduous trees (regularly spaced)	5	Forest land
25	Coniferous trees (irregularly spaced)	5	Forest land
26	Coniferous trees (regularly spaced)	5	Forest land
27	Mixed tree forest	5	Forest land
28	Tropical rain forest	5	Forest land
30	BUILT-UP AREA	[Further differentiation needed]	
31	Sparse houses	7	Residential
32	Village center	7	Residential
33	Suburban	7	Residential
34	Dense suburban	8	Mixed Urban/buildings
35	Urban	8	Mixed Urban/buildings
36	Dense urban	8	Mixed Urban/buildings
37	Industrial zone	9	Commercial/Industrial
40	DRY GROUND	1	Open land
42	Sand dunes	1	Open land
43	Desert	1	Open land

Table 18 - Local Clutter Attenuation in dB as a Function of Frequency and Land Use Classification

	Frequency (MHz)					
Classification	**30-50**	**136-174**	**220-222**	**380-512**	**746-941**	**Reclassified Number**
Open land	1	3	3	3	5	1
Agricultural	2	3	3	4	18[1]	2
Rangeland	1	9[1]	9	10[1]	10	3
Water	0	0	0	0	0	4
Forest land	3	8[1]	9	12	25[1]	5
Wetland	1	3	3	3	3	6
Residential	3	14[1]	15	16[1]	20[1]	7
Mixed urban/ buildings	4	15[1]	16	17[1]	20[1]	8
Commercial/ industrial	4	14[1]	14	15[1]	20[1]	9
Snow & Ice	0	0	0	0	0	10

1. Taken from [Rubinstein 98]. Non-superscripted values are derived from industry sources.
2. The density of foliage in a particular urban environment can heavily influence values for urban settings. Heavily forested urban environments can exhibit clutter losses in excess of those published here.

6.8.2 NLCD Re-sampling

Depending on its application, it might be desirable to resample the NLCD-92, NLCD-01, NLCD-06, or NLCD-11 raw 30-meter square cells to some coarser resolution, e.g., 3 arc-second. The following procedure describes a method of re-sampling the NLCD data with the intent of selecting a classification that favors the most realistic propagation environment for the new cell.

1. Map the classifications from NLCD as described above.
2. Translate the NLCD native projection and coordinate system to the desired projection and coordinate system.
3. Determine the location in the NLCD database where the desired data point resides (x, y).
4. Use the area of x ± n columns by y ± n rows around the point and extract the data from the NLCD database. “n” is half the resolution of the new database.
5. Determine the number of occurrences for each classification.
6. Multiply the number for each classification by the weighting factor in Table 19.
7. Determine the classification with the greatest result from the above step. This is the classification for the resampled cell. In the event that more than one classification has equal results select the classification with the largest weighting factor.

By way of example suppose after step 5 that there were 20 points of Forest and 18 points of Residential. After applying the weighting factor there would be a score of 120 for Forest and 144 for Residential. The cell would be classified as Residential even though the majority of the data is Forest.

Table 19 - NLCD Re-sampling Weights

Classification	Weight
Open Land	3
Agricultural	4
Rangeland	5
Water	1
Forest land	6
Wetland	2
Residential	8
Mixed urban/buildings	9
Commercial / Industrial	7
Snow & Ice	1

6.8.3 Clutter Loss Measurement in a Mobile Environment

Clutter loss measurements are desirable to refine signal strength predictions beyond the accuracy that is possible when more general methods are employed.

6.8.3.1 Methodology

A standard communications receiver can be used for the clutter loss measurement. If the receiver's Received Signal Strength Indicator (RSSI) bus is considerably more sensitive than the sensitivity corresponding to the desired CPC, a preamplifier might not be necessary to extend the measurable range; otherwise, a low noise preamplifier can be connected between the antenna and the receiver. Calibrate the receiver. Connect a signal generator to the input of the preamplifier (or the receiver if no preamplifier is used). In the low signal range, calibrate in 1-decibel intervals. Repeat each calibration point many ($\geq$ 30) times to ensure a valid reading. All of this can be automated by a data acquisition device/system. Calibrate in accordance with §4.1.2.3 of [845]

The actual readings are taken by driving around the evaluation area using a test setup to take readings in an automated fashion[16]. A typical test setup would consist of the antenna and receiver, a notebook computer, and an analog-to-digital (A/D) converter on a PCMCIA card. A more fully automated system could include GPS or DGPS data to eliminate user interface for location information.

---

[16] The measurement methods of TSB-176 [TIA 09] are recommended. The data recording format of TIA-845-B [TIA 10] is also recommended.

A computer program can be written to take the necessary readings subtract the effects of the antenna system, compare the results to the calibration curve, and note the results corresponding to a given location. This gives a power value, typically in dBm.

After taking the data, the user can then establish signal contours for the area and frequency band of interest.

6.8.3.2 Associating Local Signal Measurements with Land Cover categories

The signal strength measurements that Table 18 is based upon were taken in specific areas. While many of the values are based upon measurements [Rubinstein 98] that were taken in three different types of terrain (urban and suburban with sparse trees, suburban with dense trees, and forested rural), locally taken measurements are best for predicting those values over a more diverse, but still local, set of terrain. Where practical, it is recommended that signal measurements be taken over a local sample area. The values in Table 18 provide a good estimate where such measurements are not practical.

To implement a local land cover survey, consider the following material:

a. Choose a Land Cover dataset to use in categorizing the data. If available in the area of interest, use NLCD-11 as it is the most current.

b. Based upon the Land Cover category data create a route that covers as many tiles containing each Land Cover Category of interest as possible. It is recommended that at least 30 tiles for each category be covered and that the test sample area be selected, insofar as is practical, such that each category is found in more than one portion of the sample area; i.e. not a single grouping. Note also, because shadow loss varies over small distances and is difficult to accurately predict, only make measurements along unshadowed paths to prevent introducing that inaccuracy into the measured data.

c. Make a signal strength survey according to the principles described in §6.8.3.1 above and in TSB-176 [TIA-09].

d. Select a model (e.g. the model of §6.1) against which you wish to compare the measured data and run a prediction using that model.

e. For each measurement point, calculate the difference between the predicted value and the measured value.

f. Gather the data on a Category-by-Category basis. Plot the data for each category using box-and-whisker plots[17] [Hoaglin 83].

g. See sidebar box adjacent to §5.3.3.2 Visually inspect the plots to determine whether the data is reliable[18]. If it is, use the median value in preference to the more general values in Table 18.

h. Like all data, this data should be ought to in a form that can be easily identified and retrieved.

6.9 Propagation Modeling and Simulation Benchmarks

The following referenced path profiles and tabulated path losses are to serve as benchmark results of the propagation prediction model. Those interested in creating computer implementations of the model described in this section can use these tests to verify their implementation.

From the NBS measurement program reported by McQuate *et al* [McQuate 68] and studies by Hufford [Hufford 91], the following path numbers were selected:

R1-20-T1	R2-10-T3	T1-10-R1
R1-20-T3	R2-10-T4	T1-10-R3
R1-20-T7	R2-10-T7	T1-10-R6
R1-50-T4	R2-20-T5	T1-20-R5
R1-50-T5	R2-20-T8	T1-80-R7
R1-50-T6	R2-20-T9o	T4-50-R7
R1-50-T7	R2-50-T3	T5-20-R7
R1-50-T8	R2-50-T4	T6-10-R2
R1-50-T9	R2-50-T5o	T7-80-R6o
R1-80-T1	R2-120-T2	
R1-120-T5	T1-5-R1	

The exact endpoint coordinates for these paths are contained in the above-cited documents. Measured path losses, as a function of receive antenna height above ground and at several frequencies, are shown on graphs in[Lustgarten 77]
Lustgarten, M.N. & J.A. Madison, "An empirical propagation model", *IEEE Trans Electromag Compat*, 19(3), Aug 1977.

[17] While other methods of considering outliers and dispersion of a dataset exist, the box-and-whisker plot is recommended because of its simplicity and intuitiveness.
[18] Indications of possible data unreliability include the following: (i) widely-spread inter-quartile range, (ii) greatly unbalanced 2nd vs. 3rd quartiles, (iii) large number of outliers.

[the above-cited documents. The same information can also be found at the following URL: http://www.its.bldrdoc.gov/resources/radio-propagation-data/radio-propagation-data.aspx.

For modeling broadband LTE systems, simulators may be calibrated using Section A.2.2 of [3GPP 10]. This procedure addresses: downlink and uplink configurations; coupling gain (for multi-antenna systems); predicted SINR; user throughput; and spectral efficiency. It is applicable for the broadband path loss models listed in Table B.1.2.1-1 of [3GPP 10].

6.10 Recommendations Concerning Tiled vs. Radial Metaphors

A number of possibilities exist for defining the plane of the service area. The most widely used are the following:

- The Radial method
- The Stepped Radial method
- The Grid Mapped from Radial Data method
- The Tiled Method

6.10.1 Radial Method

In the radial method, many radials are drawn at equal angular intervals from the site to the far edge of the service area. Elevation points are extracted from the database at intervals along each radial. Each point represents an annular segment of service area. Since the radials get farther and farther apart as the distance from the site increases, take care to ensure that the number of radials is sufficient to adequately characterize the area near the outer edge.

6.10.2 Stepped Radial Method

In the stepped radial method, the angular interval is stepped with distance. For example, in the Communications System Performance Model method (CSPM) [Jennings 77], 8 radials are drawn from 0 to 2 km, 16 radials for 2 to 4 km, and so on up to 2,048 radials at distances of greater than 256 km. This results in a distance between radial ends not exceeding 1.57 km for all distances up to 512 km. Once again, each point along a radial represents an annular segment.

6.10.3 Grid Mapped from Radial Data Method

With this method, basic path loss information is calculated at points along radials as described in §6.10.1 and §6.10.2, and this information is then mapped into a uniform grid using linear or other interpolation methods. The derived signal levels at the grid locations can be then used for analyzing signals from multiple transmitters at common tiles being analyzed. This method combines the calculation speed advantages of radial methods over tiled methods, while still providing a common grid or tile structure for uniform multi-transmitter, multi-site system analysis.

6.10.4 Tiled Method

In the tiled method, rectangular[19] tiles of a given size are predefined throughout the service area. Radials are drawn to each of these tiles. This results in unequal angular spacing necessitating a greater number of radials to predict signal levels in a given geographical area. The advantage is that a specific path loss calculation has been done to each tile centroid rather then being interpolated from nearby path loss calculation points.

6.10.5 Discussion of Methods

In predicting signal strength, only the radial method presents any kind of problem and, if the user is willing to increase the number of radials sufficiently, that problem can be averted. In predicting interference or simulcast performance, however, new problems arise. In the tiled method, all predictions from all sites are done to the same set of endpoints. Therefore, signal strength and delay spread prediction values can be calculated at those points. The grid mapped from radial data method provides a similar feature by using a set of interpolated endpoints.

Conversely, however, either radial method predicts to arbitrary endpoints. For a two-site system, the situation is not hopeless. The program needs to calculate the crossing points between the radials originating at the two sites and calculate its capture ratios, signal strengths, and delay spreads at those points. However, radial crossings become extremely far apart at angles approximating the azimuth between the two sites. Overall, the results of the radial approach to simulcast or interference prediction in a two-site system are mediocre at best.

In a system of three or more sites, the problem becomes more complicated. The tiled method still works well because the calculation points are predefined. The grid mapped from radial method also does the job. The radial method, however, becomes even more problematic. It is highly improbable that there are ANY crossings that exist between radials from three or more sites. This means that any straight radial system is unable to be used.

---

[19] In practice, the tiles might be squares or curvilinear trapezoids as well.

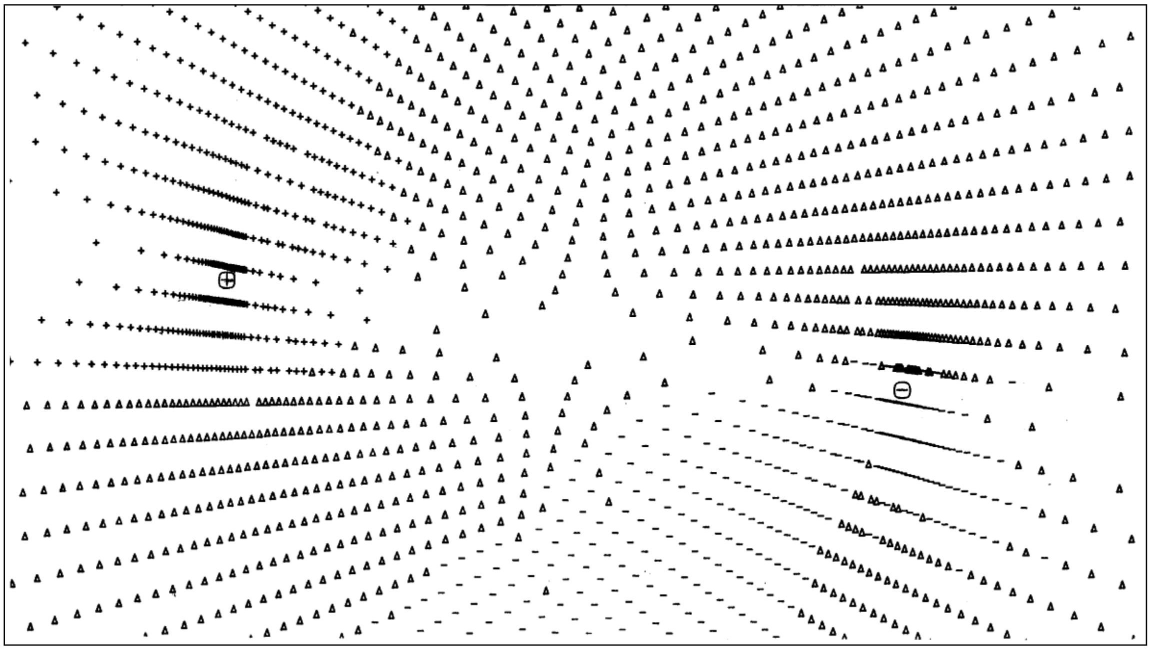

Figure 17 - Radial Crossings in a 2-Site System

Notes to Figure :
1: Figure is a randomly-selected capture ratio map
2: Symbols:
  Circled "+" = Site 1
  "+" = Signals from Site 1 exceed those from Site 2 by predetermined ratio
  Circled "-" = Site 2
  "-" = Signals from Site 2 exceed those from Site 1 by predetermined ratio
  "∆" = Capture ratio does not exceed predetermined value
3: In the example, the "+" site is omni and the "-" is directional toward 240°

6.10.6 Summary and Recommendations

All four of the methods listed above can provide acceptable results for predicting signal strengths in the region around a single transmitter if proper consideration is given to the resolution of the study method and the objectives of the signal strength prediction. However, for broadband, simulcast, interference, best server, and other studies involving two or more transmitters, of the four methods listed, the grid mapped from radial method (§6.10.3) and the tiled method (§6.10.4) are best suited to providing acceptable results and are therefore recommended for such applications. For broadband communications as defined in [88.4], tile based methods are recommended.

6.11 Reliability Prediction

The prediction of mean signal strength at a given location can vary from the measured signal for many reasons, including the following:

- Prediction algorithm not adequate
- Terrain database imperfections
- Land cover database imperfections
- Measurement made at slightly different location than prediction

Because of this, the signal at any one location can vary from that predicted by the model. It is suggested that an additional margin of 1 dB be added for these "uncertainty" effects.

Additionally, signal variations due to land clutter tend to follow a lognormal distribution with a standard deviation of 5.6 dB, which includes a measurement error standard deviation of 1 dB. This value is applicable only when the terrain database recommendations of §6.7 are followed, including the local clutter database from Table 18.

In determining the amount of extra margin to include, apply the user's requested reliability level, and (because the only interest is in the signal equaling or exceeding a given value, rather than being in a given range) apply the "one-tailed" statistical test. Values of suggested margins for particular predicted reliabilities follow; these values are applicable only when the terrain database recommendations of §6.7 are followed:

Table 20 - Tile Reliability Margins

Tile Reliability	Clutter Margin	Uncertainty Margin (if used)	Necessary Margin
90 %	7.2 dB	1.0 dB	8.2 dB
95 %	9.2 dB	1.0 dB	10.2 dB
97 %	10.5 dB	1.0 dB	11.5 dB

For narrowband models, no additional margin is included for time (temporal reliability). This implies that measurements taken at different times over the same locations would produce similar results. Evaluate seasonal changes for worst case scenarios, such as tree losses with leaves rather than without.

For broadband coverage modeling, a per tile Monte Carlo is recommended. Broadband systems allow significant changes in frequency and uplink power allocations per user on a much finer temporal scale than narrowband LMR systems. LTE intracell interference changes every TTI (1ms) due to new resource assignments and log normal shadowing. As the link environment changes, broadband systems optimize performance for the current link SINR. A Monte Carlo approach is better suited to modeling the complexities of traffic patterns, interactions between base station schedulers, device location and broadband interference mitigation features.

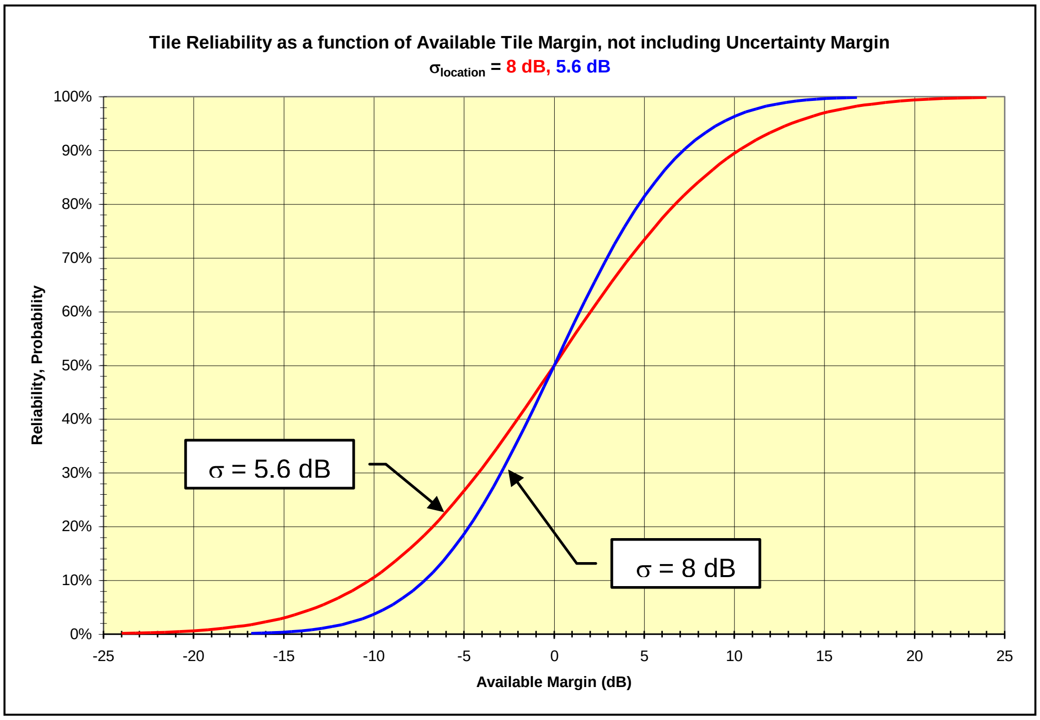

Figure 18 - Tile Reliability, No Uncertainty Margin

6.12 Interference Calculations

Two methods of calculating interference from multiple lognormally-distributed sites are presented here: Monte Carlo simulation, and the "Equivalent Interferer" method. The Monte Carlo method can produce a more precise representation for the sum of lognormal interferers. However, for this application, the inherent accuracy of both methods is limited by the accuracy with which the constituent interference distributions are known.

Monte Carlo is recommended for broadband coverage modeling described in [88.4]. Broadband equipment possess a variety of interference mitigation features including interference rejection combining, frequency selective scheduling and inter-cell interference coordination. Radio Access parameters such as type of modulation, coding rate, and power control vary independently for each link. Interference impact to broadband communications is a function of proprietary implementations of these features as well as loading. For all of these reasons, aggregating interference sources into a single equivalent interferer is not feasible for broadband communications systems. The complexity of choices is better suited to Monte Carlo modeling. See [88.4] for additional details on broadband interference mitigation features.

6.12.1 Equivalent Interferer Method

If there is only one potential interferer, use its mean and standard deviation. If there are more than one, calculate the statistics of the "equivalent interferer" as follows:

$$\mu_j = 10^{\frac{m_{jdB}}{10}} \times \exp\left(\frac{\sigma_{jdB}\ln(10)}{20}\right) \qquad (23)$$

$$D_j^2 = 10^{\frac{m_{jdB}}{5}} \times \left[\exp\left(\frac{\sigma_{jdB}\ln(10)}{5}\right) - \exp\left(\frac{\sigma_{jdB}\ln(10)}{10}\right)\right]$$

$$\mu = \sum \mu_j \qquad (24)$$

$$D^2 = \sum D_j^2$$

$$\sigma_{nat}^2 = \ln\left(\frac{D^2}{\mu^2} + 1\right) \qquad (25)$$

$$m_{eq(nat)} = \ln(\mu) - \frac{\sigma_{nat}^2}{2} \qquad (26)$$

$$m_{eq(dB)} = m_{eq(nat)} \times 10\log_{10}(e)$$

Where:

m_{jdB} ≡ The mean signal level of the j^th potential interferer in dB

σ_{jdB} ≡ The standard deviation of the j^th potential interferer in dB

$m_{eq(dB)}$ ≡ The median strength of the equivalent interferer

Note: Use the same standard deviation for all interferers, except for the background noise level and receiver internal noise. Use a standard deviation of 0 dB for the background noise and internal noise.

If $[\tau/(2s_d)] \geq 0$, substitute into the following equation:

$$R = 1 - 0.5 erfc\left[\tau / \left(2s_d\right)\right] \quad (27)$$

Where:

$$\tau = m_d - m_{eq} - C/I_{cri} \quad (28)$$

i.e., the mean desired - equivalent interferer - criterion C/I in dB

s_d = the standard deviation of the desired signal in dB, ***not*** the calculated value in natural units. If $[\tau/(2s_d)] < 0$, solve for R by substituting the absolute value of $\tau/(2s_d)$ for $\tau/(2s_d)$ in the equation for R, then by subtracting this result from 1.

Example of Equivalent Interferer Method:

Assume the following:

- A proposed analog FM system desiring DAQ-3 coverage, $C/(I+N) \geq 17$ dB is required for DAQ-3..
- At a given location, the desired station has a signal strength of -75 dBm.
- Three potential interferers of -102, -108, and -111 dBm.
- Standard deviation of 5.6 dB. (*Example only)*
- Noise for an ENBW of 16 kHz at 150MHz in a residential district.
- Receiver internal thermal noise of -126.6 dBm

m_{1dB} = -102 σ_{1dB} = 5.6 μ_1 = 120.2264E-12 D_1^2 = 380.2635E-22

m_{2dB} = -108 σ_{2dB} = 5.6 μ_2 = 30.1995E-12 D_2^2 = 23.9930E-22

m_{3dB} = -111 σ_{3dB} = 5.6 μ_3 = 15.3156E-12 D_3^2 = 6.0268E-22

Calculate m_{4dB}, the noise value, from § 0.

m_{4dB} = -114 σ_{4dB} = 0 μ_4 = 3.9811E-12 D_4^2 = 0

Calculate m_{5dB}, the thermal noise value

m_{5dB} = *-126.6* σ_{5dB} = 0 μ_5 = 0.2188E-12 D_5^2 = 0

$$\mu = \sum \mu_j = 169.7614E-12 \qquad D^2 = \sum D_j^2 = 410.2833E-22$$

$$\sigma_{nat}^2 = \ln\left[\frac{4.102833\text{x}10^{-20}}{\left(1.697614\text{x}10^{-10}\right)^2} + 1\right] = \ln\left[\frac{4.102833\text{x}10^{-20}}{\left(2.881984\text{x}10^{-20}\right)} + 1\right]$$

$$= \ln(2.423658) = 0.88527813$$

Example (cont'd)

$$m_{eq(nat)} = \ln\left(16.976142\text{x}10^{-10}\right) - \frac{0.88527813}{2} = \text{-}22.939266 nats$$

$$m_{eq(dB)} = \text{-}22.939266 \text{ x } 4.343 = \text{-}99.6\ dB$$

Substituting into [Eq. 26]

τ = -75 - (-99.6) - 17 = 7.6

Where -17 is the C/I value corresponding to DAQ-3.

$$R = 1 - 0.5\text{x}\ erfc\left(\frac{7.6}{2\text{x}5.6}\right)$$

$$= 1 - 0.5\text{x}\ (0.337)$$

$$= 0.832 = 83.2\%$$

6.12.2 Monte Carlo Simulation Method

Treating the remaining sites as potential interferers, run Monte Carlo simulations for points uniformly distributed over the proposed service area. For each point in the proposed service area, do the following in §6.12.2.1 through §6.12.2.6.

6.12.2.1 Calculate Deterministic Signal Strengths

Calculate the (deterministic) signal strengths from the desired station and for all potential interferers at the location currently of interest using the methods of §§0 -6.11. Express the results in dB values (e.g., dBm).

6.12.2.2 Draw from a Pseudorandom Number File

For the proposed station and for all potential interferers, draw a small number of times (e.g., 500) from a pseudorandom number file which has the following distribution: Type = Normal, standard deviation = 1, mean = 0. [For a proposed station and three potential interferers, this results in 2000 draws, 500 corresponding to each station.]

6.12.2.3 Multiply by Known Standard Deviation

Multiply the values thus found by the known standard deviation[20] for the area under consideration. See §6.11.

6.12.2.4 Offset the Calculated Signal Strengths

Offset the calculated signal strengths by the values just calculated; i.e., add 500 of the values calculated in §6.12.2.3 to the proposed station value calculated in §6.12.2.1, add the next 500 to the first interferer's value, etc. Note that, since the values calculated in §6.12.2.3 can have both positive and negative values, the results of §6.12.2.3 can sometimes be larger and sometimes smaller than §6.12.2.1.

6.12.2.5 Calculations for Each of the Samples

For each of the (500) samples, convert the values for the potential interferers to absolute (not dB) values, sum them, and convert the sum back to dB. Subtract this value from the value for the corresponding draw for the desired signal. If this number equals or exceeds the $C/(I+N)$ goal, it is a "pass". Otherwise, it is a "fail".

6.12.2.6 Determine the Probability of a "Pass"

To determine the probability of a "pass" at a given location, divide the number of "passes" by the total number of samples (in the example, 500).

6.12.3 Alternative Methods

6.12.3.1 Alternative Contour Method

The FCC allows for engineering studies for more difficult scenarios. The Model described in §6.1 can be applied to create contours by generating the signal strengths over an area, then finding the distance for a given field strength along each radial. Include only a single Land Usage Correction Factor, representing the land usage in the area where desired and interfering contours intersect.

6.12.3.2 Tile Method

The use of contours has the inherent limitation of preventing the interfering adjacent channel contour from overlapping the desired channel contour - which essentially defines the service area. An interfering adjacent channel contour overlapping or being totally within - such as in the case of co-location, the desired channel contour might be acceptable where the adjacent channel has a large ACCPR value. In these cases, the use of the tile method is recommended.

---

[20] Normally the standard deviation is assumed to be 5.6 dB. This assumption is based on using the high resolution terrain data base as well as the land usage data. When less accurate data is provided then a higher standard deviation is recommended.

Caution: While this might be acceptable for talk-out, talk-in might still be problematic unless additional measures to reduce adjacent channel power (e.g. automatic subscriber output power management, reduced carrier deviation) or network design attributes (e.g. satellite receivers - macro diversity) are employed to mitigate potential interference. The potential for this to occur is raised for trunked systems as the control channel may be interference free while an assigned traffic channel may have an adjacent channel. The extension of the field strength restrictions to 3 or 5 miles (depending on the Regional Frequency Plan) and high ACPR values can create cases where the Near/Far problem in the talk-in direction is increased.

6.13 Building Losses

Building loss is a function of many variables. In general, the loss decreases with increasing frequency due to the mechanisms involved. The materials commonly used in building constructions consists of steel, copper mesh, reinforcing steel mesh and metallic sheets. These are highly lossy and cause the windows to become the main method of penetration. At low frequencies, windows act as waveguides below cutoff, or small slots. Because the wavelength decreases with increasing frequency, the efficiency of coupling improves as more energy can pass through the same aperature. Many new buildings utilize metalized glass which can dramatically increase the penetration loss.

The penetration losses in wooden frame buildings works in the opposite direction. Materials commonly used include glass, brick and mortar, drywall, plywood, wood, and cinder blocks. In this case, the penetration is primarily via the walls and the loss normally increases with frequency [Berg 96]. Stucco buildings use wire mesh and therefore trend more toward industrial building losses. Many new residential structures employ metalized roofing materials which makes the penetration loss more reliant on window coupling.

Buildings incorporating glass with low-emittance coatings ("Low-E" glass), so-called "Green" buildings, experience a propagation mechanism closer to that experienced in wood frame buildings because the windows are much less RF-transparent than normal glass windows. Only a few published papers [Asp 14][Rodriguez 14] have presented measurements of this phenomenon in a Terrestrial Land Mobile environment. These papers suggest that medium buildings incorporating Low-E glass experience an increase in attenuation between 12 and 20 dB at 800-900 MHz as compared to buildings with "ordinary" windows. However, because of the sparseness of the data available, caution is urged in applying this information.

Building loss generally decreases with height [Plets 09]. As the number of stories increases, the loss on the higher floors decreases. . While this can be beneficial from a coverage standpoint, the fact that the probability of interference also increases ought to be considered in system design.

Lower floor losses can increase due to the increased amount of structural steel used. Buildings in earthquake prone areas generally have higher steel content.

Floor to floor losses are considerably higher than penetration loss. This is especially important in high rise buildings where a unit on the main floor could be limited in how many floors higher a desired unit can be and still communicate. In fire ground situations, an external unit is more desireable as it can relay communications and illuminate more of the building.

The following figures provide generalized medium building[21] loss [Davidson 96] [Davidson 97] and standard deviation [Davidson 97]. They are provided as a general reference as they are an amalgamation of many different studies and measurements. Local conditions might change these values. Use the methods in §5.6.4.1 or §5.6.4.2 of [88.3] to determine if the indicated values are applicable. It should be noted that the measurements cited in the Davidson papers were performed before so-called "green" buildings were common, so the losses derived from them and shown in the figures may not be applicable in the case of green buildings.

In general, applying one building loss value across an entire service area is not recommended. It is recommended that specific criteria be applied to defined areas appropriate to the current or envisioned type of construction. The specification can be applied within a geographically specified polygon.

[21] According to [Davidson 97], 'Medium Buildings' are defined as industrial or commercial buildings of reinforced concrete, steel, aluminum, and brick where the loss through the material is very high, and the dominant penetration is through slots (windows, cracks, etc.).

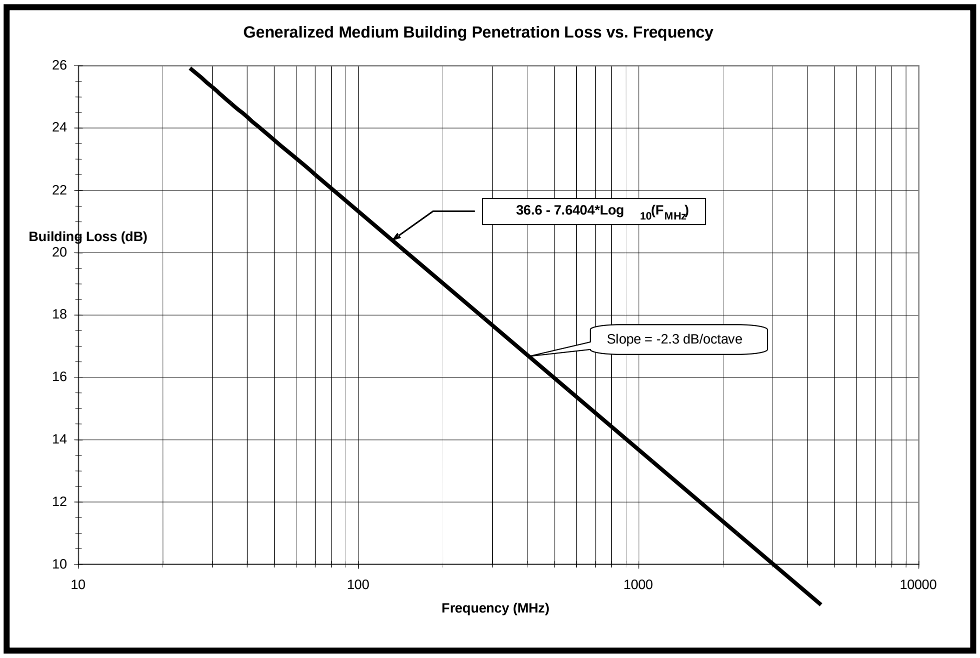

Figure 19 - Generalized Medium Building[21] Penetration Loss

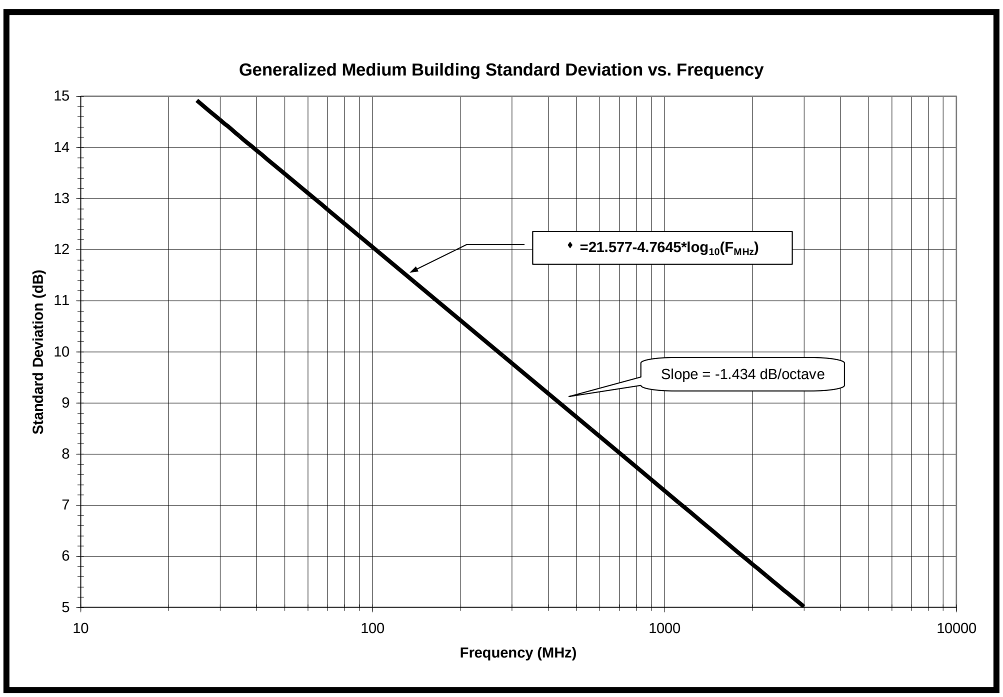

Figure 20 - Standard Deviation, Generalized Medium Buildings[21]

7. Site Diversity

Diversity techniques can be utilized to improve a system's channel performance. The amount of improvement is dependent on a number of factors. The following discussion provides the theory behind the recommendation to only use Aperture Gain in making coverage predictions.

- Number of antennas (Aperture Gain)
- Type of Signal Combiner
- Type of fading
    - Rayleigh Distribution
    - Rician Distribution
- Cross-correlation (ρ) of the arriving signals
    - Antenna Configuration
        - Omnidirectional
        - Sectored (directional)
    - Horizontal Separation of the Base Receive Antennas
    - Arrival angle relative to the Base Receive Antennas
    - "Radius of mobile local scatterers"
    - Mobile distance from the site

The amount of diversity gain that can be realized is composed of two separate factors, aperture gain and fading gain.

7.1 Aperture Gain

The aperture gain is a function of the number of identical antennas.

$$ApertureGain = 10 \times log_{10} NumberOfAntennas \tag{29}$$

Typical configurations in the Land Mobile bands consist of 2 or 3 antennas. As is discussed in § 0 below, 2 antenna configurations are typically sectored due to high correlation in the end-fire direction whereas 3 antennas are typically omnidirectional as the end-fire issue is no longer applicable.

As will be discussed further, the aperture gain is the conservative value to use for diversity gain. When comparing a Rician- to a Rayleigh-distributed signal, there is an apparent fading gain or reduction in fading penalty in the Rician signal. However, this gain is not unique to the multi-branch diversity configuration. Indeed, a Rician-distributed signal received by a single-branch configuration realizes a possibly greater reduction in fading penalty.

An accurate prediction of any change in fading gain is difficult to make. When Rayleigh fading is not present, mobile unit antenna directivity can affect received signal levels. At VHF and UHF sub-microwave frequencies in the mobile environment, it is more practical to assume constant Rayleigh fading and dismiss any mobile unit antenna directivity rather than try to determine complex fading distributions and include mobile antenna directivity and orientation.

7.2 Fading Gain

The amount of fading gain is a function of the fading distribution (e.g. Rayleigh or Rican) and the cross-correlation of the arriving signals.

Figure shows how the various factors affect the cross-correlation (ρ) factor.

The most fading gain is realized when ρ is low and the received signal(s) are Rayleigh faded.

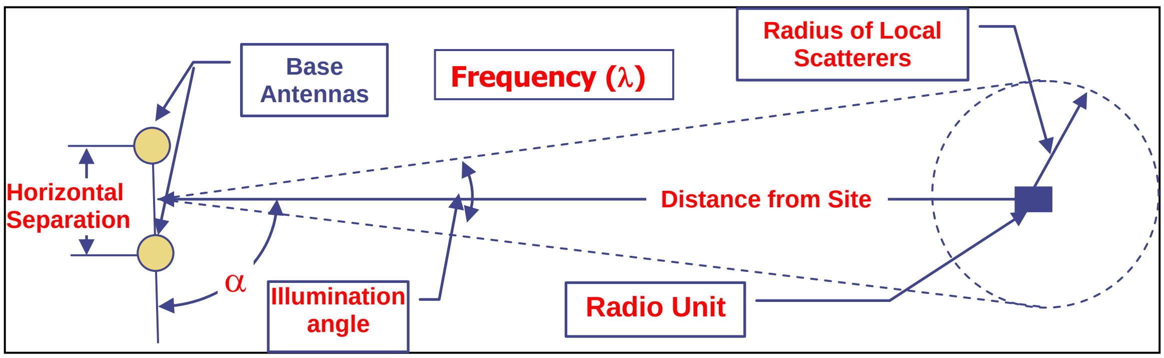

Figure 20 Model of Cross-correlation Factors

The following characteristics impact cross-correlation:

- Antenna Horizontal Separation. The greater the separation, the lower the value of ρ.
- Frequency. The value of ρ is inversely proportional to frequency such that, the shorter the wavelength the lower the resulting value of ρ. Therefore the lower bands with longer wavelengths are less efficient in realizing fading gain.
- Arrival Angle (α). This angle is referenced to a broadside antenna configuration, 90 degrees. Broadside arrival produces the lowest ρ as compared to other angles.
- Radius of Mobiles Local Scatterers. The concept of a radius of local scatterers is useful in predicting fading gain. It is really not a circle, but lends itself to measurement by sounding methods. The larger the radius the lower the cross-correlation until the radius is so large that reflections off local scatterers no longer provide multiple signal rays. See §0 for a more detailed discussion
- Illumination angle. The angle varies with the distance from the site and the radius of local scatterers. The wider the illumination angle the lower

the cross-correlation due to increased path differences. Therefore as the distance from the site increases, the angle narrows for a given radius and the cross-correlation approaches unity.

The value of ρ can be estimated from Equation (30) from [Adachi 86] Equation 18.

$$\rho = \sqrt{e^{-\left[\left[\frac{2\pi}{\lambda} x \left(\frac{H_{separation} \ x \ \text{Radius}_{scatterers} \ x \ Sin(\alpha)}{\text{Distance from Site}}\right)\right]^2\right]}} \tag{30}$$

where the distance units used are all the same; e.g. all in meters or all in feet.

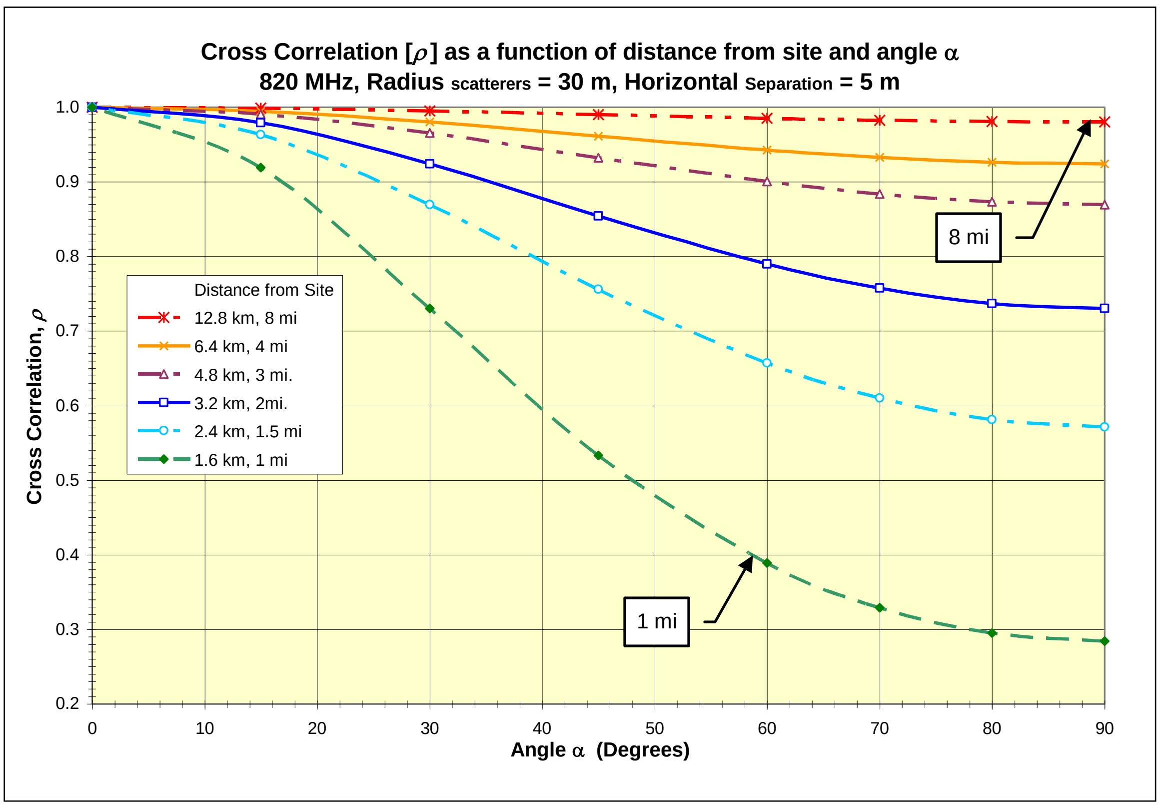

Figure 21 Cross-correlation Example

In a number of publications, notably [Lee 71], a correlation coefficient, ρ, of 0.7 is recommended as the maximum practical value in a diversity system. In Figure , the lowest ρ, i.e. the highest fading gain, occurs close to the site when α is 90 degrees. The example is based on a frequency of 820 MHz, a radius of local scatterers of 30 m.(100 ft.) and a horizontal separation of 5 m (16 ft.). At distances over 3.2 km (2 mi.), ρ exceeds 0.7.

Based on limited measured data, provided by [Butler 96], the amount of fading gain (allowable reduction in C/N) can be approximated at signal levels approaching faded reference sensitivity. Curve fits to the measured data creates equations (31) & (32) which when used in conjunction with equation (30) can estimate the Diversity Gain in a fully Rayleigh faded environment. Figure plots equations (31) & (32).

$$\text{F2br}_{\text{gain}} = 6.3054 - 1.5542(\rho) + 4.858(\rho^2) - 14.343(\rho^3) + 18.867(\rho^4) - 11.218(\rho^5) \quad (31)$$

$$\text{F3br}_{\text{gain}} = 7.7993 - 0.65176(\rho) - 1.7482(\rho^2) + 6.2936(\rho^3) - 6.9929(\rho 4) - 4.9696(10^{-5})(\rho^5) \quad (32)$$

The fading gain can then be estimated by subtracting the aperture gain.

$$Fading\ Gain_{dB} = Diversity\ Gain_{dB} - Aperture\ Gain_{dB} \quad (33)$$

An example of the estimated Fading Gain is shown in Figure for three different frequency bands.

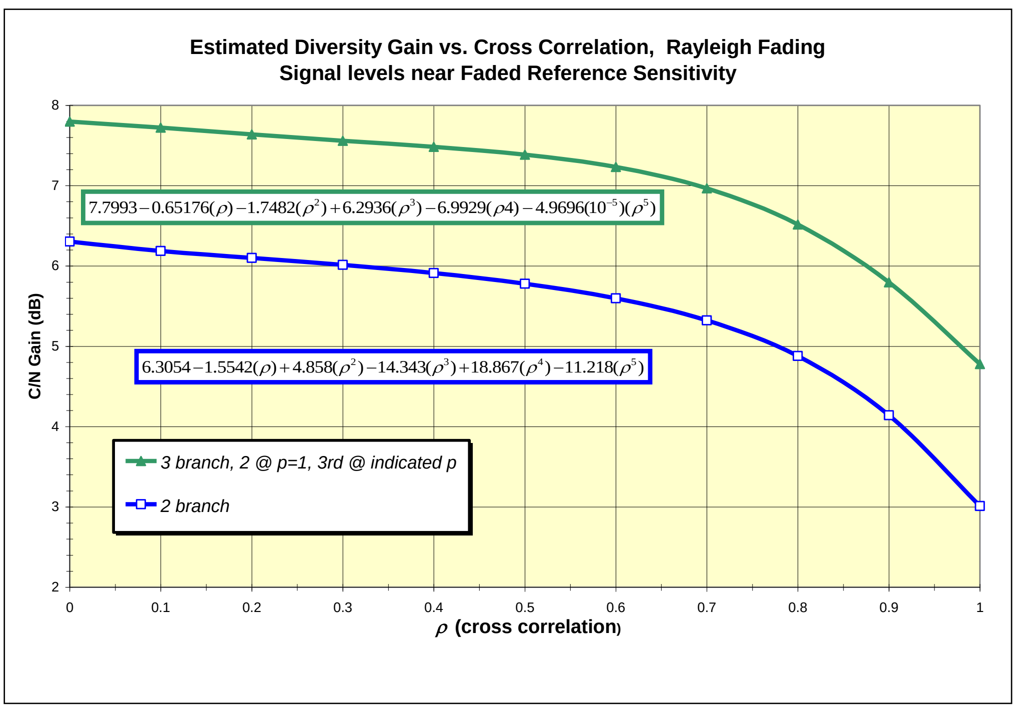

Figure 22 Estimated Diversity Gain

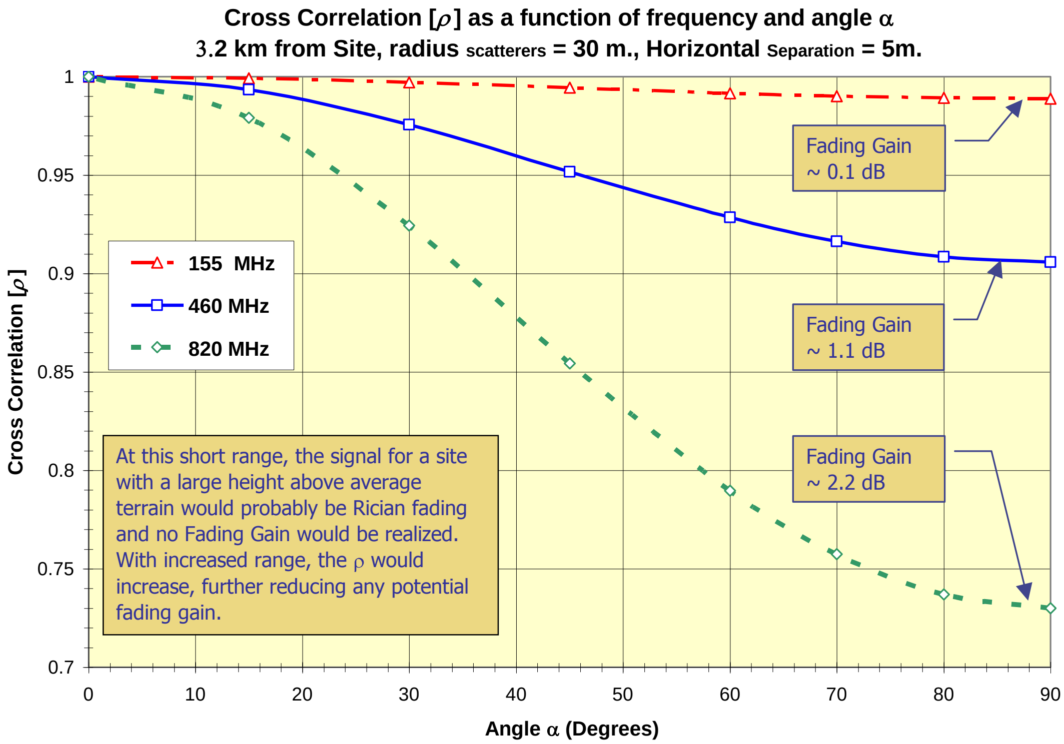

Figure 23 Fading Gain Example

7.3 Fading Gain Conclusions

From the preceding discussions, it can be generalized that fading gain is realized only under the following conditions:

- The scattered component is large compared to the direct component.
- Close to the Site (when needed the least)
- When cross-correlation is low
    - When α approaches 90º.
    - Larger radius of scatterers
    - Increased horizontal separation

Furthermore, fading gain is greatly limited at lower frequency bands

Further discussion on some of these factors follows.

7.4 Antenna Configurations

As previously discussed, when the arrival angle (α) approaches 90º, the cross-correlation is minimized. However the arrival angle depends on the number of antennas and the area to be covered. Figure demonstrates that ρ becomes high when the signal arrives at a small arrival angle.

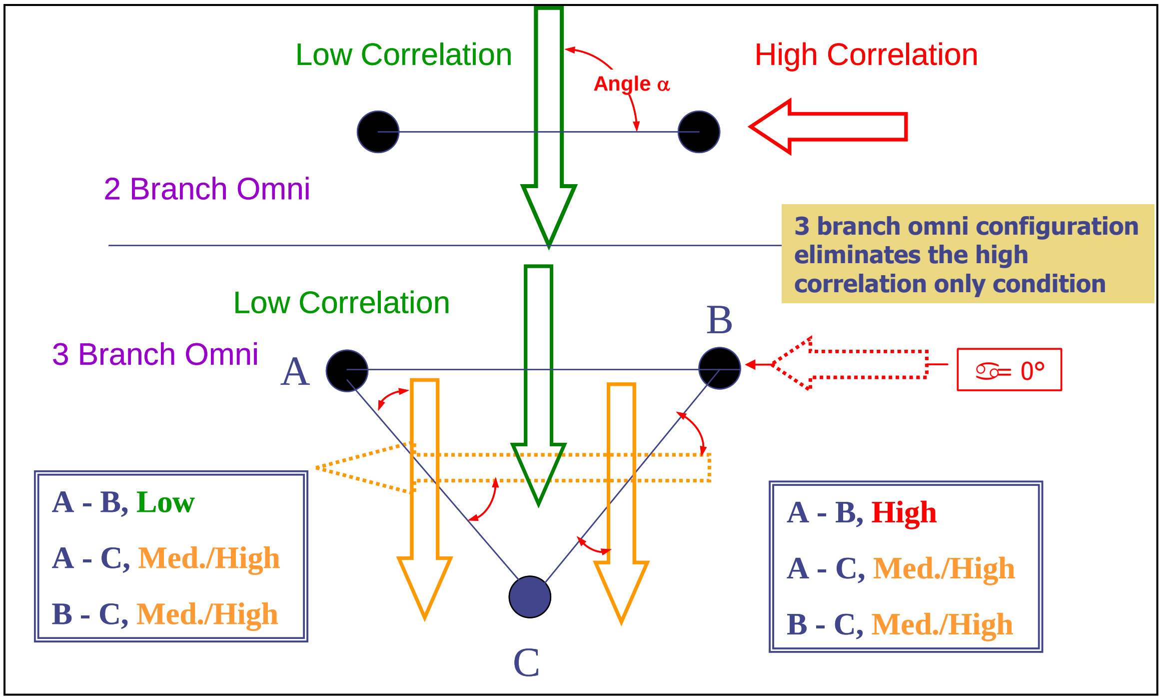

Figure 24 Cross-correlation vs. Arrival Angle

This increase in correlation can be compensated for by using a three branch omnidirectional configuration. In this case, when the arrival angle for antennas A-B is low, the arrival angle to antenna configurations A-C and B-C have an arrival angle that can produce a lower level of correlation. This can result in an overall improvement in the fading gain, limited by the other controlling factors as discussed in §7.3.

Sectored configurations do not have the same limitations. Therefore, only consider omnidirectional antenna configurations for more than two antennas.

Some 2-antenna omnidirectional configurations can potentially provide additional interference suppression when used in conjunction with a coherent receiver. This is due to the ability to essentially evaluate the received signals and optimize the antennas' inputs to favor the desired while rejecting the undesired signal. However, this is purely a function of the relative locations of the desired and undesired sources and the combined antenna patterns. Hence this optimization cannot be assured.

7.5 Horizontal Separation

Horizontal separation is the preferred deployment. Other configurations, such as vertical separation, are possible. However, this configuration can create signal level differences which diminish the diversity enhancements. This will be discussed in more detail below.

The type of structure has a great deal of influence over how much horizontal separation can be achieved. We will discuss the following types of structures:

- Tall Towers
- Shorter Towers on High HAAT Sites
- Building Tops

7.5.1. Tall Towers

Tall towers are limited by the amount of separation that can be achieved by side arms. Receive antennas are most frequently mounted at the top of the tower. This allows the 3-branch-omni configuration to be deployed. If omnidirectional receive antennas are side-mounted, the patterns are no longer identical (pattern distortion) and signal level differences reduce the amount of gain achievable.

As previously discussed, the maximum fading gain occurs when Rayleigh-faded and at distances close to the site. In this case, tall towers and close range produce Rician fading with a significant direct component and the fading gain is reduced to Aperture Gain only.

7.5.2. Shorter Towers on High HAAT Sites

High HAAT Sites (e.g. mountain tops) typically prevent users from close proximity to the site. Since the distance is great, the amount of Fading Gain is minimal.

7.5.3. Building Tops

Greater separation is possible on building tops. However, local obstructions frequently produce antenna pattern distortion. Pattern distortion limits the fading gain, particularly when omnidirectional patterns are employed. In this case, a sectored antenna configuration might be the preferred deployment, as is the case with cellular radio systems. Note that sectored configurations might need additional frequency resources as well as additional infrastructure.

7.5.4. Low HAAT Sites

Most of the research into diversity has been conducted for cellular systems that are characterized by low HAAT sites. For any environment, the low effective tower height limits the range. Thus, the illumination angle is relatively large due to the short distance from the site compared to the same environment at a greater distance. Thus, the cross-correlation is low and because of the lower effective antenna heights. The direct component becomes negligible and the signal distribution approaches Rayleigh. This works well for cellular systems but is not useful for private systems because, unlike cellular systems, private mobile radio systems do not generate revenue at each site as well as increasing potential system loading capability. In private systems, increased distances from the site increases the cross-correlation and lower potential fading gain.

7.6 Radius of Local Scatterers

The concept of a radius of local scatterers is never fully realized but is useful in making fading gain estimates. Sounding measurements can be used to determine the delay spread of pulses[22] and from that information a radius of local scatterers can be estimated for use in equation (14) p. 40 [Lee 82].

In general, the greater the local environment density is, the smaller the radius of local scatterers. This minimizes the illumination angle resulting in a large value for ρ, lowering potential fading gain.

Open areas have few reflective surfaces. As a result the direct component of the Rician Distribution becomes stronger, so that it no longer approaches a Rayleigh distribution. Rician fading reduces the Rayleigh fading penalty, but it is not exclusive to a diversity deployment. In addition, the increase in the direct component can cause mobile antenna directivity to become more noticeable, resulting in lower signal levels at the base receive site.

In lower frequency bands (e.g., the 160 MHz or the 460 MHz band) local scatterers become less efficient, further reducing the effectiveness of fading gain.

7.7 Combiner Types

There are several different types of diversity combiners available.

- Selective
- Equal Gain
- Maximal-ratio

The amount of C/N improvement is the least for the selection combiner and best for the maximal-ratio combiner.

7.7.1 Selective Combiner

This type of combiner compares the inputs and selects the best. As a result, the least amount of C/N is achieved as only one output is available.

7.7.2 Equal Gain Combiner

This type of combiner compares the inputs, co-phases them and combines them equally until one input is preferred over the other(s) by some preset value. When this condition exists, only the preferred input is used.

[22] Extremely narrow, impulse function, pulses are transmitted. At the receive location the arrival time differences provide sufficient information to generalize the radius of local scatterers

7.7.3 Maximal-ratio Combiner

This is the preferred configuration as the co-phased inputs are combined after being weighted for their C/N. This is the case where the Aperture Gain can be realized. The maximal-ratio combiner can be used by either a coherent or non-coherent receiver subject to the ability to co-phase the signals for proper detection. As a result, coherent receivers are not necessary to achieve the gain of a maximal-ratio combiner.

7.7.3.1 Coherent Detection

Coherence needs the signals to be aligned in both phase and time. Coherent detection therefore needs both phase and amplitude to be detected.

In a coherent receiver configuration this can be accomplished post detection.

7.7.3.2 Non-coherent Detection

A non-coherent receiver can only detect phase or amplitude post detection. However pre-detection still preserves both phase and amplitude. Therefore, a non-coherent receiver can achieve the maximal-ratio combining gain if the signals are co-phased prior to detection. This eliminates the need for a coherent receiver.

7.8 Theoretical Gain

Examples of theoretical gain calculations are found in many text books. From [Lee 82] p. 310-311 a comparison for maximal-ratio combiners is shown in Figure . This specific case has signals fully Rayleigh faded and independent channels ($\rho = 0$). This implies sectored antennas as $\rho \neq 0$ for all antennas in omnidirectional configurations as discussed in §7.4.

The amount of Diversity Gain at 95% probability is quite large, 8.4 dB for 2 branches and 12.0 dB for 3 branches. However, this gain is only available with the stipulated conditions.

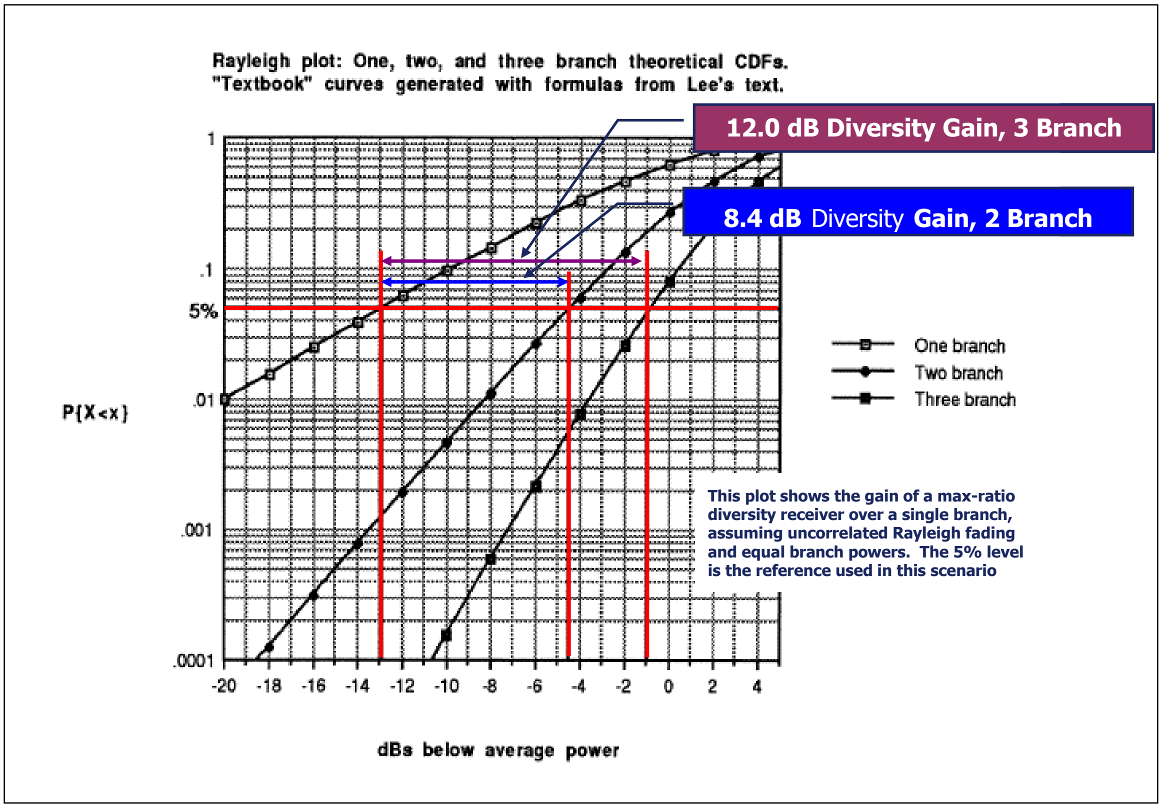

Figure 25 Theoretical Diversity Gain for Maximal-ratio combining, independent channels

7.8.1 Measured Comparisons

Measured data by [Butler 96] for different conditions provide examples of what can be expected in actual deployments. Extensive data was collected and segments identified as to existing conditions so comparisons could be made between theoretical and measured results.

7.8.1.1. Rayleigh Fading with Cross-correlation = 0

When full Rayleigh fading with low cross-correlation is present, the measured data agrees with the theoretical predictions. Figure has both the theoretical and measured probabilities plotted and the results agree with the theoretical predictions. However, this is a special case using sectored antennas, no cross-correlation, Rayleigh fading and maximal-ratio combiners.

When these conditions are not present, the amount of Diversity Gain changes as will be shown in the following subclauses.

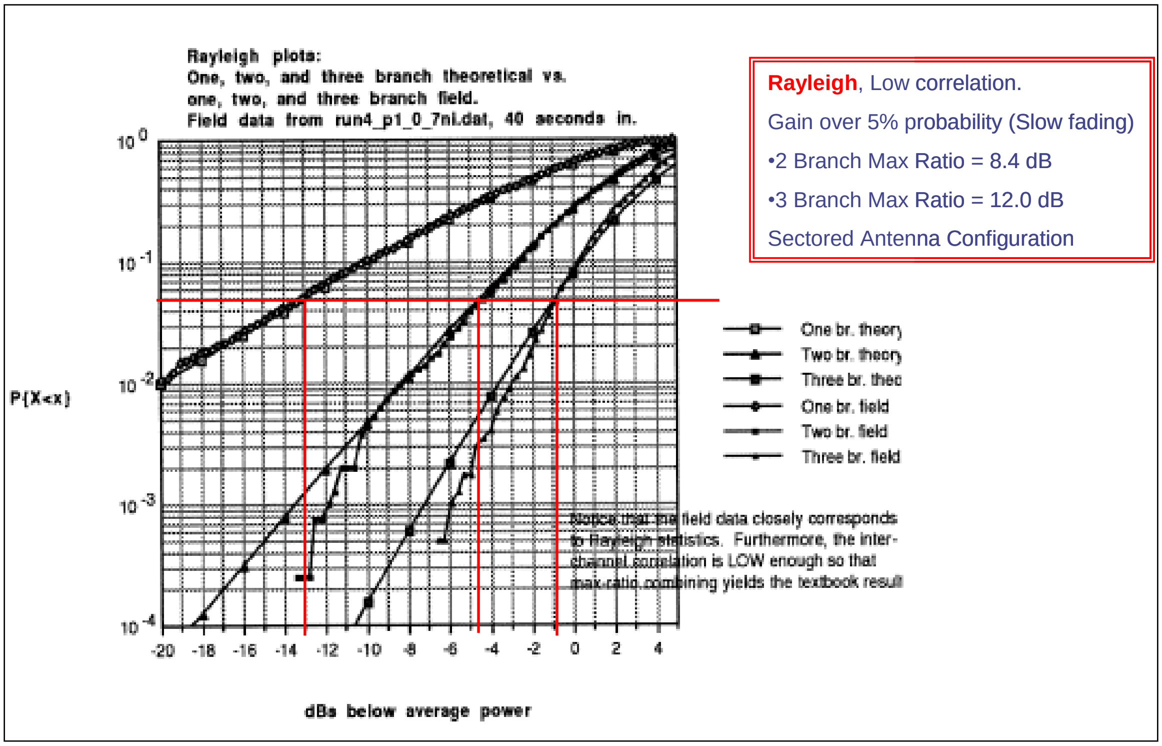

Figure 26 Full Rayleigh Fading

7.8.1.2. Rayleigh Faded, Medium Cross-correlation

As the cross-correlation increases, the amount of Diversity Gain is reduced. Figure 26 shows that the fading gain is reduced to approximately 2 dB and the rest of the gain is aperture gain. The parallel measured distributions are indicative of high correlation. As discussed in §7.4 omnidirectional configurations will have different cross-correlation based on the arrival angle (α).

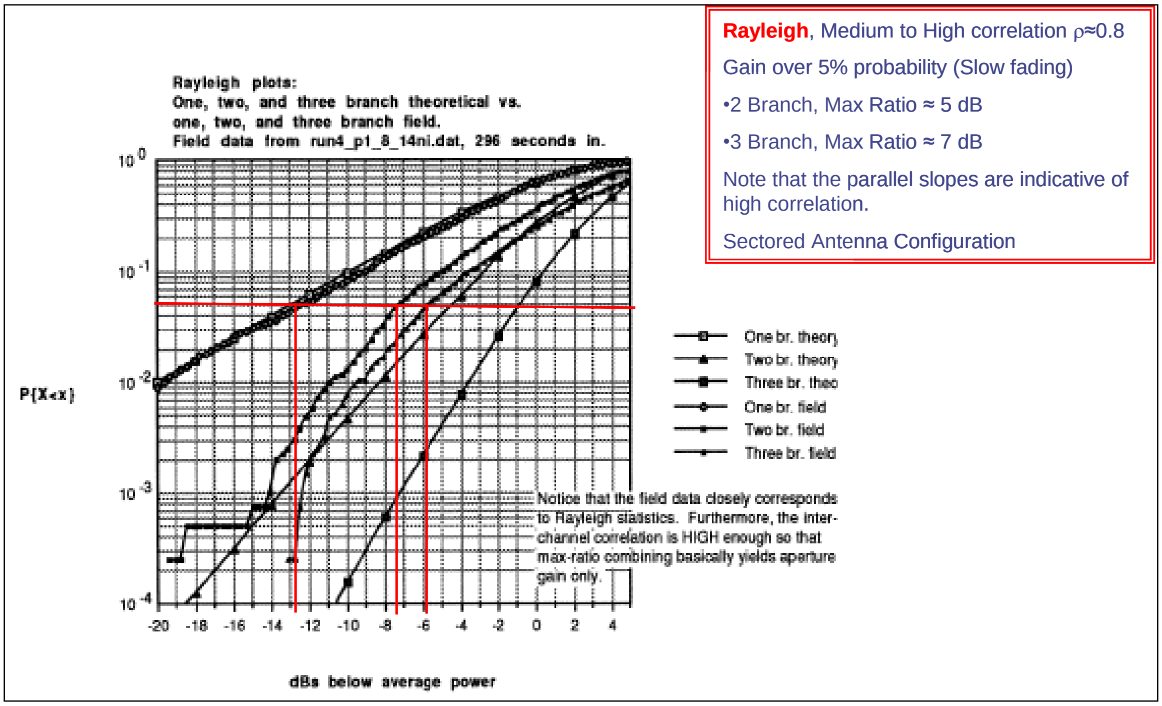

Figure 27 Rayleigh Faded, Medium Cross-correlation

7.8.1.3. Rician Fading

Rician fading exists when there is a strong line-of-sight component in the received signals. Figure demonstrates that the difference between the configurations is merely the aperture gain. There certainly is fading gain, but it applies equally to the non-diversity configuration as well as the 2 and 3 branch configurations. Therefore only aperture gain can be assured due to the diversity configuration.

Rician fading occurs primarily when units are close to the site or where the site has a large HAAT providing either a line-of-sight path or near line-of-sight path to the site. In both cases, the non diversity configuration has the same reduction in fading.

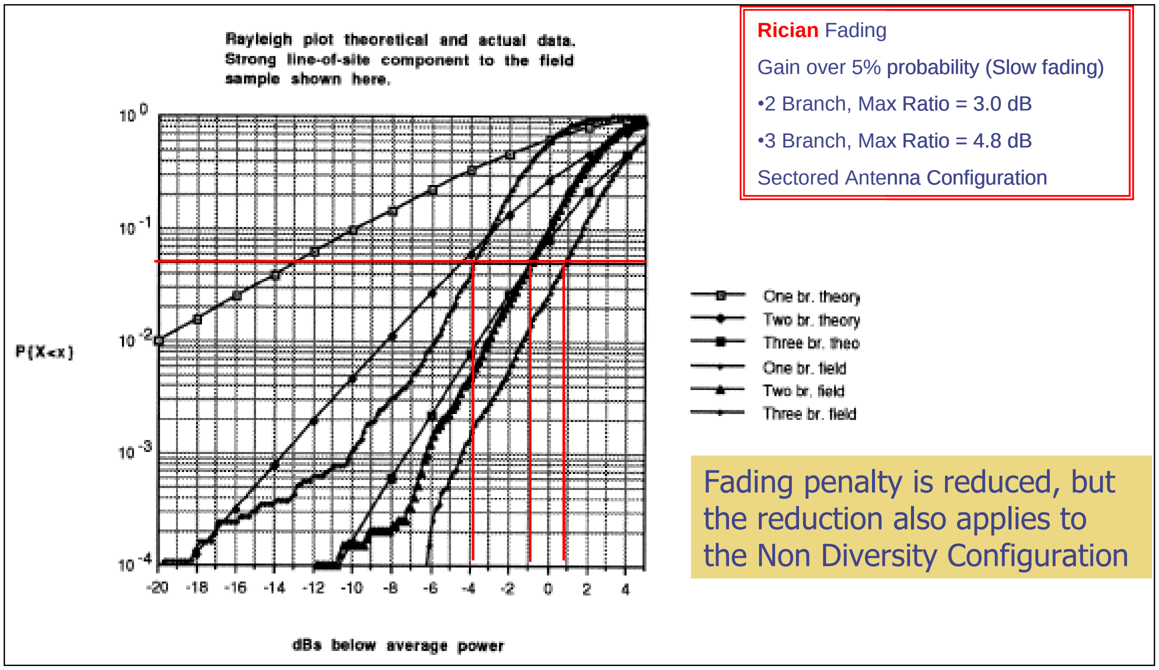

Figure 28 Rician Fading

7.8.2 Rayleigh vs. Rician fading distributions

As previously discussed, Rician fading has less of a fading penalty than does Rayleigh fading. Figure represents the fading distributions of Rayleigh fading and an example of Rician fading when k = 0.15. The value of k represents the fraction of the total power carried by the multipath (random) component. For this example, there is a 7.2 dB reduction in the necessary C_f/N, median signal levels, when this scenario is present. This penalty reduction is applicable to the non diversity configuration as well as the multi-branch diversity configurations.

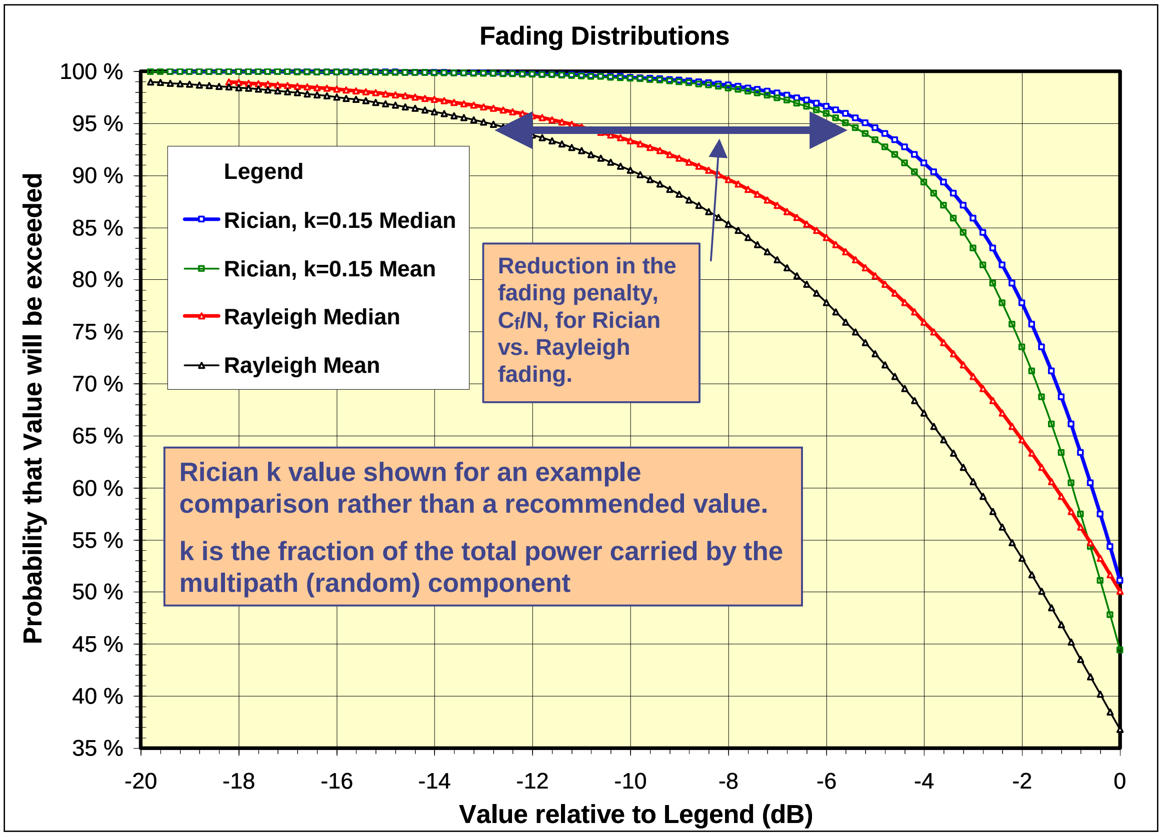

Figure 30 Rayleigh vs. Rician Fading

7.9 System imbalances effect on Gain

System imbalances reduce the amount of Diversity Gain. The unbalance can be caused by unequal signals in the branches while having equal noise in all branches. This type of condition can be caused by:

- Unequal antenna gains or patterns
- Unequal cable loss prior to amplification
- Unequal amplifier gains
- Unequal HAAT per antenna

The other case is where the signals in all branches are equal, but the noise in each branch is different. This type of condition can be caused by:

- Unequal branch Noise Figures
- Unequal distribution of Gains or Losses

These types of unbalances are difficult to predict prior to actual deployment. This type of degradation essentially eliminates vertical spacing diversity due to both type of factors, unequal signal levels and unequal distribution of gains or losses.

From a practical view, designers are not always familiar with the actual physical constraints, and installers have to deal with the actual physical constraints of the installation. As a result, exact predictions are difficult to make.

7.10 Macro-Diversity (Voting)

Macro-diversity relies on different sites receiving inbound signals. As a result of the wide separation of sites and the signal paths, the cross-correlation is normally zero.

7.11 Summary

It is recommended that only aperture gain be utilized when performing coverage predictions.

- Diversity, both micro and macro are applicable to all modulations
    - Micro-diversity necessitates co-phasing before detection for non-coherent receivers
- Diversity Gain is difficult to calculate or rely on
    - Only aperture gain can be assured
    - One approach does not fit all cases
    - Available when needed the least: close to the site
    - Unavailable when needed the most: far from the site
    - Additional equipment cost and increased tower loading
- Fading gain is not possible, or extremely small, in many cases, such as the following:
    - For high-HAAT sites (Rician fading)
    - Local scatterers
        - Small radius, high urbanization
        - Sparse or no local scatterers
    - Lower Frequency bands (longer wavelengths)
    - End-fire, 2 branch omnidirectional configurations
    - Limited horizontal separation on towers
    - Large unbalances in system gains
    - Different antenna patterns

BIBLIOGRAPHY

The following is a list of generally applicable sources of information relevant to this document.

[3GPP 06] *Specification Group Radio Access Networks; Deployment Aspects,* Report TR 25.943, 3rd Generation Partnership Project, 2006

[3GPP 10] 3rd Generation Partnership Project; Technical Specification Group *Radio Access Network; Evolved Universal Terrestrial Radio Access (E-UTRA); Further advancements for E-UTRA physical layer aspects*, 3GPP TR 36.814 (Release 9)

[3GPP 14a] 3rd Generation Partnership Project; Technical Specification Group Radio Access Network; *Spatial channel model for Multiple Input Multiple Output (MIMO) simulations*, 3GPP TR 25.996 V12.0.0.

[3GPP 14b] 3rd Generation Partnership Project; Technical Specification Group, *Study on LTE device to device proximity services; Radio aspectsI*, #GPP TR 36.843 (Release 12).

[3GPP2 03] *1xEV-DV Evaluation Methodology,* 3GPP2 TSG-C.R1002, 3GPP2 Technical Specifications Group C, 2003.

[Adachi 86] Adachi, Fumiyuki, *et al*, "Crosscorrelation between the envelopes of 900 MHz signals received at a mobile base station site", *IEE Proceedings vol. 133, Pt. F, no. 6,* pp. 506 – 512, October 1986

[Aguirre 94] Aguirre, S.; L.H. Loew, Yeh Lo, "Radio propagation into buildings at 912, 1920, and 5990 MHz using microcells", *3rd Int Conf on Univ Pers Comm*,1994, Page(s): 129 –134.

[Akima 73] Akima, H., "A method of bivariate interpolation and smooth surface fitting based on local procedures", *OT Report 73-7*, NTIA Office of Telecommunications, March 1973, NTIS Accession Number COM 75-10812/AS.

[Allsebrook 77] Allsebrook, Keith & J. David Parsons, "Mobile Radio Propagation in British Cities at Frequencies in the VHF and UHF Bands", *IEEE Trans Veh Tech*, vol. 26, no. 4, Nov 1977, pp 313 - 323.

[Anderson 76] Anderson, James R. *et al*, "*A Land Use and Land Cover Classification System for Use with Remote Sensor Data*, Geological Survey Professional Paper 964", USGPO, 1976.

[Asp 14] Ari Asp *et al*, "Impact of Modern Construction Materials on Radio Signal Propagation: Practical Measurements and Network Planning Aspects", *79th IEEE Veh Tech Conf*, VTC-2014 Spring, Seoul.

[Barry 87] Barry, P.J. and A.G. Williamson, "Modelling of UHF radiowave signals within externally illuminated multi-storey buildings," *Journal of the Institution of Electronic and Radio Engineers*, 57(6), (Supplement), Nov/Dec 1987, pp. S231-S240.

[Barry 89] Barry, P.J., *A Statistical Model for UHF Radiowave Signals Within Externally Illuminated Multi-Storey Buildings*, Sch of Engrg Rep # 474, University of Auckland (NZ), Aug 1989.

[Berg 96] Berg, J.-E., "Building penetration loss along urban street microcells", *PIMRC'96*., Oct. 1996 , Volume: 3 , pp 795 –797.

[Blomquist 74] Blomquist, A. & L. Ladell, "Prediction and Calculation of Transmission Loss in Different Types of Terrain", *1974 AGARD Conf Proc*, pp. 32/1-32/25.

[Bullington 47] Bullington, K., "Radio propagation at frequencies above 30 megacycles", *Proc IRE*, October 1947, pp. 1122-1136.

[Bullington 57] Bullington, K. "Radio propagation fundamentals", *BSTJ*, 36(3), May, 1957, pp. 593-626.

[Bullington 77] Bullington, K., "Radio propagation for vehicular communications", *IEEE Trans Veh Tech*, 26(40, Nov 1977, pp 295-308.

[Butler 96] Butler, James A., *Base Station Diversity Considerations for the Prodigy/MIRS System*, May 1996. Motorola Internal Publication.

[Camwel 87] Camwel, P.L. and J.G. McRoy, "Experimental results of in building anisotropic propagation at 835 MHz using leaky feeders and dipole antenna," *IEEE Montech '87 Cong*., Montreal, Nov. 1987, pp. 213-216.

[Carey 64] Carey, Roger B., *Technical Factors Affecting the Assignment of Facilities in the Domestic Public Land Mobile Radio Service*, Report No. R6406, Office of Chief Engineer, Federal Communications Commission, Washington, D.C., 1964.

[Correia 99] Correia, Luis M. (ed.), *Digital Mobile Radio Towards Future Generation Systems:* Final Report, Cost Action 231, European Communities, 1999, ISBN 92-828-5416-7.

[Correia 01] Correia, Luis M. (ed.), *Wired Flexible Personalised Communications:* COST 259: European Co-operation in Mobile Radio Research, Wiley, 2001, ISBN 0-471-49836-X.

[Cox 83] Cox, D.C., R.R. Murray, and A.W. Morris, "Measurements of 800-MHz radio transmission into buildings with metallic walls," *BSTJ*., 62(9), 1983, pp. 2695-2717.

[Cox 84] Cox, D.C., R.R. Murray, and A.W. Norris, "800-MHz attenuation measured in and around suburban houses," *BSTJ*, 63, (6), 1984, pp. 921-955.

[Craig 08] Craig, K.H. *et al*, *Diffraction Model Comparisons Using the ITU-R 3K1 Correspondence Group Database*, ISART 08, Boulder CO, p. 58**.**

[Dadson 75] Dadson, C.E., et al, “Computer prediction of field strength in the planning of radio systems”, *IEEE Trans Veh Tech*, vol. 24, no. 1, pp. 1-8, Feb 1975.

[Dadson 79] Dadson, C.E., “Radio network and radio link surveys derived by computer from a terrain data base”, *1979 AGARD Conf Proc*, pp25-1 to 25-17, 1979.

[Daly 10] Daly, M. & S. O’Hara, *Large Scale Spectrum Management and Coverage Optimization*, presented at IWCE 2010, Las Vegas, Mar 10 2010.

[Damelin 66] Damelin, Jack et al, *Development of VHF and UHF Propagation Curves for TV and FM Broadcasting*, FCC Report R-6602, Federal Communications Commission, Washington DC, 1966, NTIS Accession Number PB 174 288.

[Davidson 96] Davidson, Allen *et al* , “Frequency Band Selection Analysis” White Paper, Public Safety Wireless Advisory Committee Final Report, 1996. Not included in final report. TIA TR-8.18/04-01-0001.

[Davidson 97] Davidson, Allen *et al*, “Measurement of building penetration into medium buildings at 900 and 1500 MHz”, *IEEE Trans Veh Tech*, 46(1) , Feb. 1997, pp 161 –168.

[deBot 94] de Bot, P.; *et al*.; “Propagation of broadcast signals into buildings at 762 MHz“, *IEEE Second Symposium on Communications and Vehicular Technology in the Benelux*, 1994, pp 28 –37.

[DeMinco 08] DeMinco, N. & P. McKenna, *A Comparative Analysis of Multiple Knife-Edge Diffraction Methods*, ISART 08, Boulder CO, p. 65.

[Dietz 73] Dietz, Jules *et al*, *Examination of the feasibility of Conventional Land-Mobile Operation at 950 MHz*, FCC OCE Report R-7202, May 1973.

[Deygout 66] Deygout, Jacques, “Multiple knife-edge diffraction of microwaves”, *IEEE Trans Ant Prop*, 14(4), Jul 1966, pp 480-489.

[Deygout 91] Deygout, Jacques, “Correction factor for multiple knife-edge diffraction”, *IEEE Trans Ant Prop*, 39(8), Aug 1991, pp 1256-1258.

[Dougherty 64] Dougherty, H.T. and L.J. Maloney, "Application of diffractions by convex surfaces to irregular terrain solutions", *Radio Sci*, 68D(2), Feb 1964, pp 239-250.

[Durante 73] Durante, James M., “Building penetration loss at 900 MHz, *23rd IEEE Vehicular Technology Conference Record*, 1973.

[Durkin 77] Durkin, J., “Computer prediction of service areas for VHF and UHF land mobile radio services”, *IEEE Trans Veh Tech*, vol. 26, no. 4, pp. 323-327, Nov 1977.

[Edwards 69] Edwards, R. and J. Durkin, "Computer prediction of service areas for V.H.F. mobile radio networks", *Proc IEE*, 116(9), September 1969, pp. 1496-97, §§3.2 - 3.2.4.

[Egli 57] Egli, John J., "Radio Propagation Above 40 Mc Over Irregular Terrain", *Proc IRE*, vol 45, no 10, Oct 1957, pp 1383 - 1391.

[Epstein 53] Epstein, Jess & Donald W. Peterson, "An experimental study of wave propagation at 850 Mc", *Proc IRE*, 41(5), May 1953, pp 595-611.

[Erceg 03] Erceg, Vinko *et al*, *Channel Models for Fixed Wireless Applications*, IEEE 802.16a-03/01, IEEE, June 27, 2003.

[ETSI 98] *Universal Mobile Telecommunications System (UTMS); Selection procedures for the choice of radio transmission technologies of the UMTS,* ETSI Report TR 101 112 v 3.2.0, 1998, §B.1.4.2.

[ETSI 14a] *LTE; Evolved Universal Terrestrial Radio Access (E-UTRA); User Equipment (UE) radio transmission and reception* (3GPP TS 36.101 version 12.5.0 Release 12), Annex B, ETSI TS 136 101, 2014.

[ETSI 14b] *LTE; Evolved Universal Terrestrial Radio Access (E-UTRA); Base Station (BS) radio transmission and reception* (3GPP TS 36.104 version 12.5.0 Release 12), Annex B, ETSI TS 136 104, 2014.

[Frazier 83] Frazier, William E., *Master Propagation System Users' Manual*, NTIA/DF-83/001a, National Telecommunications and Information Admin., Annapolis, MD, 1983, NTIS Accession No. PB83-178624, pp 2-1 to 2-16.

[Freeman 87] Freeman, Roger L., *Radio System Design for Telecommunications (1-100 GHz)*, New York: Wiley, 1987, ISBN 0-471-81236-6.

[Gahleitner 94] Gahleitner, R. & E. Bonek, "Radio wave penetration into urban buildings in small cells and microcells", *44th IEEE Vehicular Technology Conference Record*, 1994, pp 887-891.

[Green 95] Green, J.A. & I.R. Pullen, "Building penetration loss measurements for digital analog broadcasting", *IEE Colloq on Propagation in Buildings*, 1995, Digest No 1995/134, pp 1/1 – 1/6.

[Hata 80] Hata, Masaharu, "Empirical formula for propagation loss in Land Mobile radio services", *IEEE Trans Veh Tech*, 29(3), Aug 80, pp 317-325.

[Hess 93] Hess, G., *Land Mobile Radio System Engineering*, Boston, Artech House, 1993, ISBN 0-89006-680-9.

[Hoaglin 83] Hoaglin, David C., Fredrick Mosteller, and John W. Tukey, *Understanding Robust and Exploratory Data Analysis,* Wiley, New York, 1983, pp.58-77.

[Hoffman 82] Hoffman, H.H. and D.C. Cox, "Attenuation of 900 MHz radio waves propagation into a metal building," *IEEE Trans Ant Prop*, 30(4), 1982, pp. 808-111.

[Homer 04] Homer, C. *et al*, "Development of a 2001 National Landcover Database for the United States". Photogrammetric Engineering and Remote Sensing, 70(7), July 2004, pp. 829-840.

[Homer 15] Homer, C.G. *et al*, "Completion of the 2011 National Land Cover Database for the conterminous United States-Representing a decade of land cover change information", *Photogrammetric Engineering and Remote Sensing*, 81(5), pp. 345-354, May 2015.

[Hoppe 99] Hoppe, R., G. Wolfle,F.M. Landstorfer, "Measurement of building penetration loss and propagation models for radio transmission into buildings", *50th IEEE Veh Tech Conf*, VTC 1999 - Fall. Sept. 1999, pp 2298 - 2302

[Horikoshi 86] Horikoshi, J. K. Tanaka, and T. Morinaga, "1.2 GHz Band Wave Propagation Measurements in Concrete Buildings for Indoor Radio Communications," *IEEE Trans. Veh. Tech*., 35(4), 1986, pp 146-152.

[Hufford 79] Hufford, George A., *The Longley-Rice Model -- An Implementation, 1979: Programmer's and User's Guide*, Institute for Telecommunication Sciences, Spectrum Utilization Division, Boulder, July 1979.

[Hufford 82] Hufford, George A. et al, *A Guide to the Use of the ITS Irregular Terrain Model in the Area Prediction Mode*, NTIA Report 82-100, National Telecommunications and Information Administration, Boulder, Colorado, 1982.

[Hufford 85] Hufford, George A., MEMORANDUM TO: Users of the ITS Irregular Terrain Model SUBJECT: Modifications, Institute for Telecommunication Sciences, Boulder, January 30, 1985

[Hufford 91] Hufford, George A., *Tabulations of Propagation Data over Irregular Terrain in the 75 to 8400 MHz Frequency Range, Part V*: Virginia, *NTIA Report No. 91-282*, December 1991.

[IEEE 00] *The Authoritative Dictionary of IEEE Standards Terms,* 7th Ed., Institute of Electrical and Electronics Engineers, 2000.

[IEEE 04] *Channel Models for IEEE 802.20 MBWA System Simulations,* IEEE C802.20-04/66, 2004.

[ITU 97] *Guidelines for evaluation of radio transmission technologies for IMT-2000,* ITU-R Rec. M.1225, International Telecommunication Union, Geneva, 1997.

[ITU 99] *Digital Topographic Databases for Propagation Studies*, Recommendation P.1058-2, International Telecommunication Union, Geneva, 1999.

[ITU 09a] *Guide to the Application of the Propagation Methods of Radiocommunication Study Group 3*, Recommendation P.1144-5, International Telecommunication Union, Geneva, 2009.

[ITU 09c] *Multipath propagation and parameterization of its characteristics*, ITU-R Rec. P.1407-4, International Telecommunication Union, Geneve, 2009.

[ITU 12] *Propagation curves for aeronautical mobile and radionavigation services using the VHF, UHF and SHF bands*, ITU-R Rec. P.528-3, International Telecommunication Union, Geneva, 2012.

[ITU 13b] *Propagation by diffraction*, ITU-R Rec. 526-13, International Telecommunication Union, Geneva, 2013.

[ITU 13d] *A general purpose wide-range terrestrial propagation model in the frequency range 30 MHz to 50 GHz*, ITU-R Rec. 2001-1, International Telecommunication Union, Geneva, 2013.

[ITU 13e] *Method for point-to-area predictions for terrestrial services in the frequency range 30 MHz to 3 000 MHz*, ITU-R Rec. P.1546-5, International Telecommunication Union, Geneva, 2013.

[ITU 15a] *Prediction procedure for the evaluation of interference between stations on the surface of the Earth at frequencies above about 0.1 GHz*, ITU-R Rec. 452-16, International Telecommunication Union, Geneva, 2015.

[ITU 15b] *Propagation data and prediction methods for the planning of indoor radiocommunication systems and radio local area networks in the frequency range 900 MHz to 100 GHz*, ITU-R Rec. P.1238-8, International Telecommunication Union, Geneva, 2009.

[ITU 15c] *Propagation data and prediction methods for the planning of short-range outdoor radiocommunication systems and radio local area network in the frequency range 300 MHz to 100 GHz*, ITU-R Rec. P.1411-8, International Telecommunication Union, Geneva, 2015.

[ITU 15d] *A path-specific propagation prediction method for point-to-area terrestrial services in the VHF and UHF bands*, ITU-R Rec. 1812-4, International Telecommunication Union, Geneva, 2015.

[ITU 15e] *A general purpose wide-range terrestrial propagation model in the frequency range 30 MHz to 50 GHz*, ITU-R Rec. P.2001-2, International Telecommunication Union, July 2015.

[Jennings 77] Jennings, Raymond D. and S. Jean Paulson. *Communication System Performance Model for VHF and Higher Frequencies.* OT Report 77-128, Office of Telecommunications, U.S. Department of Commerce, October 1977, NTIS Accession No. PB274458.

[Kalagian 76] Kalagian, Gary S., “*Field Strength Calculation for TV and FM Broadcasting (Computer Program TVFMFS), Report FCC/OCE RS76-01*”, Federal Communications Commission, Office of the Chief Engineer, Washington DC, January 1976, NTIS Accession Number PB 249 144.

[Karadimas 09] Karadimas, P & S. Kostopoulos, "The Weibull–lognormal fading channel: Analysis, simulation, and validation, *IEEE Trans Veh Tech*, 58(7), p. 3808, 2009.

[Komura 77] Komura, N., T. Hogigira, and M Ogasawara, "New radio raging [sic] system and its propagation characteristics," *IEEE Trans Veh Tech*., VT-26, Nov. 1977, pp. 362-366.

[Lee 71] Lee, William C.Y., “Antenna spacing requirement for a mobile radio base-station diversity”, *BSTJ*, 50(6), Jul-Aug 1971, pp1859-76.

[Lee 82] Lee, William C.Y. *Mobile Communications Engineering*, McGraw-Hill, 1982, ISBN 0-07-037039-7.

[Lee 85] Lee, William C. Y., “*Estimate of Local Average Power of a Mobile Radio Signal*”, *IEEE Transactions on Vehicular Technology*, Vol. VT-34, No. 1, Feb 1985.

[Lee 93] Lee, William C.Y., *Mobile Communications Design Fundamentals*, New York, John Wiley & Sons, Inc., 1993, ISBN 0-471-57446-5.

[Longley 68] Longley, Anita G. & Philip L. Rice, *Prediction of Tropospheric Radio Transmission Loss Over Irregular Terrain: A Computer Method-1968*, ESSA Technical Report ERL79-ITS67, Institute forTelecommunication Sciences, Boulder, Colorado, 1968.

[López 84] López Giovaneli, Carlos, “An analysis of simplified solutions for multiple knife-edge diffraction”, *IEEE Trans Ant Prop*, 32(3), Mar 1984, pp 297-301.

[Lustgarten 77] Lustgarten, M.N. & J.A. Madison, "An empirical propagation model", *IEEE Trans Electromag Compat*, 19(3), Aug 1977.

[McQuate 68] McQuate, P.L. et al., *Tabulations of Propagation Data over Irregular Terrain in the 230- to 9200 MHz Frequency Range, Parts I and II*, ESSA Technical Report ERL 65-ITS 58, Institute for Telecommunications Sciences, Boulder, CO, March 1968.

[Molkdar 91] Molkdar, D, "Review on Radio Propagation Into and Within Buildings," *IEE Proceedings-H*, 138(1), Feb 1991, pp. 61-73.

[Nakagami 40] Nakagami, M, "Study of the resultant amplitude of many vibrations whose phases and amplitudes are at random". *J Inst Elec Commun Engrs Japan*, *24*(202), 17-26, 1940.

[NPSTC 14] "Defining Public Safety Grade Systems and Facilities", National Public Safety Telecommunications Council, 2014. http://npstc.org/download.jsp?tableId=37&column=217&id=3066&file=Public_Safety_Grade_Report_140522.pdf

[Okumura 68] Okumura, Y. et al, "Field Strength and Its Variability in VHF and UHF Land Mobile Radio Service", *Rev Elect Comm Lab*, 16(9-10), September-October 1968, pp. 825-873.

[Palmer 78] Palmer, Frank H., "The CRC VHF/UHF Propagation Prediction Program: Description and Comparison with Field-Measurements", *1978 AGARD Conf Proc*, pp49-1 to 49-15.

[Palmer 79] Palmer, Frank H., "VHF/UHF Path-Loss Calculations Using Terrain Profiles Deduced From a Digital Topographic Data Base", *1979 AGARD Conf Proc*, pp 26-1 to 26-11.

[Parsons 92] Parsons, J. David, *The Mobile Radio Propagation Channel*, New York-Toronto, Halsted Press, 1992, ISBN 0-471-21824-X

[Picquenard 74] Picquenard, A., *Radio Wave Propagation*, Wiley, 1974, p. 296.

[Plets 09] David Plets *et al*, "Extensive Penetration Loss Measurements and Models for Different Building Types for DVP-H in the UHF Band, *IEEE Trans Brdcst*, 55(2), p. 213. June 2009.

[Prasad 96] Prasad, R. & A. Kegel, "Effects of Rician Faded and Log-Normal Shadowed Signals on Spectrum Efficiency in Microcellular Radio", *IEEE Trans Veh Tech*, 42(3), p. 274, 1996.

[Reudink 74] Reudink, Douglas O., "Chapter 2: Large-Scale Variations of the Average Signal", IN: W. C. Jakes ed., *Microwave Mobile Communications*, New York, Wiley, 1974, Reprinted by IEEE Press, 1993, ISBN 0-471-43720-4

[Rice 59] Rice, L.P., "Radio transmissions into buildings at 35 and 150 Mc", *BSTJ*, v38, Jan 1959, pp 197-210.

[Rice 67] Rice, Philip L. et al, *Transmission Loss Predictions for Tropospheric Circuits*, National Bureau of Standards, Rev. 1967, NTIS Accession No. AD-687 820.

[Rice 48] Rice, Stephen O., "Statistical properties of a sine wave plus random noise", *BSTJ*, 27(1), pp 109-157, Jan 1948.

[Rodriguez 14] Ignacio Rodriguez *et al*, "Radio Propagation into Modern Buildings: Attenuation Measurements in the Range from 800 MHz to 18 GHz", *80th IEEE Veh Tech Conf*, VTC-2014 Fall, Vancouver.

[Rubinstein 98] Rubinstein, Thomas N., "Clutter losses and environmental noise characteristics associated with various LULC categories", *IEEE Trans Broadcasting*, 44(3), September 1998, pp. 286-93.

[Shibuya 87] Shibuya, Shigekazu, *A Basic Atlas of Radio-Wave Propagation*, Wiley, 1987, §3.3.

[Soares 71] Soares de Assis, Mauro, "A simplified solution to the problem of multiple diffraction over rounded obstacles", *IEEE Trans Ant Prop*, 19(3), March 1971, pp. 292-5.

[Spaulding 74] Spaulding, A.D. & R.T. Disney (1974), *Man-Made Radio Noise*, OT Report 74-38, U.S. Department of Commerce, Office of Telecommunications, Boulder, 1974.

[Strutt 80] Strutt, J.W. (3rd Baron Rayleigh), "On the resultant of a large number of vibrations of the same pitch and of arbitrary phase," *Philosophy Mag*., vol. 10, pp. 73-78; August, 1880

[Suzuki 77] Suzuki, H., "A Statistical Model of Mobile Radio Reception", *IEEE Trans.Comm*, 25(7), July 1977, pp 673-680.

[Tanis 93] Tanis, W.J., II; Pilato, G.J., "Building penetration characteristics of 880 MHz and 1922 MHz radio waves", *43rd IEEE Vehicular Technology Conference Record*, 1993, pp 206-209.

[TIA 97] *A Report on Technology Independent Methodology for the Modeling, Simulation and Empirical Verification of Wireless Communications System Performance in Noise and Interference Limited Systems Operating on Frequencies Between 30 and 1500 MHz*, TIA TR8 Working Group 8.8 Technology Compatibility, Telecommunications Industry Association, 1997.

[TIA-08] *Wireless Communications Systems --- Performance in Noise- and Interference-Limited Situations --- Part 3: Performance Verification*, TSB-88.3-C, Telecommunications Industry Association, Arlington VA, 2008.

[TIA 09] *Radiowave Propagation --- Path Loss --- Measurement & Validation*, TSB-176, Telecommunications Industry Association, Arlington VA, 2009.

[TIA 10] *Radiowave Propagation — Path Loss — Measurement Presentation Format*, TIA-845-B, Telecommunications Industry Association, Arlington VA, 2010.

[TIA 12] *Wireless Communications Systems --- Performance in Noise- and Interference-Limited Situations --- Part 1: Recommended Methods for Technology-Independent Modeling*, TSB-88.1-D, Telecommunications Industry Association, Arlington VA, 2012.

[Turkmani 87] Turkmani, A.M.D. *et al*, “Radio propagation into buildings at 441, 900, and 1400 MHz”, *Conf on Land Mobile Radio*, Dec 1987, pp 129-138.

[Turkmani 93] Turkmani, A.M.D. and A.F. de Toledo, "Modelling of radio transmissions into and within multistorey buildings at 900, 1800, and 2300 MHz," *IEE Proceedings-I*, 140(6), Dec. 1993, pp. 462-470.

[USGS 07] *National Land Cover Database 2001 (NLCD 2001)*, March 7, 2007, U.S. Geological Survey, September 5, 2007, http://www.mrlc.gov/ .

[USGS 11] *NLCD 2006 Product Description Provisional Version*, March 14, 2011, U.S. Geological Survey, April 21, 2011, http://www.mrlc.gov/nlcd_2006.php

[Vogelmann 01] Vogelmann, J.E.*et al*, *Completion of the 1990s National Land Cover Data Set for the Conterminous United States from Landsat Thematic Mapper Data and Ancillary Data Sources, Photogrammetric Engineering and Remote Sensing*, 67:650-652, 2001.

[Walker 83] Walker, E.H., “Penetration of radio signals into buildings in the cellular radio environment”, *BSTJ*, 62(9), Nov 1983, pp 2719-2734.

[Wells 77] Wells, Paul I., “The attenuation of UHF radio signals by houses”, *IEEE Trans Veh Tech*, 26(4), Nov 1977, pp 358-362.

[Whitteker 85a] Whitteker, James H., *Users Guide to the C.R.C. VHF UHF Propagation Prediction Program*, Communications Research Centre, Ottawa, April 1985.

[Whitteker 85b] Whitteker, James H., *Users Guide to the C.R.C. Topographic Data Base*, Communications Research Centre, Ottawa, April 1985.

[Wong 82] Wong, Harry K., *“A Computer Program for Calculating Effective Interference to TV Service, Technical Memorandum FCC/OST 82-2”,* Federal Communications Commission, Office of Science and Technology, Washington DC, 1982, NTIS Accession Number PB 82-250911.

[Yao 92] Yao and Sheikh, “Investigation into Cochannel Interference in Microcellular Mobile Radio Systems”, *IEEE Trans. On Vehicular Tech.*, vol. 41, no. 2, May 1992, pp 114-123.

[Yamaguchi 86] Yamaguchi, Y., T. Abe, and T. Sekiguchi, "Experimental study of radio propagation characteristics in an underground street and corridors,"*IEEE Trans Electromag Compat*., 28(3), 1986, pp. 148-155.

THE TELECOMMUNICATIONS INDUSTRY ASSOCIATION

TIA represents the global information and communications technology (ICT) industry through standards development, advocacy, tradeshows, business opportunities, market intelligence and world-wide environmental regulatory analysis. Since 1924, TIA has been enhancing the business environment for broadband, wireless, information technology, cable, satellite, and unified communications.

TIA members' products and services empower communications in every industry and market, including healthcare, education, security, public safety, transportation, government, the utilities. TIA is accredited by the American National Standards Institute (ANSI).

ADVANCING GLOBAL COMMUNICATIONS

TELECOMMUNICATIONS INDUSTRY ASSOCIATION

1320 N. Courthouse Road, Suite 200
Arlington VA, 22201, USA

+1.703.907.7700 MAIN
+1.703.907.7727 FAX